Public Works Canada
Travaux publics Canada

Architectural and Engineering Services
Services d'architecture et de génie

AES/SAG 1-2:88-6

DEVELOPMENT OF A MODEL FOR PROGRESSIVE DAMAGE IN ICE

July 1988

Canada

Public Works Canada
Architectural and Engineering Services
Technology

AES/SAG 1-4:88-6

DEVELOPMENT OF A MODEL FOR PROGRESSIVE DAMAGE IN ICE

July 1988

Preparation Agency:
Det norske Veritas Canada Ltd.

Sponsoring Agency:
Panel for Energy Research
and Development (PERD)
Marine Product Line, Headquarters
Project Manager: M.S. Cheung

The contents of this document represent the views of the authors and are not necessarily the views or policies of the Department of Public Works.

The Minister of Public Works makes no representation or warranty, express or implied, with respect to this publication or the programs or information described in this publication, their quality, merchantability, or fitness for any particular purpose, or their adequacy to produce any particular result. In no event shall the Minister or Her Majesty the Queen in right of Canada, Her employees, servants or agents be legally liable to any person or persons for any damage, whether direct, indirect or consequential, resulting from the use of said publication or the programs or the information contained herein.

Published by Architectural and Engineering Services
Public Works Canada

© Minister of Supply and Services Canada 1988

Cat. No. W62-11/88-6E

ISBN 0-662-16292-7

Public Works Canada / Travaux publics Canada

DOCUMENT DATA

1. Document Title DEVELOPMENT OF A MODEL FOR PROGRESSIVE DAMAGE IN ICE	2. Control Number AES/SAG 1-2:88-6
	3. Date JULY 1988
4. Author(s) A. Cormeau, I.J. Jordan, M. Maes	5. Consultant's Ref. No.
6. Project Manager M.S. Cheung	7. Discipline Series No.
8. Preparation Agency and Address Det norske Veritas Canada Limited Suite 1110, 10201 Southport Rd., Southwest Calgary, Alberta T2W 4X9	9. Document Type Technical Report
	10. No. of Pages 121
11. Sponsoring Agency and Address Panel for Energy Research and Development (PERD) and Public Works Canada, Marine Product Line Sir Charles Tupper Bldg., Riverside Drive Ottawa, Ontario K1A 0M2	12. PWC File No. 6200-31
	13. PWC Project No. 601061
14. Supplementary Notes	15. SSC Publication No. W62-11/88-6E
	16. ISBN 0-662-16292-7

17. Abstract

This report addresses two important aspects of the interaction between ice and fixed structures: progressive damage to ice during compression, and the clearing of pulverized material around and indentor. Computer models were developed using finite element methods to emulate and analyze the behaviour of ice.
Scarcity of relevant data on ice crushing led to a number of assumptions based on existing damage theories for metals, concrete and rocks. An isotropic shear degradation model was implemented and uniaxial loading tests were applied, showing strain softening effects.
A shear damage model was successfully applied to the spread of microcracks during an ice sheet indentation test. An accurate prediction of the shape of the crushed layer was inhibited by the restrictions associated with the explicit time step algorithm.
A relationship among velocity, viscosity, ice thickness and pressure on the indenter was derived. Further investigations are recommended to quantify damage, to measure mechanical stress, and to measure flow, viscosity and shape of the crushed layer. Development of an implicit algorithm is proposed as a possible extension to this work. Further work is also called for in the development of an energy-based criterion relating to the shape of the crushed ice layer.

18. Distribution Statement Copies are available from: Documentation Centre Public Works Canada Sir Charles Tupper Bldg. Riverside Drive Ottawa, Ontario K1A 0M2	19. Keywords Ice forces; finite element; ice/structure interaction	
	20. Documentation Centre Catalogue No. MA102	21. Price no charge

DPW 2398 (86/09)

Travaux publics Canada | Public Works Canada

FICHE SIGNALÉTIQUE DE DOCUMENT

1. Titre du document MISE AU POINT D'UN MODÈLE DE DÉTÉRIORATION PROGRESSIVE DES GLACES	2. Numéro de contrôle AES/SAG 1-2:88-6
	3. Date Juillet 1988
4. Auteur (s) A. Cormeau, I.J. Jordan, M. Maes	5. No de réf. du conseil
6. Chargé de projet M.S. Cheung	7. No de la collection technique
8. Nom et adresse de l'organisme rédacteur Det Norske Veritas Canada Limited Suite 1110, 10201 Southport Road, South West Calgary, Alberta T2W 4X9	9. Type de document Rapport Technique
	10. Nombre de page 121
11. Nom et adresse de l'organisme promoteur Comité de la recherche et du développement énergétiques et Travaux publics Canada, Travaux maritimes, Immeuble Sir-Charles-Tupper, Promenade Riverside, OTTAWA (Ontario) K1A OM2	12. No de dossier de TPC 6200-31
	13. No de projet de TPC 601061
14. Notes	15. No de publication de ASC W62-11/88-6E
	16. ISBN 0-662-16292-7

17. Résumé

Le présent rapport aborde deux importants aspects de l'interaction entre les glaces et des ouvrages fixes, soit la détérioration progressive des glaces en compression et la pulvérisation suivie du dégagement des glaces autour d'un pénétrateur. Des modèles informatiques ont été élaborés par méthode des éléments finis, afin d'imiter et d'analyser le comportement des glaces. La rareté des données pertinentes à l'égard de l'écrassement des glaces a favorisé un certain nombre d'hypothèses fondées sur des théories existantes touchant les dommages causés aux métaux, au béton et à la roche. Un modèle de détérioration par cisaillement isotrope a été mis en oeuvre et des essais de charge uniaxiale ont été réalisés démontrant des effets de déformation réduite. Un modèle de détérioration par cisaillement a été appliqué avec succès à la propagation des microfissures lors d'un essai de pénétration de la couche de glace. Une prévision précise de la forme de la couche broyée a été entravée par des contraintes liées à l'algorithme de saut de temps explicite. Un rapport entre la vélocité, la viscosité, l'épaisseur des glaces et la pression sur le pénétrateur a été établi. De nouvelles études sont recommandées pour quantifier la détérioration, mesurer les efforts mécaniques, et mesurer l'écoulement, la viscosité et la forme de la couche de glace broyée. L'élaboration d'un algorithme implicite est proposé comme prolongement possible de ces travaux. En outre, de nouveaux travaux sont réclamés pour élaborer un critère, basé sur l'énergie, touchant la forme de la couche de glace broyée.

18. Diffusion Exemplaires disponibles du: Centre de documentation Travaux publics Canada Imm. Sir-Charles-Tupper, Prom. Riverside OTTAWA, Ontario K1A OM2	19. Mots clés Forces exercées par les glaces; éléments finis, interactions glaces/ouvrages	
	20. No de catalogue du centre de documentation MA100	21. Prix Gratuit

MTP 2398 (86/09)

PREFACE

This report is one of several reports on the research work in the field of marine engineering, identified and managed by the Marine Product Line and Technology Resources groups of Public Works Canada, with funds provided by the Interdepartmental Panel on Energy Research and Development (PERD)

PERD was established in 1974 to coordinate research on energy by the Federal Government with objectives to provide, in conjunction with efforts in the private sector and the provinces, the technical basis for:

- maintaining oil self-sufficiency over the short term, in view of dwindling conventional supplies;

- developing a diversified energy economy, less dependant on oil and gas in the mid-term; and

- making Canadians less reliant on non-renewable energy sources in the long term.

The research work undertaken by Public Works Canada in Marine Engineering with funds from PERD has been directed particularly toward the following two main topics:

1. Ice/Structure Interaction
2. Construction and Towing of Reinforced Concrete Caissons in the Arctic.

This report is being published with a view to enhancing the technology in the field of Marine Engineering and contributing toward the objectives of PERD.

TABLE OF CONTENTS

PREFACE		i
LIST OF FIGURES		iii
LIST OF TABLES		v
1. INTRODUCTION		1
2. PROBLEM DEFINITION: PROCESS OF INTERACTION OF ICE WITH AN INDENTER		2
2.1	Local (Progressive) Fracture	2
2.2	Progressive Damage	7
2.3	Crushed Ice	7
3. REVIEW OF CONTINUUM DAMAGE THEORIES		10
3.1	The Damage Process	10
3.2	Definition of Damage	12
3.3	Literature Review	15
3.3.1	Progressive Damage	15
3.3.2	Behaviour of Crushed Ice	19
4. DAMAGE MODEL FOR ICE		22
4.1	General	22
4.2	Formulation of the Damage Model for Ice	23
4.3	Finite Element Implementation	27
4.4	Energy Dissipation in the Damage Model	32
4.5	Preliminary Tests	38
5. MODEL FOR THE VISCOUS FLOW OF CRUSHED ICE		50
5.1	General	50
5.2	Analogy between Hooke's Law and Stoke's Law	50
5.3	Modelling of Incompressible Elastic Behaviour	56
5.4	Finite Element Modelling	57

TABLE OF CONTENTS (cont'd)

6. MODELLING OF ICE INDENTATION TESTS AND COMPARISONS 58

6.1 Progressive Damage of Ice during Indentation 58
6.2 Viscous Flow of Crushed Ice during Indentation 65

7. CONCLUSIONS AND RECOMMENDATIONS 81

REFERENCES 84

APPENDICES

Appendix A: Relationship between Stress and Strain Increments for Particular Constraint Conditions and States of Stress

Appendix B: Comparison between an Analytical and an FE Solution to a Uniaxial Damage Problem

LIST OF FIGURES

2.1 Idealization of Zone of Crushed Ice (High Penetration Rates) 3

2.2 Contours of Accumulated Primary Creep Strains 3

2.3 Progressive Shear Damage Under a Flat Indenter 6

2.4 Failure Modes in Compression 6

2.5 Formation of a Crushed Zone Immediately in Front of a Structure at the Indenter Head. The Velocity Dependence of Pressure 9

3.1 Stress-Strain Curves for Concrete 11

3.2 An Identical Load F Acting on Materials with Varying Degrees of Damage 14

3.3 Viscoplastic Layer of Crushed Ice Under the Ball 20

LIST OF FIGURES (cont'd)

4.1	(a) Progressive Damage (b) Damage accompanied by the development of permanent strains	25
4.2	Illustration of Equation 4.9 in a Stress-Strain Diagram	27
4.3	Illustration of a term J_{ijkl} in a Material Jacobian Matrix	31
4.4	Illustration of the Different Energy Density Components (Equation 4.34)	37
4.5	Uniaxial Load Test Models	39
4.6	Uniaxial Stress/Strain Curves for Various Damage Laws	43
4.7	Cyclic Loading History for a Uniaxial Strain-Driven Test	44
4.8	Uniaxial Stress/Strain Curve for a Damaging Material Loaded According to Figure 4.7	45
4.9	Stress-Strain Curve Corresponding to Equation 4.43	46
4.10	Uniaxial Stress/Strain Relation for Creep Damage	47
4.11	Stress/Strain Curves for Uniaxial Loading	48
4.12	Constant Stress Test	49
6.1	Plane Stress Finite Element Mesh of Ice Loaded by an Indenter	59
6.2a,b,c	Spreading of Damage as a Function of Time	61-63
6.3	Maximum Shear Stress Distribution under the Indenter	64
6.4	Damage Evolution at a Certain Point under the Indenter	66
6.5	Simplified Model for Ice Indentation	66
6.6a	Contours of Constant Shear Stress from Boussinesq-Flamant Analytical Solution	68

LIST OF FIGURES (cont'd)

6.6b	Shape of Crushed Layer under the Indenter	68
6.6c	Possible Shapes of the Layer of Crushed Ice	69
6.7	Flow of Crushed Ice in the Layer Adjacent to the Indenter	70
6.8	Amount of Ice Crushed during Θt in an Indentation Test	70
6.9	Finite Element Analysis of a Typical Layer of Crushed Ice Using the Elastic-Viscous Analogy	72
6.10	Various Layer Geometries to Model the Crushed Ice Flow in Plane-Stress	73
6.11	Stresses, Exerted by Crushed Ice on the Indenter	75
6.12	Interact Force as a Function of Thickness of the Layer of Crushed Ice	76
6.13	Flow of Crushed Ice in the Midplane of the Ice Sheet	78
6.14	Distribution of Velocity Vectors on Top of the Ice-Layer Boundary	79

LIST OF TABLES

5.1	The Analogy Between the Elastic Analysis of an Incompressible Solid and the Flow of a Viscous Fluid	55
6.1	Forces from Indentation Tests	77

1. INTRODUCTION

Ice features interacting with structures at even moderate velocities exhibit progressive fracturing and damage in the ice in the immediate vicinity of the structure. On the other hand, creep processes, in which the ice flows and deforms, are predominant only at very small rates of loading. The ability of the ice to transmit forces is dictated by the mechanical behaviour of the ice. First, floes or features may split, and in doing so, can redistribute some of their energy into creating rotational kinetic energy of large ice pieces. In the zone near the ice-structure interface, the ice crushes, pulverizes and clears by motion of relatively small forces, involving a "flow" with frictional effects between particles.

The large-scale splitting problem referred to above has been dealt with in previous report to the Department of Public Works (Tomin et. al, 1985) so the main focus of the present report is on the pulverizing and subsequent movement or clearing of the ice. This will yield valuable information on the forces transmitted from the ice to the structure and also on the distribution of local ice pressures. The process of pulverization results from progressive damage in the ice, and this is discussed in some detail.

2. PROBLEM DEFINITION: PROCESS OF INTERACTION OF ICE WITH AN INDENTER

2.1 Local (Progressive) Fracture

During the initial contact of the ice with an indenter, the virgin ice is loaded along the contact length. As the load increases, microcracks develop in the ice and local failure occurs. A layer of crushed ice develops in front of the indenter (see Figure 2.1) and as the penetration proceeds, the crushed ice clears around it. This layer of crushed ice behaves quite differently from the intact ice and should therefore be modelled separately. This phenomenon has been observed before in tests carried out by dropping a ball on an ice surface (Kheisin and Likhomanov, 1973, Garcia et al., 1985, Yen et al., 1970). In the present study, a criterion for the onset of local microcracks is described.

Onset of internal cracking (damage) can be regarded as a certain type of failure. Gold was the first to study systematically the formation of internal cracks in ice during compressive creep. This work, together with a thorough review of crack nucleation theories is summarized in Gold (1972). Gold concluded that the pile-up dislocation model of crack initiation is applicable to ice. It was shown experimentally that a stress threshold (approximately 6.2 MPa at $-10^{\circ}C$) exists for crack nucleation in uniaxial compression. Although the cracks observed formed during uniaxial compression, Gold inferred that local tensile stresses led to the crack formation (basically a cleavage mechanism).

The number of cracks nucleated in columnar-grained ice (crack density) was given by Gold as:

$$N = A(\sigma - 0.09)^{1.7} \text{ cracks per square metre,}$$

where A is a constant, and σ is the uniaxial stress in MPa. This evidence is incompatible with results from the Zhurkov model (Zhurkov and Sanfirova, 1958) of a thermally activated process of crack formation. Zhurkov's formula has the form:

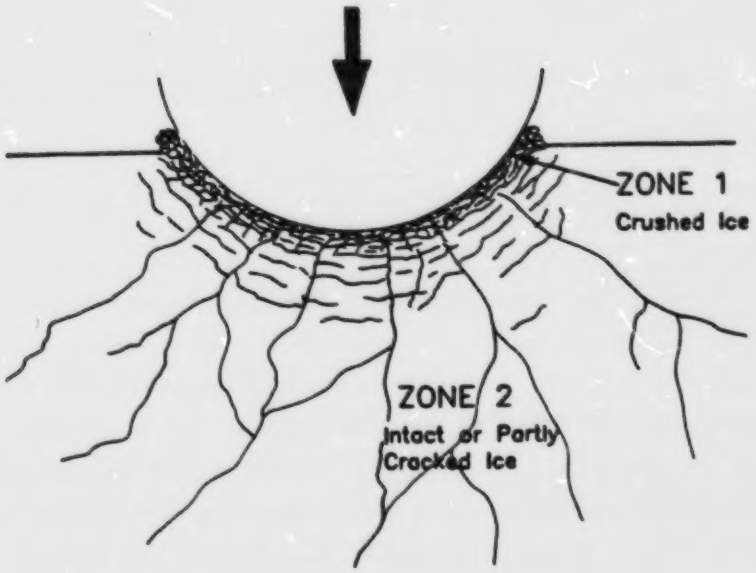

Figure 2.1. Idealization of Zone of Crushed Ice (High Penetration Rates)

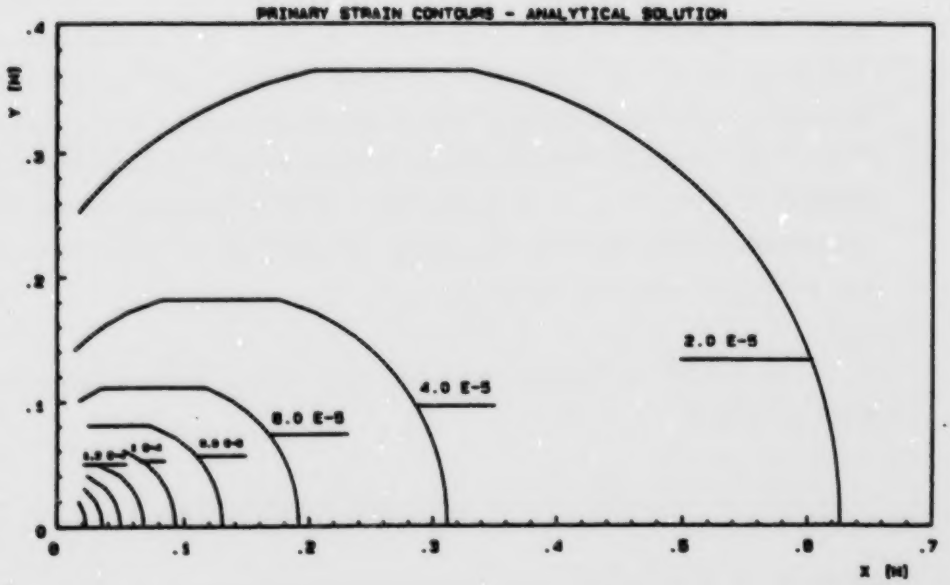

Figure 2.2. Contours of Accumulated Primary Creep Strains

$$t_f = t_o \left(\frac{Q_f - \alpha\sigma}{kT}\right)$$

where t_o and α are constants, k is the Boltzmann constant, Q_f is the activation energy of the process, σ is the stress, and T is the absolute temperatures.

This model predicts a finite time (t_f) for crack nucleation for any positive (tensile) stress, however small.

Sinha (1984) developed a model for crack nucleation in ice which relates the cracking activity to the grain-boundary sliding. The grain-boundary sliding results in stress concentrations at triple points or at irregularities or ledges at the grain boundaries, which lead to crack nucleation. The grain-boundary sliding is related to delayed-elastic strain, ε_{del}, which is a part of the total strain, ε, as follows:

$$\varepsilon = \varepsilon_{el} + \varepsilon_{del} + \varepsilon_v \qquad (2.1)$$

where

ε_{el} = elastic strain component;
ε_{del} = delayed-elastic strain component; and
ε_v = viscous (creep) strain component.

The elastic strain and viscous strain components follow the uniaxial Hooke's law and the Glen's power law respectively (Glen, 1975). The delayed-elastic strain component is given by:

$$\varepsilon_{del} = c_1 \frac{d_1}{d} \left(\frac{\sigma}{E}\right)^s \left(1 - \exp\{-(a_T t)^b\}\right) \qquad (2.2)$$

where

E = Young's Modulus;
c_1 = a constant corresponding to the unit reference grain size, d_1;
b,s = constants; and
$1/a_T$ = the relaxation time.

According to Sinha's theory, an internal crack initiates when the delayed elastic strain reaches a critical value which is directly proportional to the critical grain-boundary displacement, $\bar{x}_{cr}$:

$$\varepsilon_{del}^{cr} = \frac{K\,\bar{x}_{cr}}{d} \qquad (2.3)$$

where K is a constant and d is the grain size.

For example, if the grain size d = 1.6 mm, $\bar{x}_{cr} = 4.6.10^{-4}$ mm (found experimentally) and K = 1, the critical value of the delayed elastic strain is found to be:

$$\varepsilon_{del}^{cr} = 2.3 \times 10^{-4}$$

Results from the calculation of the accumulated primary creep strains are given in Figure 2.2, and it can be seen that these show good general agreement with the observed damage (Figure 2.3). The latter figure shows the development of damage as a process of shear degradation, a conclusion that is in general agreement with the failure mode under moderate lateral confining pressure, as suggested by Ashby and Hallam (1986). For comparative purposes, the Ashby and Hallam idealization is shown in Figure 2.4.

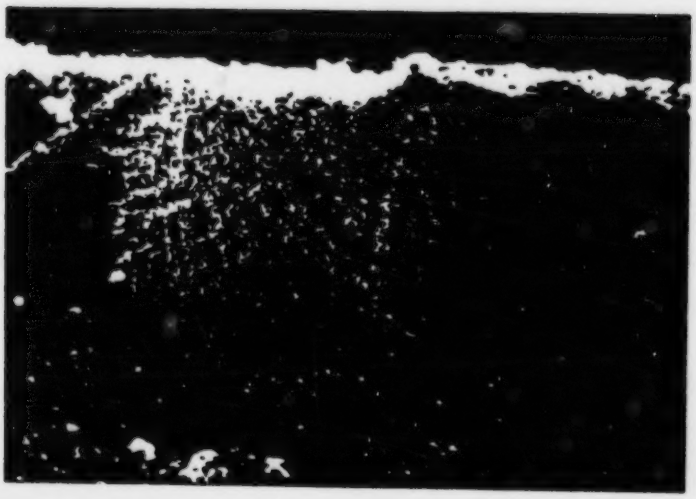

Figure 2.3. Progressive Shear Damage Under a Flat Indenter

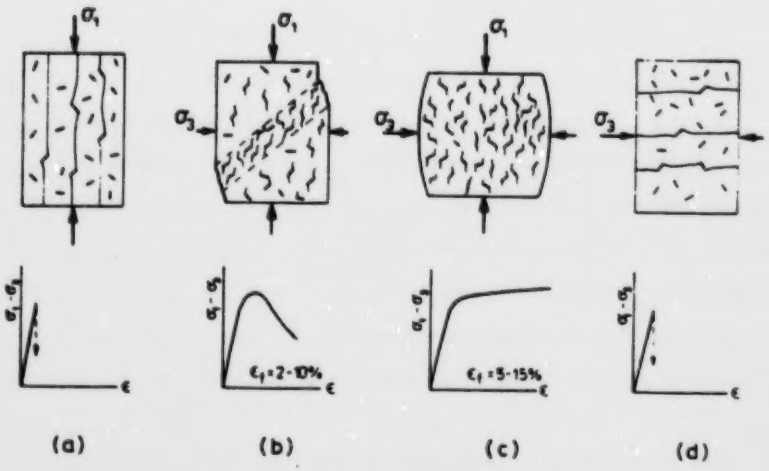

Figure 2.4 Failure modes in compression. (a) and (d) Slabbing, when one or a few cracks propagate parallel to the principal compression direction, (b) failure by aggregation of cracks to form a shear zone and (c) near-homogeneous deformation by microcracking (Ashby and Hallam, 1986)

2.2 Progressive Damage

Upon reaching the threshold of microcrack nucleation and/or propagation, the material can no longer be considered to carry external load in accordance with its original elastic properties. From that point on, the stiffness of the material changes irreversibly, that is, it is governed by gradually altering properties. This change in mechanical behaviour is the key characteristic of the damage process. In particular, it will be shown in the next sections, that the damage of ice in compression can be modelled satisfactorily by degradation of the elastic shear modulus. Progressive damage cannot proceed indefinitely. The process reaches a final stage when the microcrack network becomes so dense that the material attains zero stiffness and disintegrates entirely. This condition forms a bound for the range of applicability of damage models.

2.3 Crushed Ice

Whereas a damage analysis for engineering materials such as concrete or rock is generally limited to the investigation of the behaviour of partially damaged material, it is necessary to consider post-damage states in the case of ice. At high deformation rates, the shattered ice resembles a pasty or powdery substance which has been observed to exhibit both viscous and plastic properties. This substance has been modelled as a viscoplastic material in the analysis of dropped ball tests (Kurdyumov and Kheisin, 1976), and this approach will be applied in the present study. The properties of the crushed ice material are not as well studied as those of the intact ice, however, other models such as those for powders and soils can be implemented.

The study of the behaviour of the boundary layer of crushed ice is important, since it provides direct information regarding the ice pressures on the penetrating body. In Figure 2.5 (drawn from internal research at DnV), it is suggested that the configuration of the layer and the interaction pressure are dependent on the velocity. Results emerging from a combined treatment of virgin ice, partially damaged ice, crushed ice are consequently extremely useful for structural design.

In Section 5, the quantitative behaviour of pulverized ice is modelled using the fundamental constitutive equations of slow viscous flow. It is assumed that the powder is incompressible and that friction between the ice particles dominates inertia effects. Such a model is very beneficial from a numerical point of view, since there exists a convenient analogy between the Eulerian viscous flow of a fluid (or powder) and the Lagrangian elastic deformation of a solid.

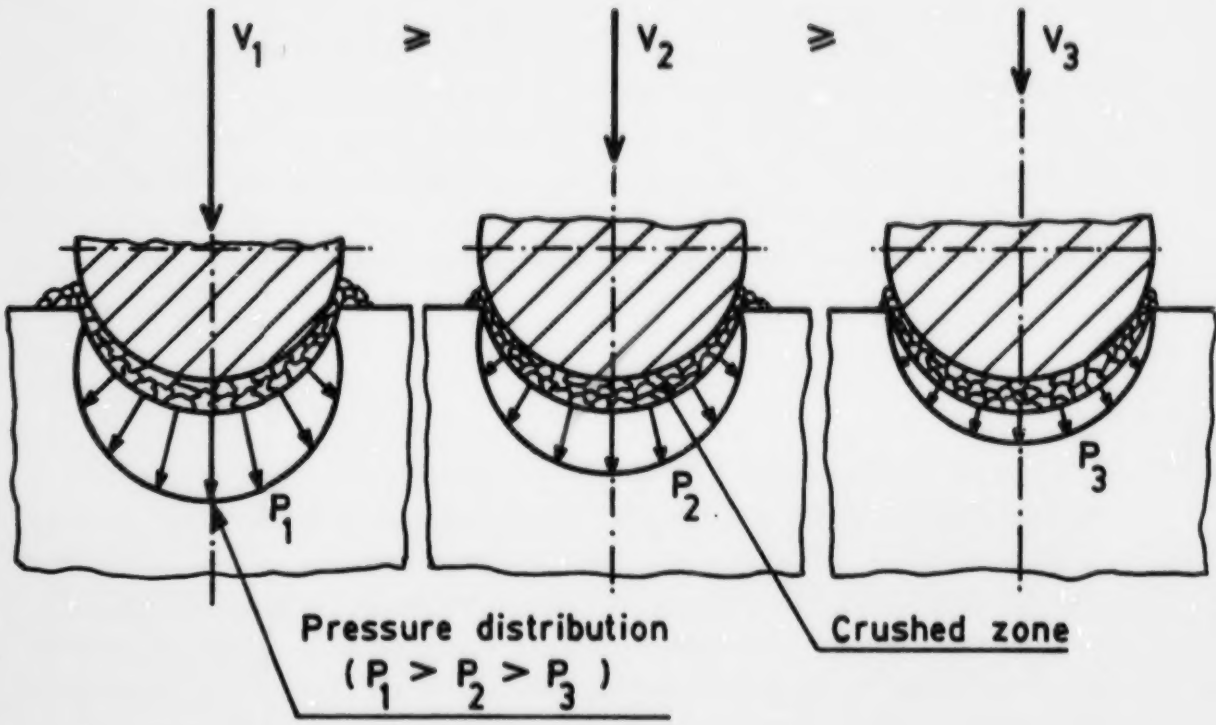

Figure 2.5 Formation of a Crushed Zone Immediately in Front of a Structure at the Indenter Head. The Velocity Dependence of Pressure.

3. REVIEW OF CONTINUUM DAMAGE THEORIES

3.1 The Damage Process

The heterogeneous structure of many materials includes dislocations, grain boundaries, microcracks and voids. These propagate and develop under compressive stresses. The propagation of large cracks is not the concern of the present work - this has been dealt with in the previous report to the Department of Public Works (Tomin et al., 1985). Rather, the system of microcracks that develop under compressive stresses is the subject of the present study.

Consider a specimen of material, such as concrete, rock, or as we shall see, ice, loaded in compression. If one subjects the material to a small incremental strain, several things can happen:

(1) There may be an increase or decrease in elastic strain energy;

(2) There may be irreversible movements associated with creep or plastic flow; and

(3) The microcrack system may extend and new microcracks could be nucleated: this is the essence of the damage process. Generally, the crack growth will be stable so that damage increases in a relatively orderly manner.

It is important to recognize that (1) and (2) do not of themselves result in material damage or degradation. Storage of elastic strain energy is a reversible process without any effect on the structure of the material, however, creep and plastic flow are irreversible (involving heat generation) nonetheless the structure of the material is restored after the movement of dislocations. The mechanism for (3) involves changes to the structure of the material; as the density and size of cracks increases, the response of a specimen of macroscopic size changes. Figure 3.1 shows the changes in the stress-strain curve for concrete under successive load cycles. This phenomenon is exhibited by many materials with a strain-softening descending branch, and one such material is ice. The damage can occur at a fast rate, without

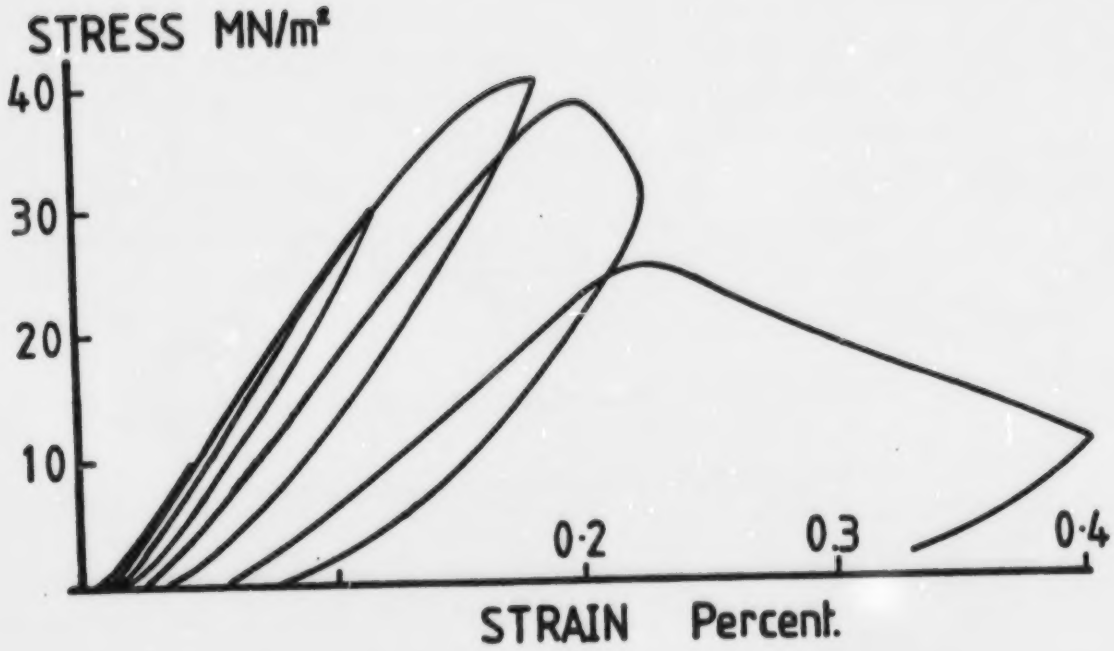

Figure 3.1. Stress-Strain Curves for Concrete
(Spooner and Dougill)

substantial time-dependent response of the ice, or slowly, leading to a gradual development of damage with time. In this case, the damage is referred to as creep damage (Leckie, 1978) although the resulting change to the material is damage, not creep (which occurs simultaneously).

The energy in the damage process is mostly dissipated as work in creating new surfaces, and this is done in the highly stressed zone near the crack tips. Some energy is conserved as surface energy, but this is a small percentage (about 10%) of the energy dissipated and cannot readily be regained. For practical purposes, the energy in damaging the material can be treated as being dissipated.

The growing network of cracks which constitutes damage of the material is characterized by techniques which are addressed in the next section. The key point is that one does not wish to follow each individual crack, but rather "smear" the cracks out over the material. The rationale for this is sensible because the number of cracks is large, and that repetitive tests on similar specimens would yield quite different detailed crack patterns, though with similar "average" behaviour.

3.2 Definition of Damage

The extent of damage is related to the density of microcracks, voids and other defects, which permanently affect the overall mechanical behaviour of the material. Generally however, there is no clear, visible distinction between virgin (undamaged) and partially damaged material. Therefore, direct visual measurements of the density of microcracks would be difficult, since they would involve complicated microscopical measurements. It is more feasible to use indirect mechanical measurement techniques, such as the following:

- dynamic ultra-sound measurements: ($\geq$ 20 kHz). Here, damage is related to the changes in longitudinal and transversal speed of sound through the material.

- measurement of the variation of electric resistance: the effect of damage on electrical resistance is purely geometrical; the denser the microcrack network, the higher the overall resistivity.

- measurement of the variation of other material or rheological properties, such as elastic moduli or creep (Lemaitre and Chaboche, 1985).

It is convenient initially to characterize damage by a single scalar function or index D (see also Section 3.3). This number represents to what extent the values of certain elastic properties are reduced and ranges between 0 (intact) to 1 (completely damaged). One could also imagine the material in different states of total damage, as in Figure 3.2. In situation (a), virtually no damage has occurred and the imposed shearing load F corresponds to a stress τ_o acting on shear area S_0. If an extensive microcrack network is present (Figures 3.2(b) and (c)), the "effective" shear area is reduced to the values S_1 and S_2. It is assumed that this reduction in area occurs in the following manner:

$$\begin{aligned} S_0 &= S_0 && \text{..., for } D = 0, \\ S_1 &= S_0\,(1-D) && \text{..., in general, and} \\ S_2 &= 0 && \text{..., for } D = 1. \end{aligned} \qquad (3.1)$$

The measured shear strain ε is equal to:

$$\varepsilon = \frac{F}{G_0 S_1} = \frac{F}{G_0 (1-D) S_0} = \frac{F}{G_1 S_0} \qquad (3.2)$$

for the general case of a partially damaged material (Figure 3.2(b)), where G_0 is the elastic shear modulus of virgin material. Consequently, damage can be considered to affect either the effective shear area S_1 or the effective modulus G_1 in an entirely similar manner. Consequently, the analysis can be carried out on the assumption that the behaviour of damaged material, characterized by a damage function D, is equivalent to the behaviour of undamaged virgin material, provided that the original elastic modulus G_0 is replaced by:

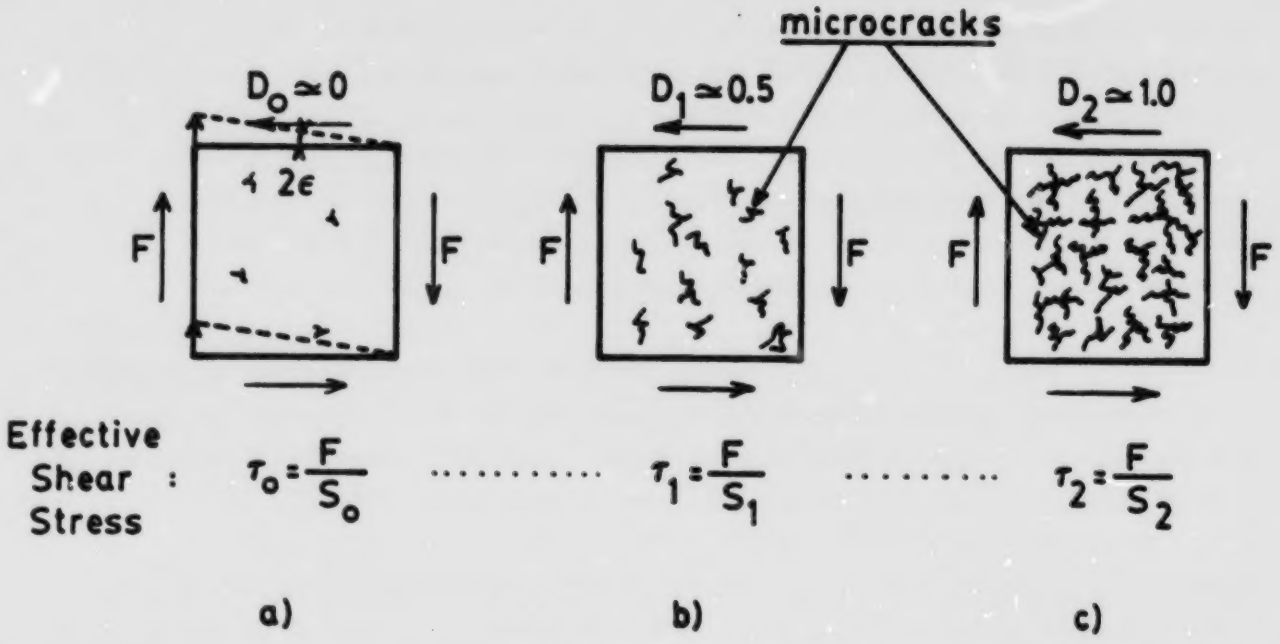

Figure 3.2. An Identical Load F Acting on Materials with Varying Degrees of Damage

$$G_1 = G_0(1 - D) \tag{3.3}$$

The behaviour of damaged material is completely defined if the damage function D is prescribed as a function of current stress and strain, and their history up to the current loading state.

In the following section, this definition of progressive damage is interpreted and discussed in the light of previously studied damage models.

3.3 Literature Review

3.3.1 Progressive Damage

During the last twenty years, phenomenological theories treating progressive fracturing in compression as a continuous process characterized by degradation of the material properties have been developed. The importance of the application of damage models to ice has been pointed out by Karr (1985).

The concept of damage as a separate state variable, having its own time history, originates from Kachanov's work (1958). He introduced a scalar state variable, D, to quantify the amount of damage which is defined as the density of voids in a given cross section. Kachanov applied the concept of damage only to the phenomenon of metal creep rupture under uniaxial load conditions. The isotropic representation was subsequently applied to ductile materials subjected to simple loading paths. In this case, damage was associated with a small concentration of spherical voids (Krajcinovic and Fonseka, 1981).

Further modifications of the scalar damage model for the ductile mode were suggested by, amongst others, Leckie and Hayrust (1973), Hayrust et al. (1975), Leckie (1978), Lemaitre and Chaboche (1978).

Additional experiments by Hayrust and Leckie showed planar microcracks perpendicular to the direction of the principal tensile strain, which provided evidence of the directional growth of damage. A vectorial model of damage was formulated by Davison and Stevens (1973), in which planar microcracks were defined by a vector normal to the plane of the crack and of magnitude equal to the area of the crack.

Vakulenko and Kachanov (1971) introduced a second order tensor notation for damage. Damage occurs either in cleavage (fracture mode I) or in shear (fracture modes II and III). However, since their model is essentially based on superposition, it is incorrect, as total damage accumulated during a combined compression and shear test is, in general, not equal to the sum of the damages associated with the individual tests. In other words, progressive damage should be considered as history dependent. Vakulenko and Kachanov's model ignores the difference between accumulated total damage and damage evolution.

The second order model was extended to the compression fracture mode by Dougill (1975 and 1983), resulting in a general theory for a progressively fracturing solid. This theory is in many ways similar to the hardening plasticity theory, in which the static variables are exchanged for kinematic variables. Instead of plastic yield surfaces in a stress space, fracture surfaces, termed "loading functions" by Dougill, are defined in a strain space. However, Dougill's theory (1983) does not include a restrictive postulate such as Drucker's plasticity postulate and it is not based on a normality assumption.

Using the principles of linear elasticity, Dougill derives a constitutive law for damage in the form of a differential equation. Stress response is purely elastic upon loading and unloading whenever straining remains inside the fracture surface. Elsewhere, stress softening occurs because of progressive fracture. The development of stress increments is governed by a flow rule. It should also be noted that unloading occurs through the origin; no permanent strains can develop (see for example Figure 4.1(a)). The fracture surface or "loading function" in a deformation space is defined by a set of parameters, in a similar way as for hardening plasticity. Dougill does not define a unique damage variable as such, but uses energy dissipation functions, which

describe the change in shape of the fracture surface. He subsequently applies the model to fibrous materials (Dougill, 1976). Damage is assumed to develop in both tension and compression, and the associated fracture surfaces are simple planes perpendicular to the axes of strain.

Of practical interest to the problem at hand is an isotropic damage model by Resende and Martin (1983). They introduced a scalar damage function together with a rate of damage evolution law. This theory was applied to progressive fracturing of granular materials such as rocks and concrete, and in particular, to Bushveld Norite rock, for which extensive data exists. Based on experimental evidence, their model includes effects such as volumetric damage, as well as different damage mechanisms for tension and compression. The elastic properties of the material degrade progressively as damage increases. Permanent volumetric strains develop simultaneously with progressive damage, whereas shearing remains purely elastic throughout the damage process. The model is conveniently formulated by means of the first and second invariants of stress, strain, and their respective rates; the material behaviour is analyzed separately using volumetric and deviatoric components.

A formal generalization of the original Kachanov's model was suggested by Chaboche (1979), who introduced the notion of effective stress and equivalence in deformation (this concept is illustrated by Figure 3.2). A main advantage of this theory is that it can be applied to any kind of material behaviour (elasticity, plasticity, creep), using the same formalism. An isotropic formulation of damage models for various materials is described, together with experimental techniques to identify the effects of damage (Chaboche and Lemaitre, 1985). In addition, anisotropic multiaxial damage is considered for simple loading cases; a fourth order tensor notation is proposed, which can be considerably simplified by separating constants relating to the direction of damage from a scalar function which represents the evolution of damage. The latter function can take into account nonlinear damage effects.

Progressive damage theories based on statistical strength models of microcracks were applied to the uniaxial compression of ice by Karr, 1985. This model was calibrated using acoustic emission data of ice samples subjected to compression.

Other theories, derived using the principles of endochronic constitutive models (Bazant, 1976) lack a consistent definition of damage and are based on a collection of data fits using variable time scaling; this procedure results in numerous material parameters.

To summarize the applicability of a progressive damage theory to ice requires a careful consideration of the following points:

1) for practical computing reasons, and also partly due to the lack of experimental evidence, a scalar damage model is preferred to a vectorial or a tensorial one; directional damage is considered to be beyond the scope of present-day ice research;

2) under compressive ice conditions, degradation of the bulk modulus (volumetric damage) is not essential. This is also suggested by Likhomonov and Kheisin (1973) who found that no significant change takes place in the volume of ice during the process of crushing;

3) the interpretation of damage must be compatible with techniques to measure it (Chaboche and Lemaitre, 1985); and

4) damage theories derived from plasticity, which include such principles as flow rule and fracture surface (Dougill, 1976), do not necessarily provide an adequate representation of the actual damage process.

In view of these considerations, a damage model similar to the one proposed by Resende and Martin (1983) for rock mechanics is judged to be suitable for ice. In addition, a law describing the evolution of permanent strains is proposed. Such a law eliminates a bothersome disadvantage of Dougill's model, namely the unloading to the origin. The development of residual strains can also be coupled with the progression of damage itself, as proposed by Kachanov.

3.3.2 Behaviour of crushed ice

Many authors have dealt with the behaviour of ice when impacted by a heavy rigid mass such as a steel ball (Yen, et al, 1970; Likhomanov and Kheisin, 1971) as well as by a lighter, but a very much faster projectile such as a bullet (Ross, 1969; Gerard, 1976). In all cases the formation of a "crater" with varying dimensions was observed. This provides evidence of the fact that ice scatters into very small fragmented particles that clear from beneath the impacting body to form a typical crater. Faced with these findings, Kheisin and Likhomanov (1973, 1976) attemped to model the behaviour of the ice powder as it clears from under an indenting body. They initially used a somewhat complicated plasticity relationship based on a spatially varying parameter dependent on a "plastic factor" and the local strain rates. This was based on flow processes in metal forming and was subsequently dropped in their analysis, since the term was insignificant compared to the coefficient of viscosity (internal friction). They considered an axisymmetrical case, as suggested in Figure 3.3, with cylindrical coordinates r, z, ϕ. The coordinate ϕ becomes irrelevant because of axisymmetry. The resulting equations are:

$$\text{grad } p = \mu \nabla^2 v \tag{3.4}$$

expressed in cylindrical coordinates, where p is the hydrostatic pressure, μ is the coefficient of viscosity, and v is the velocity vector.

The equations (3.4) are the constitutive equations governing slow-viscous flow, defined as the flow of a very viscous incompressible Newtonian fluid. Also, the Reynolds number:

$$\text{Re} = \frac{\text{inertial forces}}{\text{viscous forces}}, \tag{3.5}$$

is sufficiently small. In such a fluid the shearing stress is proportional to the velocity gradient, the proportionality factor being the viscosity. Thus, Eqs. (3.4) correspond to the Navier-Stokes equations with zero inertial terms.

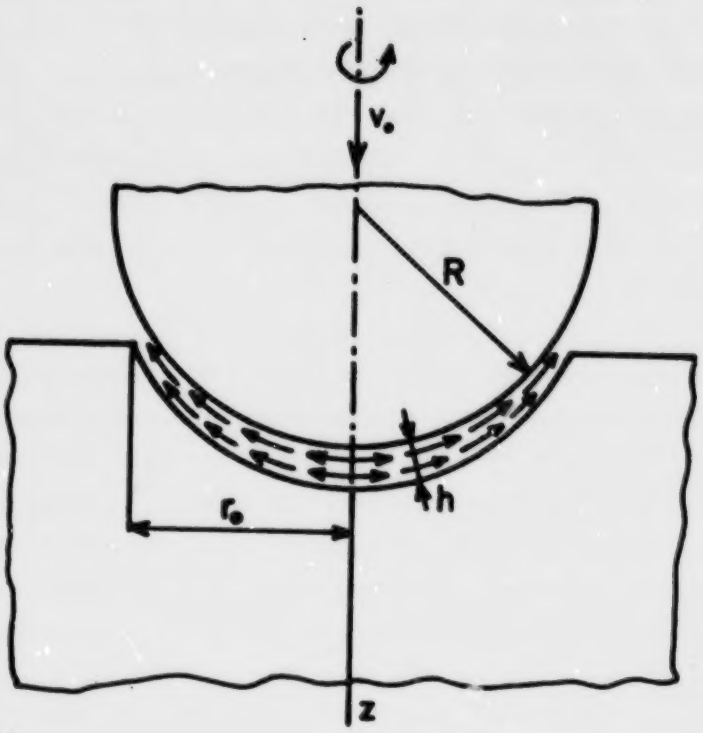

Figure 3.3

Viscoplastic Layer of Crushed Ice Under the Ball
(after Kurdymov and Kheisin, 1976)

The problem of crushed ice is essentially one of flow, and Eqs. (3.4) are based on an Eulerian formulation, which describes the flow of a fluid or a powder through a fixed grid. In general, the solution of this problem would require considerable use of difficult analytical techniques. However, there exists a very convenient analogy between Hooke's law of elasticity and Stokes' law of friction. In Chapter 5, it is demonstrated how this analogy can be used to study a slow viscous flow problem by means of a linear elastic deformation analysis.

4. DAMAGE MODEL FOR ICE

4.1 General

The purpose of this section is to develop a constitutive model for ice, which takes into account the progressive damage of ice exhibited during fast indentation tests. Under fast loading conditions, ice exhibits brittle behaviour. Strength is weakly rate dependent (G. Timco, 1985). This contrasts with slow loading conditions where creep dominates and causes a marked decline of strength with loading rate. The distinction between the two types of response is generally characterized by nominal strain rates in the order of $10^{-3}s^{-1}$ (Lainey, L. and Timarri, 1984) for uniaxial loading conditions.

In the brittle range, the behaviour of ice is essentially elastic. Under compressive state of stress, microcracks under the indenter have been observed to be aligned along maximum shear stress trajectories (Tomin et al., 1985), as illustrated in Figure 2.3. The proposed model is therefore assumed to be based on degradation of the shear behaviour using the scalar isotropic damage concept of Resende and Martin, 1985. The volumetric behaviour of ice is assumed to remain perfectly elastic and unaffected by degradation.

The degradation is expressed in terms of an internal scalar variable (see definition in Section 3.2), and an evolution law relates the rate of damage to the strain, stress and damage history. This evolution law is not to be confused with a yield/failure surface or a flow rule. It has the general form:

$$D = f\ (e,\ \dot{e},\ \sigma_m,\ \varepsilon_v,\ \dot{\varepsilon}_v,\ \ldots\ \dot{D}) \qquad (4.1)$$

In addition to the degradation of elastic shear properties, the capability of permanent deformations has been included in the model. To remain consistent with the hypothesis of shear degradation, permanent strains affect only the shear behaviour, so that, for ice sheet indentation tests, where confining pressures are low,

no permanent volumetric strains are assumed to develop. For this purpose, an additional variable representing the magnitude of permanent or residual shear strains, e^{rd} together with a new evolution law, is introduced:

$$\dot{e}^{rd} = f(e, \dot{e}, \sigma_m, \varepsilon_v, \dot{\varepsilon}_v, \ldots, \dot{D}) \tag{4.2}$$

The postulate of isotropic behaviour implies that evolution laws for damage and permanent deformation are independent of the choice of coordinate axes, and can thus be expressed as functions of tensorial invariants. Resende and Martin, 1985, postulated a dependence on stress and strain, and their time derivatives. The same assumptions are applied in the present model for ice.

4.2 Formulation of the Damage Model for Ice

The equations for linear elasticity (small deformations) for undamaged ice may be written as:

$$\sigma_{ij} = H_{ijkl} \varepsilon^{el}_{kl}, \tag{4.3}$$

which can be decomposed into equations for bulk and deviatoric behaviour (Timoshenko and Goodier, 1970), as follows:

$$\sigma_{ij} = S_{ij} + \sigma_m \delta_{ij} \tag{4.4}$$

$$\sigma_m = K \varepsilon^{el}_v \tag{4.5}$$

$$S_{ij} = 2G E^{el}_{ij} \tag{4.6}$$

where H_{ijkl} is a set of proportionality factors with two independent constants for isotropic behaviour K,G;

σ_{ij} Cauchy stress;

S_{ij} stress deviator;

σ_m mean stress: $1/3\,(\sigma_{11} + \sigma_{22} + \sigma_{33})$;

δ_{ij} Kronecker delta;

K bulk modulus;

G shear modulus;

ε_v^{el} strain in volume, $\varepsilon_{11} + \varepsilon_{22} + \varepsilon_{33}$;

E_{ij}^{el} deviator of elastic strains; and

ε_{ij}^{el} elastic strains.

It is important to distinguish two damage models. The first one is purely elastic and unloading is, at all times, associated with a return to the origin (i.e. zero strain and zero stress (Figure 4.1(a)). In the second model, additional permanent strains ε^{rd} are assumed to be obtained upon unloading (Figure 4.1(b)). Consider a material behaving in accordance with the first condition. Since progressive damage is assumed not to affect the bulk behaviour, the shearing stresses S_{ij} in a damaged material having a current degree of damage D are:

$$S_{ij} = 2\tilde{G}\, E_{ij}^{el} \tag{4.7}$$

where

$$\tilde{G} = G\,(1 - D), \tag{4.8}$$

that is, the apparent shear stiffness $\tilde{G}$ depends on the current accumulated damage D.

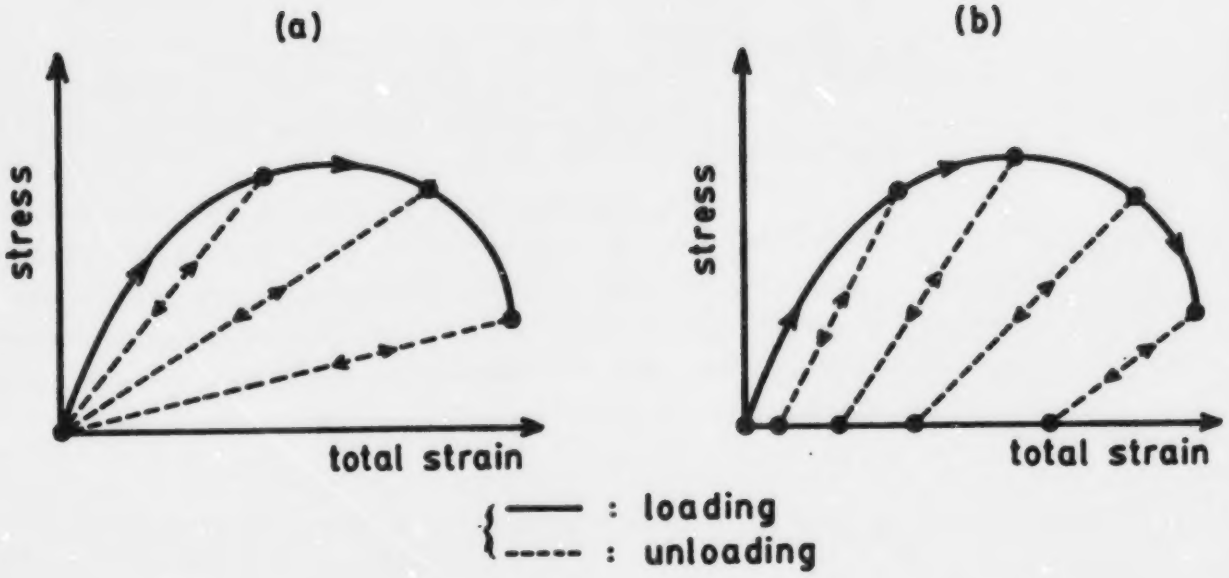

Figure 4.1 (a) Progressive Damage

(b) Damage accompanied by the development of permanent strains

To use the model under any arbitrary load history, Eq. (4.7) is differentiated with respect to time, to result in:

$$\dot{S}_{ij} = 2\tilde{G}\,\dot{E}^{el}_{ij} - \frac{\dot{D}}{1-D}\,S_{ij} \tag{4.9}$$

The first term on the right hand side represents the current degraded elastic stress and the second term represents the loss of stiffness due to the evolution of damage $\dot{D}$, during a load step (Dougill, 1980). Both terms are represented graphically in Figure 4.2.

Now, consider the simultaneous development of residual strains. In order to solve boundary value problems, the present model needs to be expressed in terms of the rate of <u>total</u> strain $\dot{\epsilon}_{ij}$. From the definition of deviatoric strain, we have:

$$\dot{\epsilon}_{ij} = \dot{E}_{ij} + \delta_{ij}\,\dot{\epsilon}_V \tag{4.10}$$

The strain rate decomposition between elastic and permanent (or residual) strain components yields:

$$\dot{E}_{ij} = \dot{E}^{el}_{ij} + \dot{E}^{rd}_{ij}, \tag{4.11}$$

where the residual strain rates are assumed to develop proportionally to an equivalent deviatoric strain rate $\dot{e}^{rd}$, that is:

$$\dot{E}^{rd}_{ij} = \frac{1}{s}\,S_{ij}\,\dot{e}^{rd} \tag{4.12}$$

where s is the uniaxial equivalent stress:

$$s = \frac{3}{2}\,S_{ij}\,S_{ij}. \tag{4.13}$$

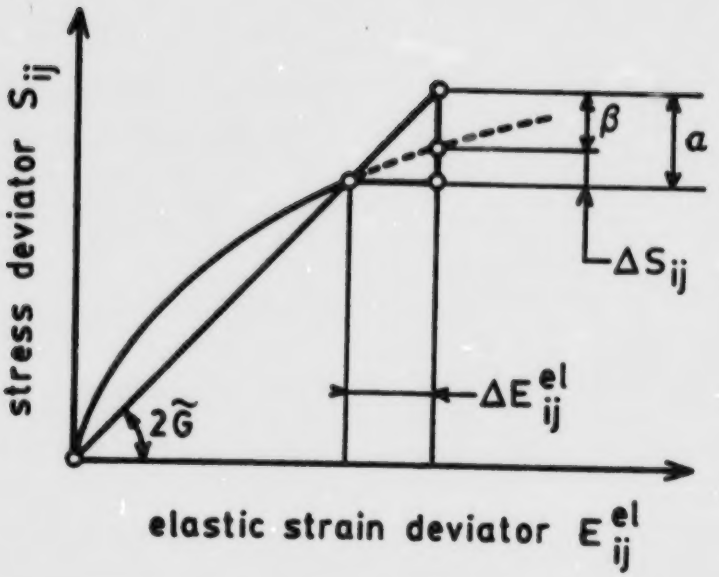

$$\Delta S_{ij} = \underbrace{2\tilde{G}\Delta E^{el}_{ij}}_{a} - \underbrace{S_{ij}\frac{\Delta D}{1-D}}_{\beta}$$

Figure 4.2. Illustration of Eq. (4.9) in a Stress-Strain Diagram

The definition of $\dot{e}^{rd}$ as a function of stress, strain, stress rate and strain rate is an essential part of the problem formulation. Together with the damage evolution function $\dot{D}$, the residual strain evolution function $\dot{e}^{rd}$ governs the spreading of damage through the material (Eq. (4.2)).

The full damage model is consequently characterized by the following equation, obtained by combining Eqs. (4.9), (4.11), and (4.12):

$$\dot{S}_{ij} = 2\tilde{G}\dot{E}^{el}_{ij} - \frac{\dot{D}}{1-D} S_{ij} - \frac{2\tilde{G}}{s} \dot{e}^{rd} S_{ij} \qquad (4.14)$$

The stress increment is consequently obtained as the sum of three terms: an elastic increment, a decrement due to the increase in damage and a final decrement due to the accumulation of permanent strain upon unloading.

The constitutive equations corresponding to (4.14) can be found by adding the hydrostatic stress component in accordance with (4.4):

$$\dot{\sigma}_{ij} = \tilde{H}_{ijkl} \dot{\varepsilon}_{kl} - \left(\frac{\dot{D}}{1-D} + \frac{2\tilde{G}}{s} \dot{e}\right) \dot{S}_{ij} \qquad (4.15)$$

where $\tilde{H}_{ijkl}$ are proportionality factors, similar to the ones in Eq. (4.3), but determined on the basis of the moduli K and $\tilde{G}$, where $\tilde{G}$ is given by Eq. (4.8). Combining equations (4.8) and (4.15) yields:

$$\tilde{H}_{ijkl} \dot{\varepsilon}_{kl} = 2\tilde{G}\dot{E}_{ij} + K \dot{\varepsilon}^{v} \delta_{ij} \qquad (4.16)$$

It should be noted that the equivalent total strains e and strain rates $\dot{e}$ are to be determined as follows:

$$\dot{e} = \frac{1}{s} S_{ij} \dot{E}_{ij}, \tag{4.17}$$

and

$$e = \int_{history} \dot{e} \, dt. \tag{4.18}$$

Recapitulating the findings of the present section, it is shown that a constitutive model of ice based on progressive damage of shear response in accordance with the evolution law $\dot{D}$ specified by (4.1), and on the simultaneous development of residual strains specified by (4.2), is governed by the differential equations (4.14), or (4.15). The integration of these equations for a given problem forms the object of the finite element analysis described in the next section.

4.3 Finite Element Implementation

The finite element program ABAQUS (Hibbit et al, 1985), provides the capability to define an arbitrary constitutive model and to link it to the incremental solution for kinematic variables. This capability is used as follows:

First, any material constants that are needed in the model are entered using a material data block. Since these models require the storage of solution dependent state variables (D, ε_V, $\dot{\varepsilon}_V$, e, $\dot{e}$, ...) at each material point, a second block is used to allocate storage for these variables. Subsequently, the user subroutine UMAT describing the appropriate constitutive relationships must be coded. As entry points, the user can avail himself of the state variables at the start of the current increment, together with the strain increments and the time increment itself. UMAT serves a double purpose:

a) to update the stresses and the solution dependent state variables to their new values at the end of the increment (damage, energy densities, equivalent strain, ...); and

b) to define the material Jacobian matrix for the constitutive model, a typical element of which is given by:

$$J_{ijkl} = \frac{\Delta\sigma_{ij}}{\Delta\epsilon_{kl}} \tag{4.19}$$

where $\Delta\sigma_{ij}$ and $\Delta\epsilon_{kl}$ are finite stress and strain perturbations, respectively, during an increment of time. Each term in the Jacobian can be interpreted as the average slope in a stress/strain diagram, as indicated in Figure 4.3.

In general, the evaluation of the Jacobian at a material point, requires the storage and integration of all the independent state variables (D, e^{rd}, e, ϵ_v, ...). The Jacobian is calculated at each integration point of every finite element, and is used in conjunction with the element interpolation functions to evaluate the current structural stiffness and the resulting nodal displacements.

Fourth order tensors are not particularly practical; their notation is hard to follow. That is why the vertical notation (engineering notation) for stress and strain is introduced for implementation in finite element codes. In this notation, six independent components are used:

$$\sigma^t = (\sigma_{xx}\ \sigma_{yy}\ \sigma_{zz}\ \sigma_{xy}\ \sigma_{xz}\ \sigma_{yz}) \tag{4.20}$$

$$\epsilon^t = (\epsilon_{xx}\ \epsilon_{yy}\ \epsilon_{zz}\ \gamma_{xy}\ \gamma_{xz}\ \gamma_{yz}) \tag{4.21}$$

with $\gamma_{xy} = 2\,\epsilon_{xy}$, $\gamma_{xz} = 2\,\epsilon_{xz}$, $\gamma_{yz} = 2\,\epsilon_{yz}$, the factor 2 being used in order to obtain energy conjugation. Using this notation, the Jacobian is a simple six by six matrix.

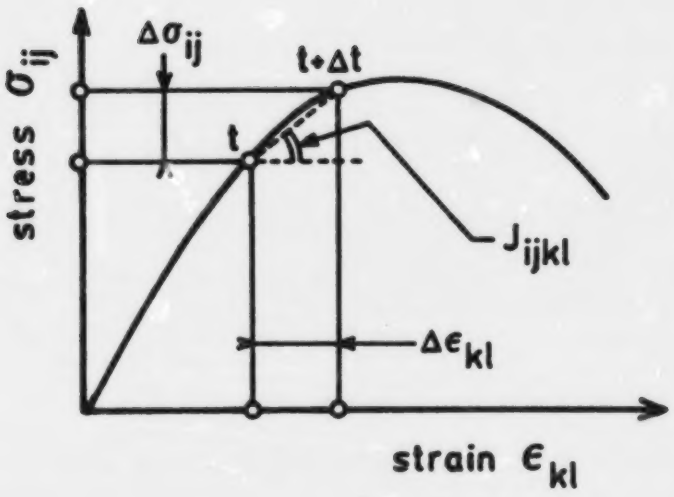

Figure 4.3. Illustration of a term J_{ijkl} in a Material Jacobian Matrix

The fundamental Eq. (4.15) governing progressive damage and residual strain development is integrated in time using a forward Euler method: if h(t) is some function, and $\dot{h}(t)$ is its time derivative at the beginning t of an increment Δt, then the integration of the function at the end of the increment $(t + \Delta t)$ is simply:

$$h(t + \Delta t) = h(t) + \dot{h}(t)\, \Delta t \tag{4.22}$$

This simple forward time integration is not difficult to implement, but, being an explicit method, it has the disadvantage of being conditionally stable. Eq. (4.15) becomes:

$$\Delta\sigma_{ij} = \tilde{J}_{ijkl}(t)\, \Delta\varepsilon_{kl} - \left\{\frac{\dot{D}(t)}{1-D(t)} + \frac{2\tilde{G}(t)}{s(t)}\, \dot{e}^{rd}(t)\right\} S_{ij}(t)\Delta t \tag{4.23}$$

and the Jacobian

$$\frac{\Delta\sigma_{ij}}{\Delta\varepsilon_{kl}} = \tilde{H}_{ijkl}(t) \tag{4.24}$$

can be interpreted as the current elasticity matrix. Equations (4.20) and (4.21) can be written in engineering notation as:

$$\begin{array}{cccccc}
K+4\tilde{G}/3 & K-2\tilde{G}/3 & K-2\tilde{G}/3 & 0 & 0 & 0 \\
 & K+4\tilde{G}/3 & K-2\tilde{G}/3 & 0 & 0 & 0 \\
 & & K+4\tilde{G}/3 & 0 & 0 & 0 \\
 & & & \tilde{G} & 0 & 0 \\
 & & & & \tilde{G} & 0 \\
\text{symmetrical} & & & & & \tilde{G}
\end{array}$$

where $\bar{G}$ and K are the current shear and bulk modulus (Zienkiewicz, 1977).

Once the Jacobian matrix (4.25) is evaluated, the stress at the end of the increment is updated using (4.23):

$$\sigma_{ij}(t+\Delta t) = \sigma_{ij}(t) + \Delta\sigma_{ij} \tag{4.26}$$

which takes into account the stress reduction due to the increase of damage $\dot{D}(t)\Delta t$ and residual strain $\dot{e}^{rd}(t)\,\Delta t$.

In addition, other state variables must be updated at the end of the increment. In particular, the conjugate shear strain 'e', defined in Eq. (4.18) as comprising an elastic component and a residual component, becomes:

$$e(t+\Delta t) = e(t) + \Delta e, \tag{4.27}$$

where, using (4.12):

$$\begin{aligned}
\Delta e &= \int_{\text{increment}} \frac{S_{ij}}{s}\, dE_{ij} \\
&= \int \frac{S_{ij}}{s}\, dE^{el}_{ij} + \int \frac{S_{ij}}{s}\, dE^{rd}_{ij} \\
&= \int \frac{S_{ij}}{s}\, dE^{el}_{ij} + \int \frac{S_{ij}S_{ij}}{s^2}\, de^{rd} \\
&= \Delta e^{el} + \frac{2}{3}\,\Delta e^{rd}.
\end{aligned} \tag{4.28}$$

In (4.28), the following definition of equivalent elastic strain was used:

$$\Delta e^{el} = \int_{increment} \frac{S_{ij}}{s} \, dE^{el}_{ij} \tag{4.29}$$

Since Eq. (4.9) can also be written as:

$$dE^{el}_{ij} = \frac{1}{2\tilde{G}} \, dS_{ij} - \frac{S_{ij}}{2\tilde{G}^2} \, d\tilde{G}, \tag{4.30}$$

The equivalent elastic strain increment (4.29) is the following function of stress and current stiffness:

$$\begin{aligned} \Delta e^{el} &= \int \frac{S_{ij}}{2\tilde{G}s} \, dS_{ij} - \int \frac{S_{ij}S_{ij}}{2\tilde{G}^2 s} \, d\tilde{G} \\ &= \int \frac{1}{3\tilde{G}} \, ds - \int \frac{s}{3\tilde{G}^2} \, d\tilde{G} \\ &= \int d\left(\frac{s}{3\tilde{G}}\right) = \frac{s(t+\Delta t)}{3\tilde{G}(t+\Delta t)} - \frac{s(t)}{3\tilde{G}(t)} \end{aligned} \tag{4.31}$$

In view of (4.13), the following integration rule for the equivalent shear strain is obtained:

$$\Delta e = \frac{s(t+\Delta t)}{3\tilde{G}(t+\Delta t)} - \frac{s(t)}{3\tilde{G}(t)} + \frac{2}{3} \Delta e^{rd} \tag{4.32}$$

The present integration scheme was coded in the ABAQUS user subroutine UMAT for a general 3-D coordinate system. Branch-off points for the uniaxial, plane stress, plane strain and axisymmetric cases are provided.

4.4 Energy Dissipation in the Damage Model

During the progressive degradation of elastic properties, and the development of permanent residual strains, it is of interest to study how the work done by external forces is converted into strain energy and dissipated through damage accumulation and permanent straining. In this context, the term dissipation has to be viewed as an energy sink, accompanied by irreversible processes. Permanent residual strains may be linked to thermal dissipation, however, damage refers to transformation of elastic strain energy into surface breakup energy, which does not imply any heat transformation.

Consider the following decomposition:

$$\dot{W}_E = \dot{W}_K^{el} + \dot{W}_S \tag{4.33}$$

where $\dot{W}_E$ is the power of the applied external forces, $\dot{W}_K^{el}$ is the rate of volumetric strain energy, and $\dot{W}_S$ is the rate of shear strain energy and dissipation (also called distortion energy). For implementation in the constitutive model for damage in ABAQUS, we seek to express the behaviour of a material point in incremental form as follows:

$$\Delta w_S = \Delta w_S^{el} + \Delta w_D + \Delta w_R$$

where
- Δw_S is the variation of the total distortion energy density during one increment;
- Δw_S^{el} is the variation of elastic shear strain energy density;
- Δw_D is the transformation of elastic strain energy density through the damage process; and
- Δw_R is the dissipation due to residual strains.

Equation (4.34) is integrated by the program, over all elements, to provide an overall energy balance. Figure 4.4 shows a graphical interpretation of the previously defined energy in terms of stress/strain equivalents (s, e, e^{el}) and their variation during the time increment (t, t + Δt).

If the stress variation is assumed to be approximately linear during the increment (this is consistent with the selected Euler integration scheme), the respective energy density components can be written as:

$$\Delta w_S = \left[s(t) + \frac{\Delta s}{2} \right] \Delta e, \tag{4.35}$$

where Δe is given by Eq. (4.32):

$$\Delta w_S^{el} = \frac{s^2(t+\Delta t)}{6\tilde{G}(t+\Delta t)} - \frac{s^2(t)}{6\tilde{G}(t)}; \tag{4.36}$$

$$\Delta w_D = \int s de^{el} - \Delta w_S^{el} = \left[s(t) + \frac{\Delta s}{2} \right] \Delta e^{el} - w_S^{el}; \text{ and} \tag{4.37}$$

$$\Delta w_R = \frac{2}{3} \int s de^{rd} = \left[s(t) + \frac{\Delta s}{2} \right] \frac{2\Delta e^{rd}}{3}. \tag{4.38}$$

The volumetric strain energy density

$$w_K = \frac{\sigma_m^2}{2K}$$

is a function of time, and is derived from the current state of stress.

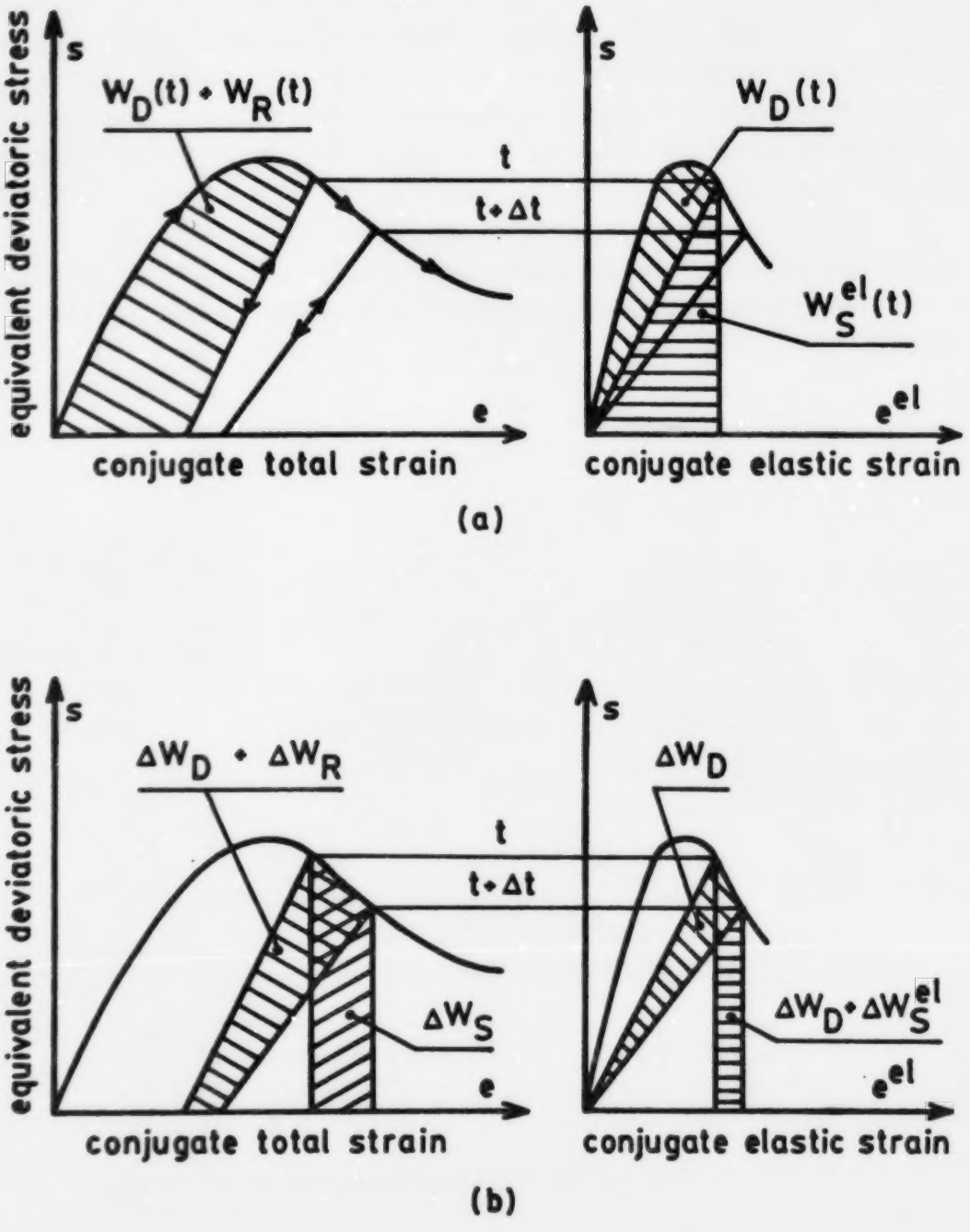

Figure 4.4. Illustration of the Different Energy Density Components (Eq. 4.34)

In the program, three entries are available for energy densities. They are selected as follows:

- strain energy;
- damage in shear; and
- dissipation through residual strains,

Each term is updated at the end of a time increment using Eqs. (4.35) to (4.38).

4.5 Preliminary Tests

There is a scarcity of data for ice in the crushing mode, compared to the large amount of data available for the ductile mode. However, in the brittle range, some data show that ice strength is weakly dependent on the strain rate (in creep tests, this dependency is more pronounced). Some simple functions were chosen to model the two evolution laws (4.1) and (4.2), and the associated shape of the stress/strain relations under uniaxial loading conditions has been studied in light of experimental data.

In order to test the the shear degradation model under uniaxial loading conditions, various meshes with different elements, cross sectional properties and material constants were studied, as shown in Figure 4.5. The initial value of Young's modulus and Poisson's ratio, are 8700 MPa and 0.33, respectively.

A constant velocity v is prescribed to one end of each mesh to simulate constant strain rate tests, while conjugate displacements and rigid body motions at opposite ends are fixed. As expected, results from the various models are identical. In Figure 4.6, a set of uniaxial stress/strain curves is compared for various evolution laws. First, the effect of constant strain rate is studied for two simple damage laws. To obtain curve (a), the damage law (4.1) is taken to be proportional to the rate of equivalent strain, $\dot{e}$, while residual strain effects are not considered:

$$\dot{D} = C_e \dot{e} \quad ; \quad \dot{e}^{rd} = 0 \qquad (4.39)$$

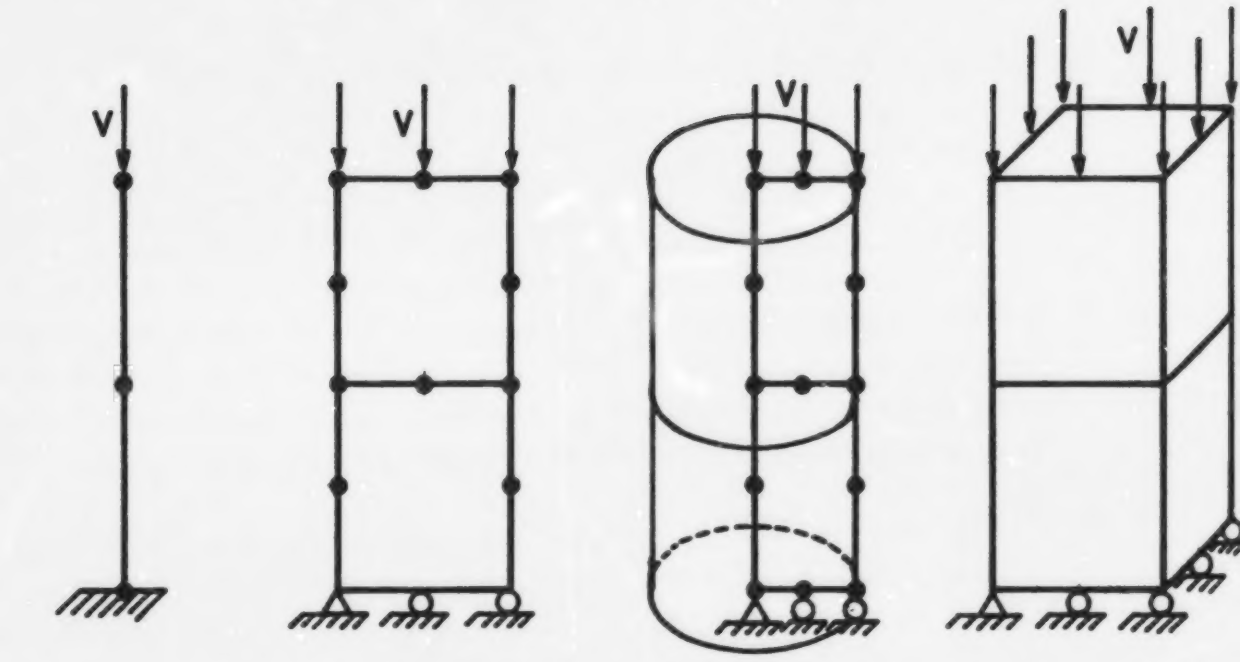

Figure 4.5. Uniaxial Load Test Models

This corresponds to a linear variation of damage between an initial state and full degradation. The proportionality constant C_e is selected to be 104, in order to impose full damage at an equivalent shear strain of 1%. The resulting uniaxial stress/strain curve is a parabola, with a shape that is not dependent on the prescribed loading rate ($2.5\ 10^{-3} s^{-1}$, $5\ 10^{-3} s^{-1}$). The response is governed solely by the elastic constants and by the value of the strain at complete failure. Comparison of these values with an analytical solution show good agreement (Appendix B).

A second damage evolution law shows direct dependency on damage, that is:

$$D = C_e\ e + D \quad ; \quad e^{rd} = 0 \tag{4.40}$$

The associated stress-strain relations are depicted by curves (b) and (c) of Figure 4.6 for prescribed loading rates of $5.10^{-3} s^{-1}$ and $2.5\ 10^{-3} s^{-1}$, respectively. The progression of damage is rate dependent.

In a subsequent set of tests, the effect of residual strains is studied by considering a simple evolution law of the form:

$$D = 104e \quad ; \quad e^{rd} = 1.04\ e \tag{4.41}$$

This corresponds to a linear variation of residual strains between initial state and full degradation:

$$e^{rd} = 0\% \quad \text{for} \quad D = 0\%$$
$$e^{rd} = 1\% \quad \text{for} \quad D = 100\% \tag{4.42}$$

The resulting stress-strain relationship is shown in (d) of Figure 4.6. The kink in the curve is due to the explicit time marching algorithm used in the integration of the damage evolution laws.

As observed for curve (a), there is no strain rate effect in the stress/strain curve (d). If a direct dependency on damage is included in the damage law according to (4.40), together with (4.41), then curve (e) shows that the resulting stress-strain relation is rate dependent. The sensitivity of the response to the residual strains in the constitutive model is reflected by increased straining, which in turn accelerates the progressive damage. This produces similar parabolic uniaxial stress/strain curves but lower strengths are obtained.

A cyclic loading test was performed, according to the history of imposed strain shown in Figure 4.7. The constitutive model is considered to be given by Eqs. (4.39) and (4.40). In Figure 4.8, the progressive damage of the shear modulus is shown during the unloading cycles, while permanent strains produce a continuous translation of the origin up to the point of full degradation.

A third evolution law of the form

$$\dot{D} = C\,\dot{e}\,(1-D) \quad ; \quad \dot{e}^{rd} = 0 \tag{4.43}$$

is chosen in order to keep a small residual strength at high strains. This alleviates some of the numerical problems linked with the complete loss of stiffness. The (1-D) term in the evolution law can be viewed as a decrease in the damage rate, when the damage asymptotically approaches 100%. The constant C is taken to be 1000, in order to obtain a realistic strength of ice in the brittle regime shown in Figure 4.9. Additional tests with (4.43) show that the ice strength is very insensitive to the strain rate.

In a last group of uniaxial tests, the concept of damage together with the development of residual strains was used to simulate creep curves corresponding to the following evolution laws are used:

$$\dot{D} = 0 \quad ; \quad \dot{e}^{rd} = C_c s^3 \quad ; \quad \text{and} \tag{4.44}$$

$$\dot{D} = 104\,\dot{e} \quad ; \quad \dot{e}^{rd} = C_c \left(\frac{s}{1-D}\right)^3, \tag{4.45}$$

where $C_c = 10^{-6}\text{MPa}^3\text{s}^{-1}$. Permanent strains are assumed to develop according to Glen's law for the creep of ice. The creep curve (a) associated with (4.44) is shown in Figure 4.10. Two different loading rates result in different creep curves (b) and (c) when (4.45) is used; both stress-strain curves exhibit strain-softening.

In another strain driven test, progressive damage is assumed to be governed by the first part of Eq. (4.43), together with a creep law corresponding to the second part of Eq. (4.44). The resulting stress-strain curves in Figure 4.11 are clearly strain-rate dependent.

Finally, a constant stress test with simultaneous degradation of creep and elastic properties, according to:

$$\begin{aligned} \dot{D} &= c_1 \dot{e}(1-D) \\ \dot{e}^{rd} &= c_2 \left(\frac{1}{1-D}\right)^3 \end{aligned} \tag{4.46}$$

is represented in Figure 4.12(b). Damage results in the development of tertiary creep, whereas a simple creep test without damage shown by curve (a), produces only secondary creep.

In conclusion, it appears that a unified model, based on progressive degradation of elastic and creep properties, could theoretically simulate the uniaxial behaviour of ice in both ductile and brittle regimes. Features, like tertiary creep and rate dependency, can be accounted for in the model. However, further experimental evidence is necessary to quantify the damage, and derive a refined functional dependence for the evolution laws, (4.1) and (4.2).

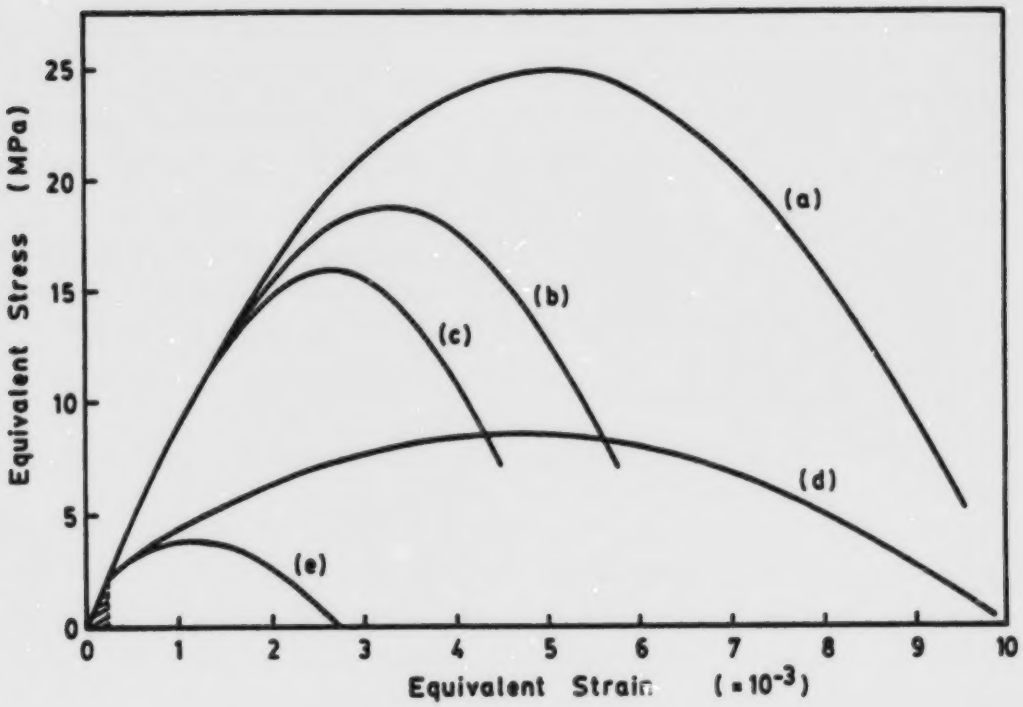

Figure 4.6. Uniaxial Stress/Strain Curves for Various Damage Laws

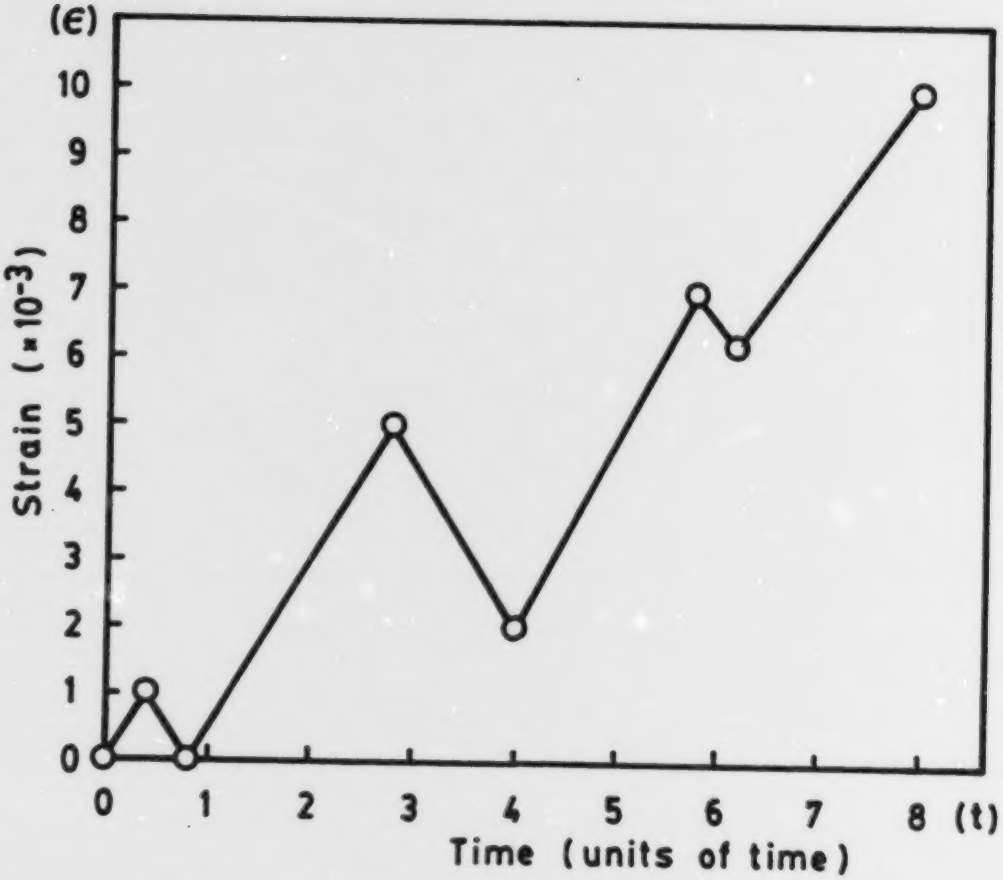

Figure 4.7. Cyclic Loading History for a Uniaxial Strain-Driven Test

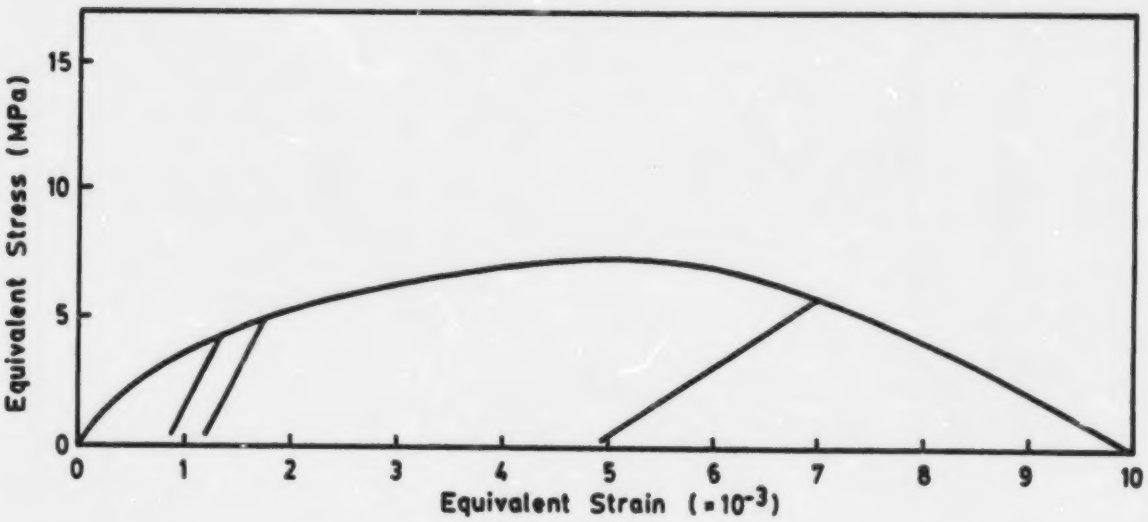

Figure 4.8. Uniaxial Stress/Strain Curve for a Damaging Material Loaded According to Fig. 4.7

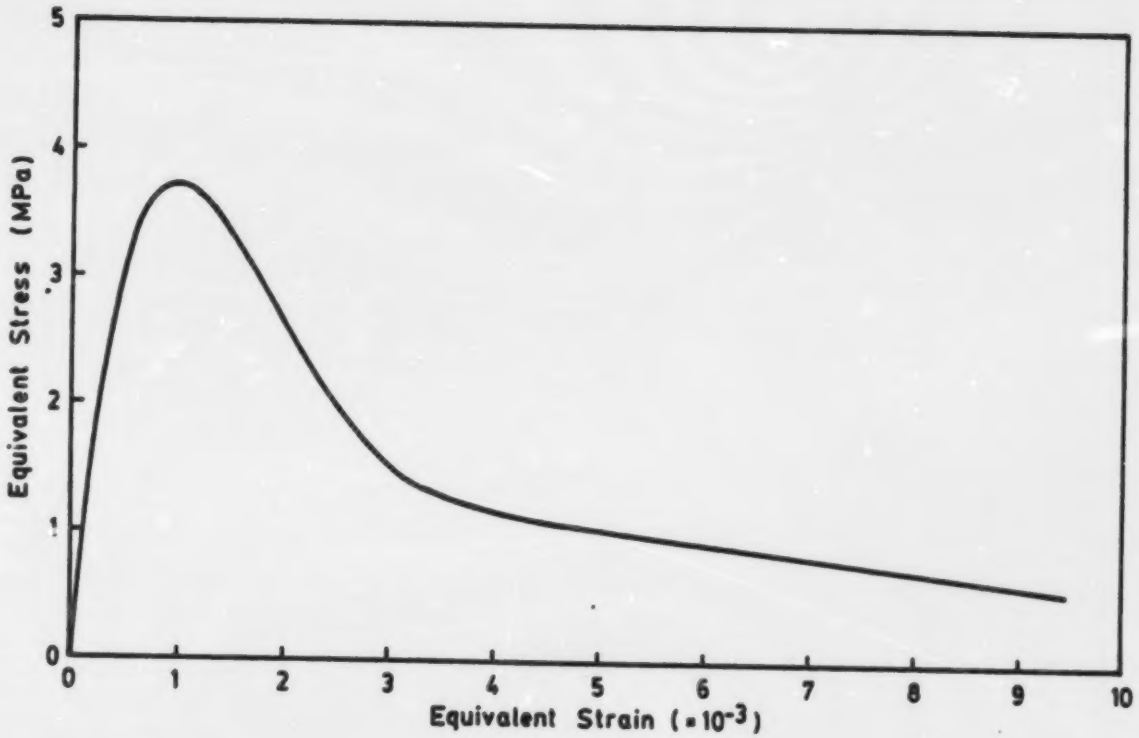

Figure 4.9. Stress-Strain Curve Corresponding to Eq. (4.43)

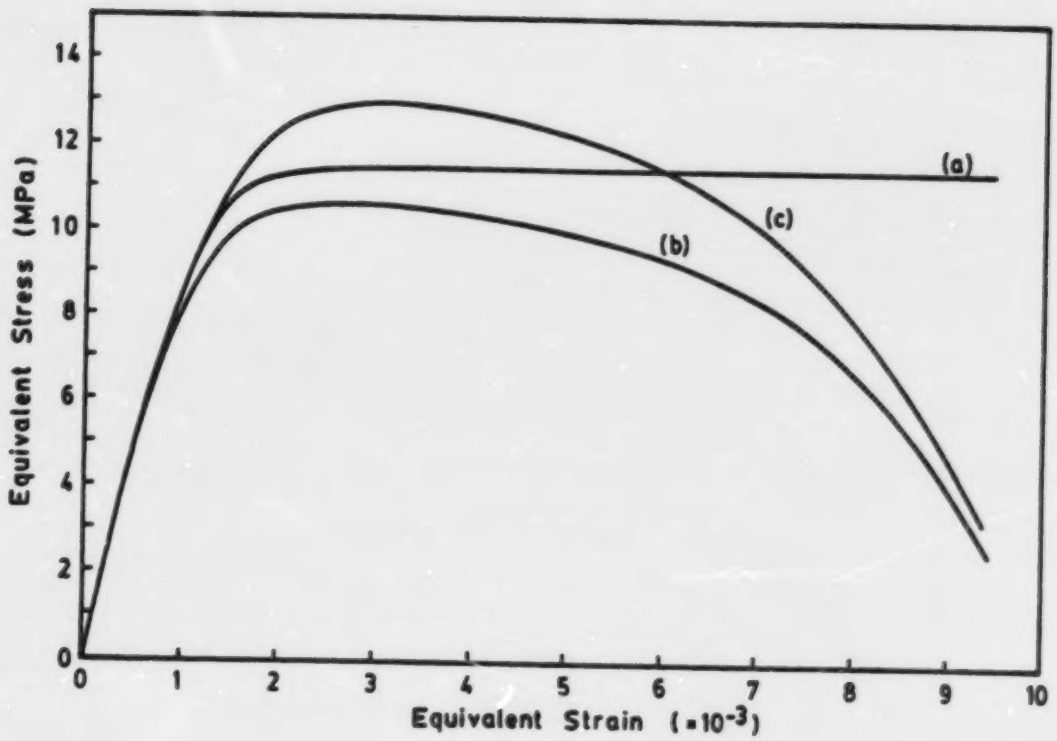

Figure 4.10. Unaxial Stress/Strain Relation for Creep Damage

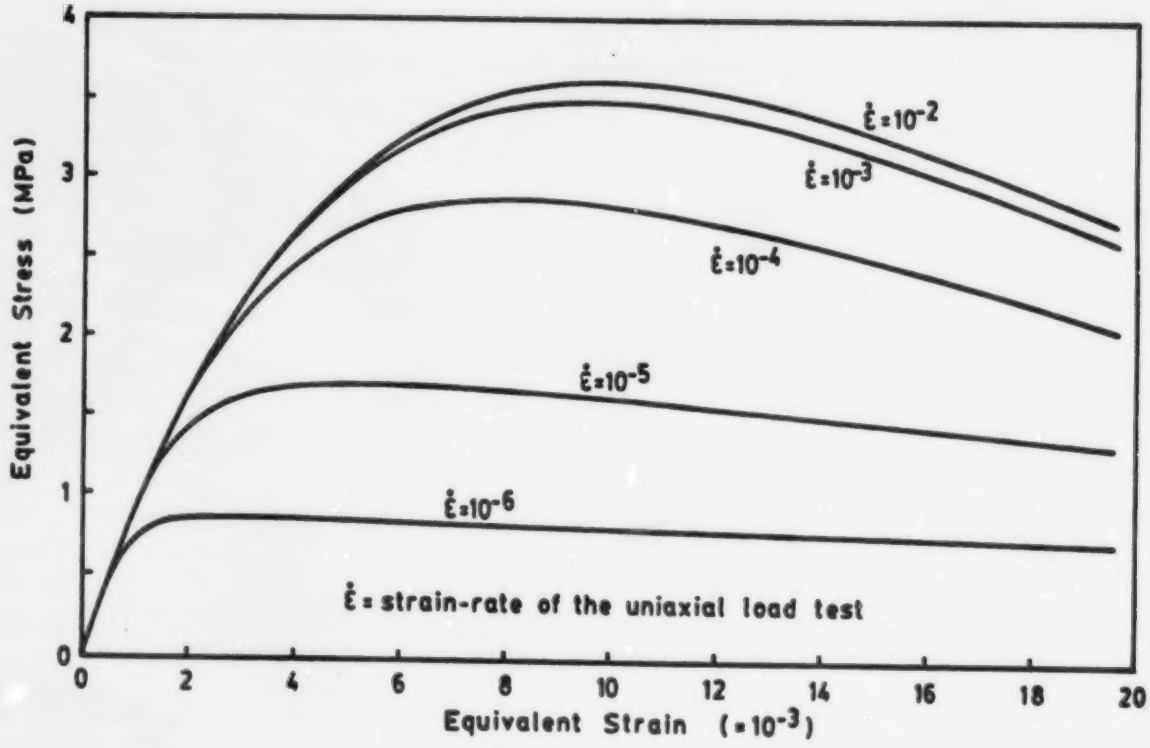

Figure 4.11. Stress/Strain Curves for Uniaxial Loading

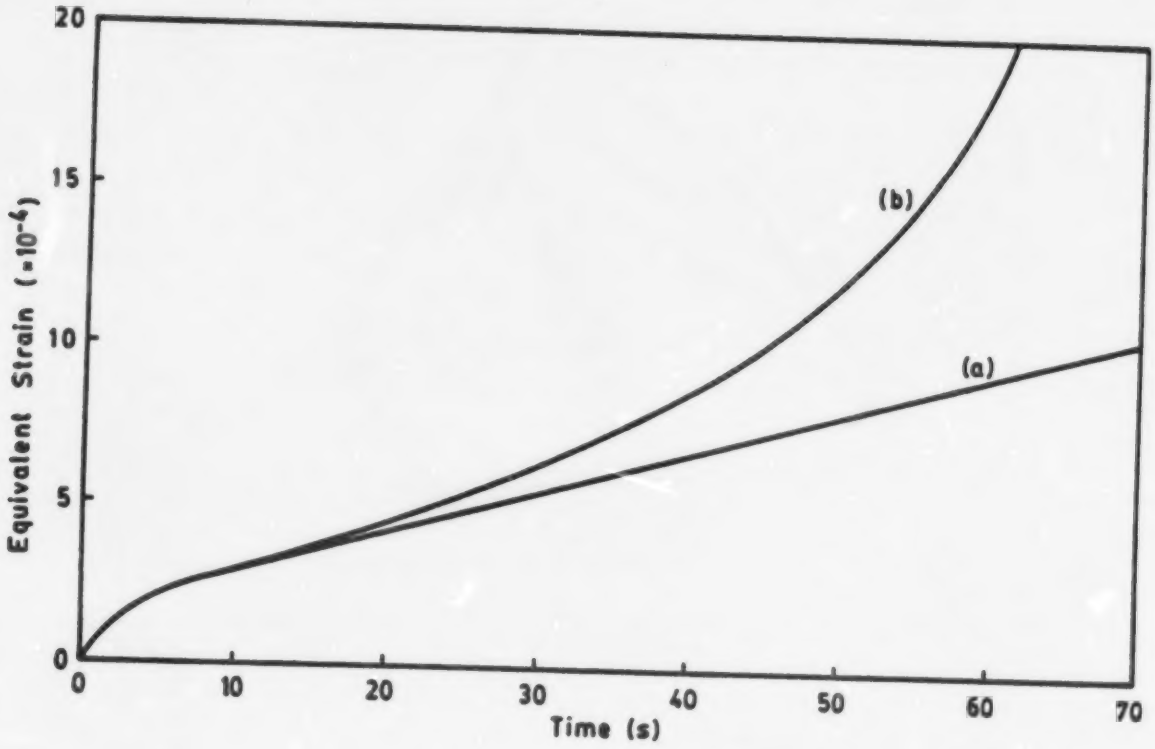

Figure 4.12. Constant Stress Test

5. MODEL FOR THE VISCOUS FLOW OF CRUSHED ICE

5.1 General

Experimental evidence, discussed in Section 3.3, indicates that intense compressive loading causes ice to pulverize into fine fragmented particles. The so called "crushed ice" behaves as a viscous powder or fluid in accordance with the differential equations (3.3). The corresponding equations in vectorial form are:

$$\frac{\partial p}{\partial x_i} - \mu \nabla^2 v_i = 0, \qquad (i = 1,2,3) \tag{5.1}$$

In Section 5.2, it is shown how the Hooke-Stokes analogy can be applied to model the flow of crushed ice in the layer that is formed at the contact zone between the indenter and ice. In subsequent sections numerical techniques are investigated, in particular those related to finite element solutions using the program ABAQUS.

5.2 The Analogy Between Hooke's and Stokes' Laws

It is helpful to begin this analysis with a consideration of the analogy between Hooke's Elasticity and Stokes' Fluid Flow Laws (Jordaan, 1986). These are:

$$\tau = G\gamma \qquad \text{(Hooke)} \tag{5.2}$$

$$\tau = \mu\dot{\gamma} \qquad \text{(Stokes)} \tag{5.3}$$

where τ = shear stress, γ and $\dot{\gamma}$ are the shear strain and shear strain rates respectively, and G and μ are the shear modulus and coefficient of viscosity, respectively. There is clearly a striking similarity between the equations, and in view of the analysis of pulverized ice using viscous methods (Kurdyumov and Kheisin, 1976), the above analogy is pursued. The basic aspects of the equations are now summarized and discussed followed by applications to ice.

Eqs. (5.2) and (5.3) above can be generalized as follows:

$$\tau_{ij} = G_{ijkl} e_{kl} \tag{5.4}$$

$$\tau_{ij} = K_{ijkl} D_{kl} \tag{5.5}$$

where τ_{ij} is the shear (viscous) stress tensor, G_{ijkl} and K_{ijkl} are the elasticity constants and viscosity coefficients, e_{kl} is the deviatoric strain tensor and D_{kl} is the rate of deformation tensor. It is worth noting that one could consider nonlinear relationships of the form:

$$\tau_{ij} = f_{ij}(D_{kl}) \tag{5.6}$$

where $f_{ij}(\cdot)$ is a nonlinear function, but for the introduction of this concept in the following, only the linear case will be considered. Eq. (5.5) is a special case of (5.6).

The equations of elasticity - as implemented in finite element codes such as ABAQUS - are based on a Lagrangian formulation. A point not always appreciated is that the rate of deformation tensor in Eq. (5.5) is based on an Eulerian formulation. This has implications for the modelling, as will be seen. Returning to the rate of deformation tensor D_{kl}, we will review briefly the theory for clarity.

The velocity gradient tensor, $\partial v_i / \partial x_j$ may be divided into its symmetric (D_{ij}) and skew-symmetric (E_{ij}) components:

$$\frac{\partial v_i}{\partial x_j} = \frac{1}{2}\left(\frac{\partial v_i}{\partial x_j} + \frac{\partial v_j}{\partial x_i}\right) + \frac{1}{2}\left(\frac{\partial v_i}{\partial x_j} - \frac{\partial v_j}{\partial x_i}\right) = D_{ij} + E_{ij} \tag{5.7}$$

The symmetric tensor D_{ij} is the material derivative of the Eulerian infinitesimal strain tensor, since

$$\frac{d\epsilon_{ij}}{dt} = \frac{1}{2}\frac{d}{dt}\left(\frac{\partial u_i}{\partial x_j} + \frac{\partial u_j}{\partial x_i}\right) = \frac{1}{2}\left(\frac{\partial v_i}{\partial x_j} + \frac{\partial v_j}{\partial x_i}\right) = D_{ij}. \tag{5.8}$$

The terms included in E_{ij} relate to rotations and do not enter into the stress-strain relations (5.5).

The problem of crushed ice is a flow problem, and should be treated as such. In continuing the development above, the classical derivation of the Navier-Stokes equations is outlined, then simplified for slow viscous flow, and finally shown how it can be applied to ice.

The degradation of ice leading to pulverization results in a material which may be regarded as incompressible (at least by comparison with the ease in which it deforms in shear). Thus,

$$\frac{\partial v_j}{\partial x_j} = 0 \quad \text{or} \quad D_{ii} = 0 \tag{5.9}$$

(summation is implied by repeated suffices).

In Cartesian coordinates, the Navier-Stokes equations are:

$$\rho\frac{dv_i}{dt} + \frac{\partial p}{\partial x_i} - F_i - \mu\nabla^2 v_i = 0, \text{ for directions } i = 1,2,3, \tag{5.10}$$

where ρ is the material density.

In (5.10), the terms represent inertia, change in pressure p, body forces with F_i = force in i direction per unit mass; lastly, the frictional resistance $\mu\nabla^2 v_i$ is derived in a very similar way to the derivation of a generalized Hooke's law, and will be briefly reviewed.

First, one can write

$$\sigma_{ij} = -p\delta_{ij} + \tau_{ij} \tag{5.11}$$

where δ is the Kronecker Delta. Now, $D_{ii} = 0$ and $-p\delta_{ij} = 1/3\ \sigma_{ii}$ for incompressible materials, and

$$\tau_{ij} = 2\mu D_{ij} \tag{5.12}$$

where μ = dynamic viscosity, and D_{ij} = deviatoric tensor. (It would be possible to include anisotropy in the analogy - referring to Eq. (5.4) - but this will not be pursued here.) Now the change in the stress in direction i, associated with viscous friction, is:

$$\frac{\partial \tau_{ij}}{\partial x_j} = \frac{\partial}{\partial x_j}\ (2\mu D_{ij}) = \mu\nabla^2 v_i\,, \tag{5.13}$$

where

$$\nabla^2 = \partial^2/\partial x_1^2 + \partial^2/\partial x_2^2 + \partial^2/\partial x_3^2$$

The terms $(\partial v_j/\partial x_i \partial x_j)$ disappear in the derivation of (5.13) because of condition (5.9).

Finally, one may write Eq. (5.10) in the familiar form for the Navier-Stokes equations:

$$\frac{\partial v_i}{\partial t} + v_j \frac{\partial v_i}{\partial x_j} + \frac{1}{\rho} \frac{\partial p}{\partial x_i} - F_i = \nu \nabla^2 v_i = 0; \quad i = 1,2,3, \tag{5.14}$$

where the first two terms are the expansion of (dv_i/dt) in the first term of (5.7) - the inertia terms - and $\nu = \mu/\rho$ is the kinematic viscosity.

If the inertia terms and the body forces can be neglected, then the equations for slow viscous flow result (alternatively steady conditions will permit the neglect of inertia terms), given in the fundamental Eq. (5.1).

The equations of elasticity can be written in the following form (Timoshenko and Goodier, 1970):

$$G\nabla^2 u_i - \frac{\partial p}{\partial x_i} \left(\frac{1.5}{1+\nu}\right) = 0 \tag{5.15}$$

where G is the shear modulus, u_i is the displacement field and ν is Poisson's ratio. It is clear that in order to obtain complete formal analogy between (5.15) and (5.1), the elastic material needs to be incompressible. Thus, ν takes on the value of 1/2 in (5.15) and the multiplier of the pressure gradient is unity. Consequently, the analogy between an elastic Lagrangian and a frictional Eulerian analysis is based on the equivalences listed in Table 5.1. The key relationship is the equivalence between the following groups of variables:

$$\left(\frac{\text{stress}}{Gu_i}\right) \leftrightarrow \left(\frac{\text{stress}}{\mu v_i}\right) \tag{5.16}$$

where u_i are the displacements and v_i are the velocities.

Table 5.1

The Analogy Between the Elastic Analysis of an Incompressible Solid and the Flow of a Viscous Fluid

Elastic Deformation		Viscous Flow	
displacement	u_i	velocity	v_i
strain	ϵ_{ij}	strain rate	$\dot{\epsilon}_{ij}$
hydrostatic pressure	$p=-1/3\ \sigma_{ii}$	pressure	p
stress	σ_{ij}	stress	σ_{ij}
shear modulus	$G\ (Nm^{-2})$	viscosity	μ (Nsm^{-2})
volumetric strain	e	0 (eq. 5.9)	
Poisson's Ratio	ν	1/2	
Lame's constant	λ	∞	
Young's modulus	E	3μ	
force	F_i	force	F_i
work done by external forces	$G u_i$	power of external forces	μv_i (eq. 5.16)

5.3 Modelling of Incompressible Elastic Behaviour

Eqs. (5.1) and (5.15) indicate that an elastic deformation analysis can be used to solve a slow viscous flow problem, provided that the elastic material is incompressible. Numerically, the modelling of incompressibility is not a trivial problem. Two methods are possible:

(a) Penalty Function Approach

Incompressible elasticity can be obtained by choosing Poisson's ratio close to, but not equal to 0.5. This method, together with reduced integration, is known as the penalty function approach (Zienkiewicz, 1977).

For a general three-dimensional problem (3 direct and 3 shear components), the elasticity matrix, expressed in terms of bulk modulus and shear modulus indicates that as Poissons ratio approaches 0.5, the solution becomes singular.

The total strain energy density w can be expressed as the sum of shear and distortional strain energies:

$$w = \text{shear strain energy} + (\alpha) \text{ volumetric strain energy.} \qquad (5.17)$$

from which is appears that incompressible behaviour can be approached by the minimization of volumetric energy, together with the additional constraint $\varepsilon_v = 0$. The factor α in (5.17) is to be interpreted as a Lagrange multiplier. With finite element discretization, this constraint is possible only if the volumetric stiffness represents a singularity, in order to avoid the trivial solution of zero displacements. This can be achieved by the use of reduced integration, that is, 2 x 2 integration with 8 node rectangular finite elements.

The penalty function technique has proven to be efficient when boundary conditions involve a low degree of constraint, or equivalently, when reduced integration induces a singularity in the structural bulk stiffness, e.g. in plane stress.

On the other hand, the technique is less adequate for plane strain conditions, where the level of constraint is much higher.

(b) Hybrid Formulation

Since the solution to an incompressible problem cannot be obtained in terms of the displacement history only, hydrostatic pressure can be treated as an additional variable without changing the displacements. The nearly incompressible case exhibits behaviour approaching this limit, in that a very small change in displacement produces extremely large changes in pressure, so that a solution based on displacements only, is too sensitive to be used numerically. This singularity is removed if the pressure is treated as an independent interpolated variable, coupled to the displacement solution through the constitutive model. Finite elements based on this mixed displacement - pressure formulation - are called hybrid incompressible elements and are available in the program ABAQUS.

5.4 Finite Element Modelling

The analysis of the flow of fragmented pulverized ice is assumed to be governed by the viscous flow Eq. (5.1). The Hooke-Stokes analogy will be applied to a linear elastic finite element analysis of the layer of crushed ice using a hybrid incompressible formulation. Table 5.1 contains a list of equivalent variables. In Chapter 6, the analogy is used to study the behaviour of ice in the vicinity of an indenter.

6. MODELLING OF ICE INDENTATION TESTS AND COMPARISONS

6.1 Progressive Damage of Ice During Indentation

In this section, a finite element model to study the progression of damage during an ice sheet indentation test is presented. Indentation tests carried out by NRC and studied by the present research group (Tomin et.al., 1985), indicate the formation of microcracks close to the indenter. An appropriate FE mesh for the analysis of the problem is shown in Figure 6.1. The coordinate axes have their origin at the indenter, with the y axis aligned perpendicular to the indenter. Dimensions and material properties are assumed to be equal to the experimental values associated with the tests quoted. The width of the indenter D is 6.35 cm; the mesh has a dimension of 3D x 2D, and a uniform ice thickness of 2.2 cm is assumed. The ice is free to move along the outer boundary. Conditions of symmetry are applied along the x axis, and the indenter moves with a uniform velocity v along the x axis.

The following damage evolution law is used:

$$\dot{D} = C_1 \dot{e} \ (1-D); \quad \dot{e}^{rd} = 0 \tag{6.1}$$

This corresponds to Eq. (4.43), which was shown to lead to satisfactory results under uniaxial compression. No residual strains are considered in this model, since all points experience a monotonically increasing strain. Eight-node isoparametric elements and plane stress conditions are used for the FE analysis.

The elastic constants for undamaged S2 freshwater ice consist of a Young's modulus of 8700 MPa and a Poisson's ratio of 0.33. The value $C_1 = 1000$ is chosen in the damage evolution law (6.1) in order to match the uniaxial strength of ice in the brittle regime (see Figure 4.9).

Generally speaking, the amount of output from finite element programs increases enormously for non-linear analyses, when the status of certain state variables is of interest throughout the full loading history. ABAQUS allows output to be written on a user file (database) in a format such that it can be selectively retrieved and post-processed by user-written programs.

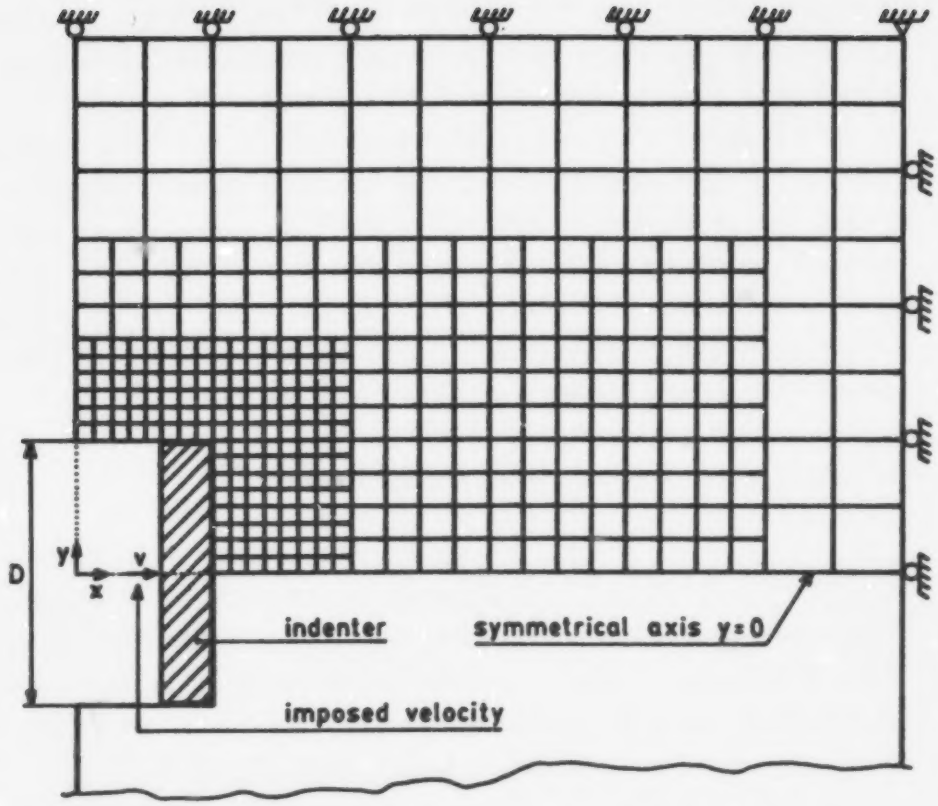

Figure 6.1. Plane Stress Finite Element Mesh of Ice Loaded by an Indenter

In Figures 6.2(a), (b), and (c), the spreading of damage is depicted as a function of time for an indentation velocity of 10^{-4} m/s. (The response is shown to be rather insensitive to velocity, which corresponds to the experimental finding that in the brittle regime the indentation load is only weakly rate-dependent). The contours of 10, 30 and 80% damage show that damage originates in the regions where shear stress is maximum, i.e. under the corners of the indenter. Subsequently, damage extends towards the axis of symmetry. Although this area is highly confined, the state of stress is, originally, almost purely hydrostatic, with very little shearing stress present in the plane. The spreading of damage is in good agreement with both experimental and analytical results (Fig. 2.3 and Fig. 6.3, respectively) of the NRC tests (Tomin et.al., 1985).

Figure 6.2 also shows that final damage occurs very rapidly. For most of the material, damage starts extremely slowly and obtains a value of 10% over a considerably long time interval. However, a small increase in load beyond this point results in an almost instantaneous collapse. This effect is illustrated in Figure 6.4 for a typical material point. In reality, damage remains confined to the immediate vicinity of the indenter and does not spread extensively into the ice sheet. The reason for this is to be found in two limitations of the present model:

(a) there is no provision for local failure, once total damage has occurred at a certain point. Ideally, the ice sheet should be remeshed locally in order to account for the transformation of continuous solid ice into a pulverized powder. When this crushed ice is squeezed out (i.e. the corresponding finite elements are destroyed), the indenter penetrates the ice sheet without causing additional damage.

(b) as compressive microcrack failure gradually weakens the zone of high shear stresses, it promotes the origination and propagation of radial cracks. Contrary to the stable development of damage in compression, the radial cracks fail due to tensile stress, and propagate in an unstable manner. Radial cracks are observed to occur frequently in combination with crushing (Timco, 1986). A separate analysis of the growth of radial cracks was carried out in the framework of the aforementioned study for Department of Public Works (Tomin et.al., 1985). However, the present analysis of progressive damage does not include this effect.

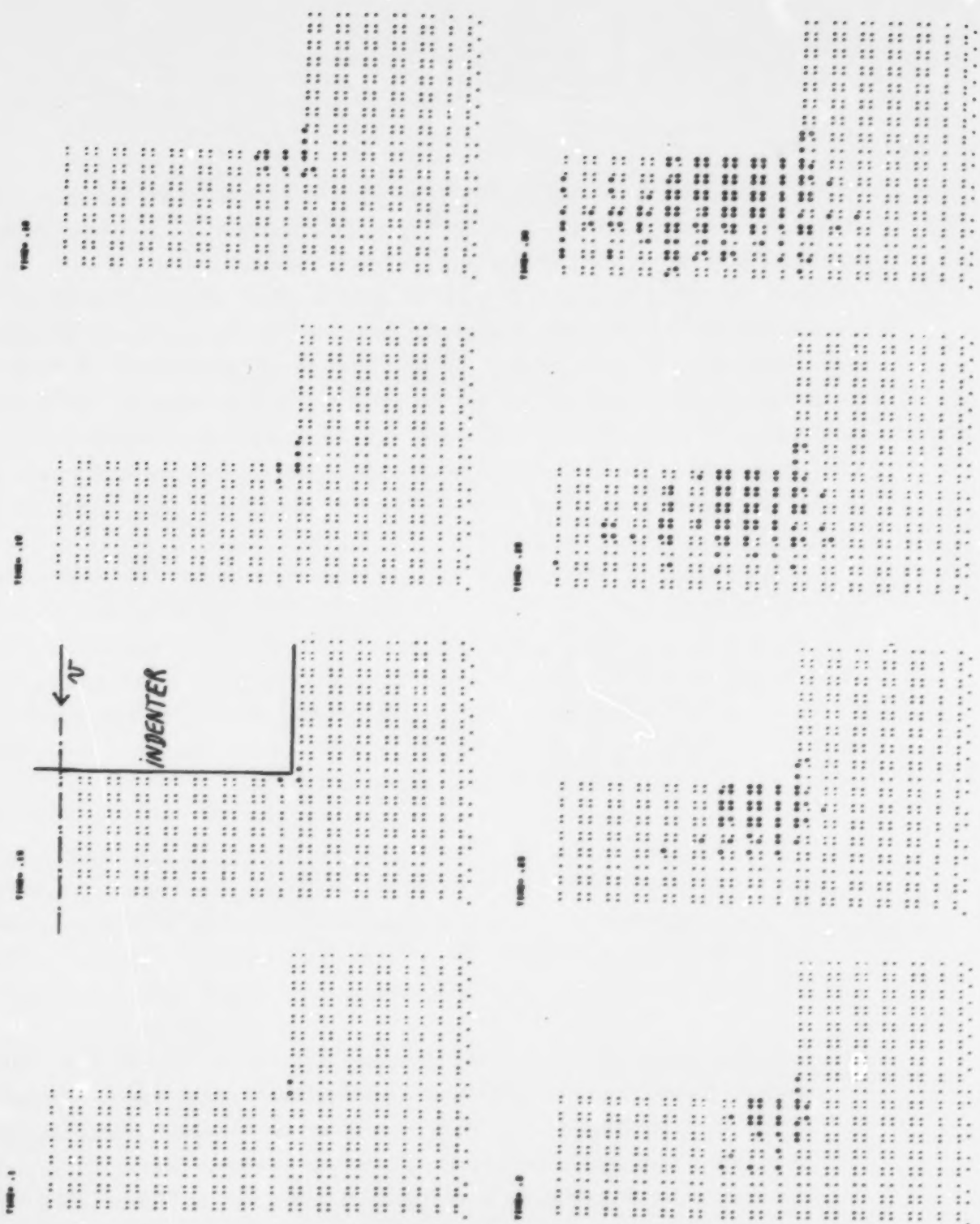

Figure 6.2(a). Spreading of Damage as a Function of Time
(asterisks denote points where D > 10%)

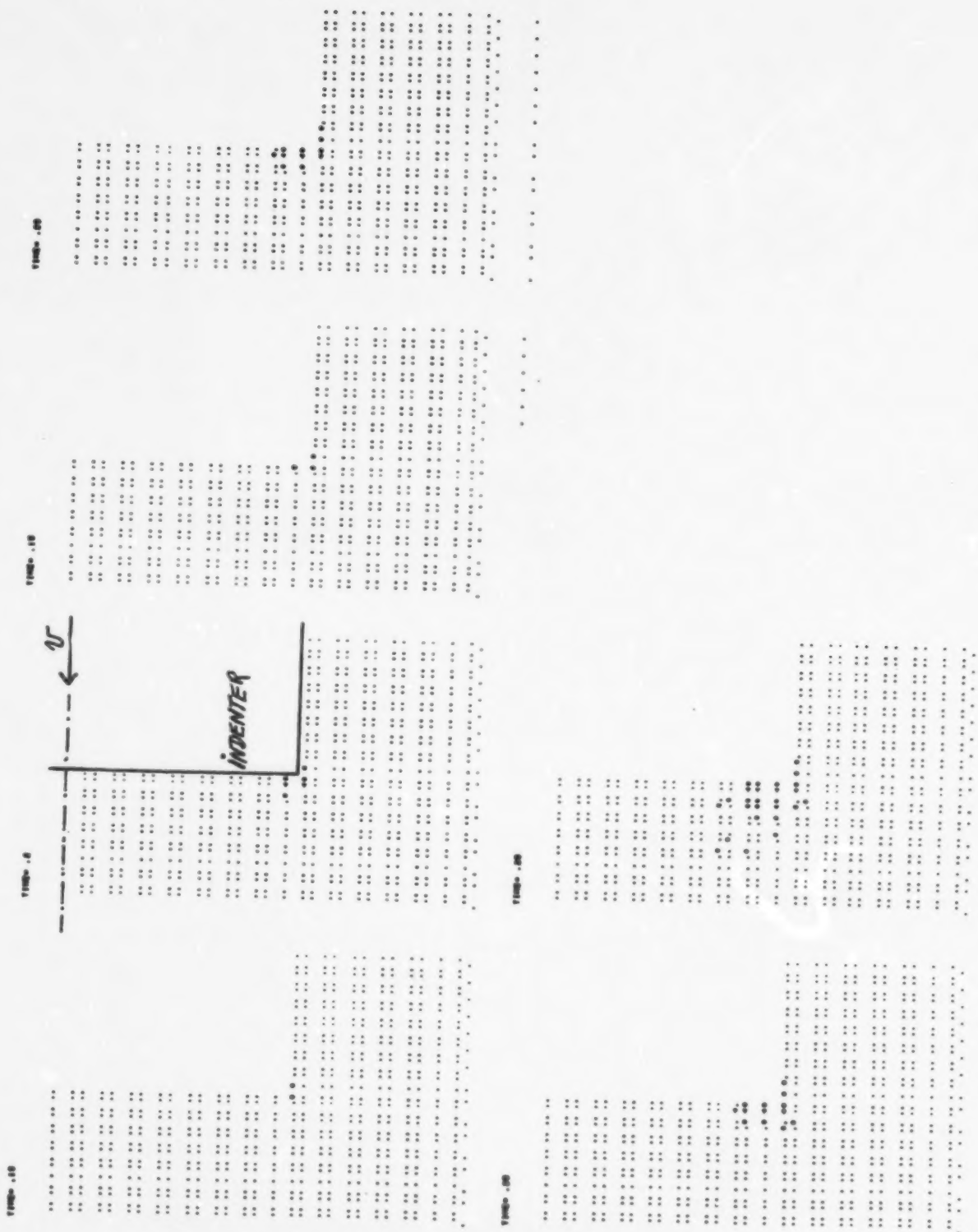

Figure 6.2 (b). Spreading of Damage as a Function of Time
(asterisks denote points where D > 30%)

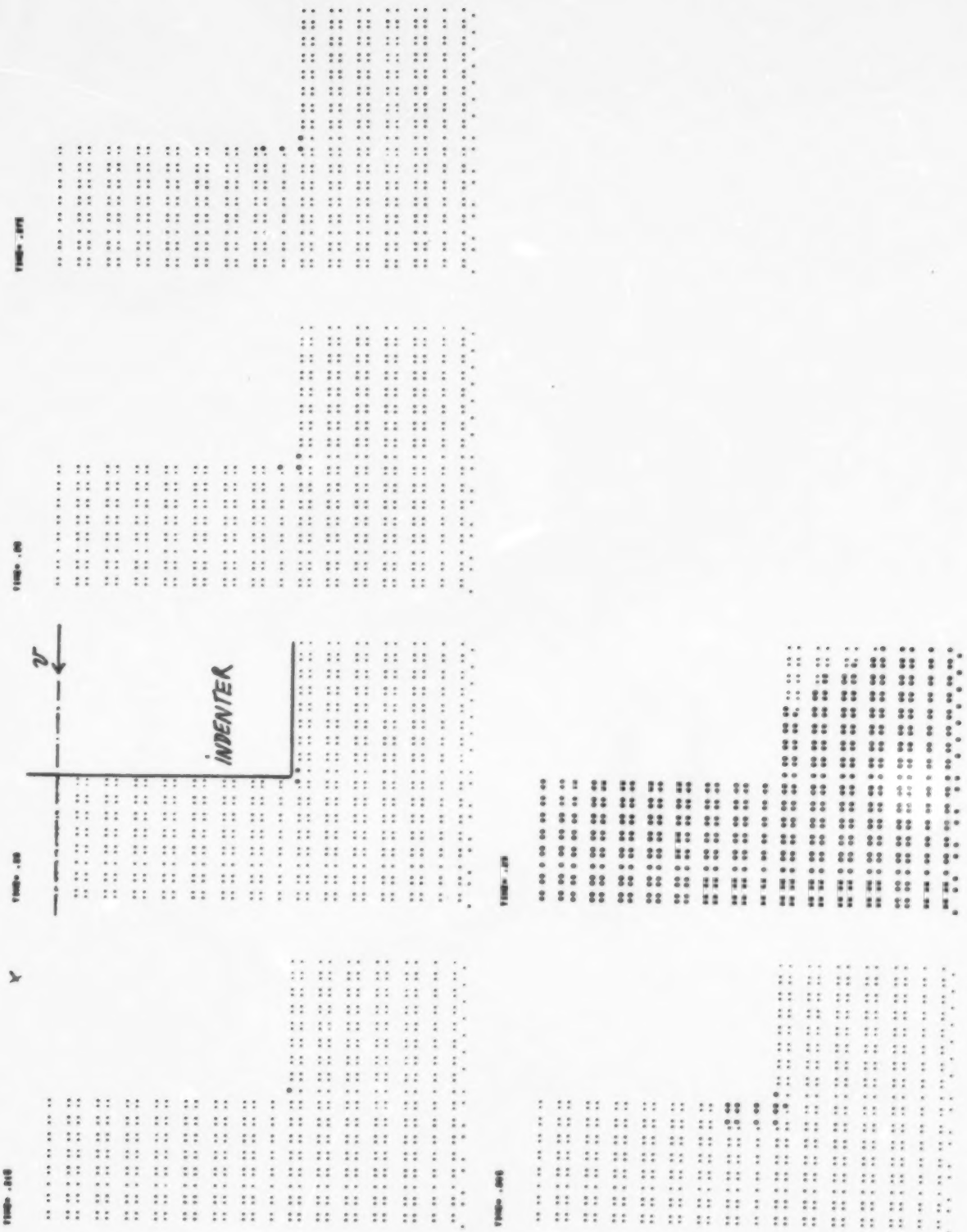

Figure 6.2 (c). **Spreading of Damage as a Function of Time (asterisks denote points where D > 80%)**

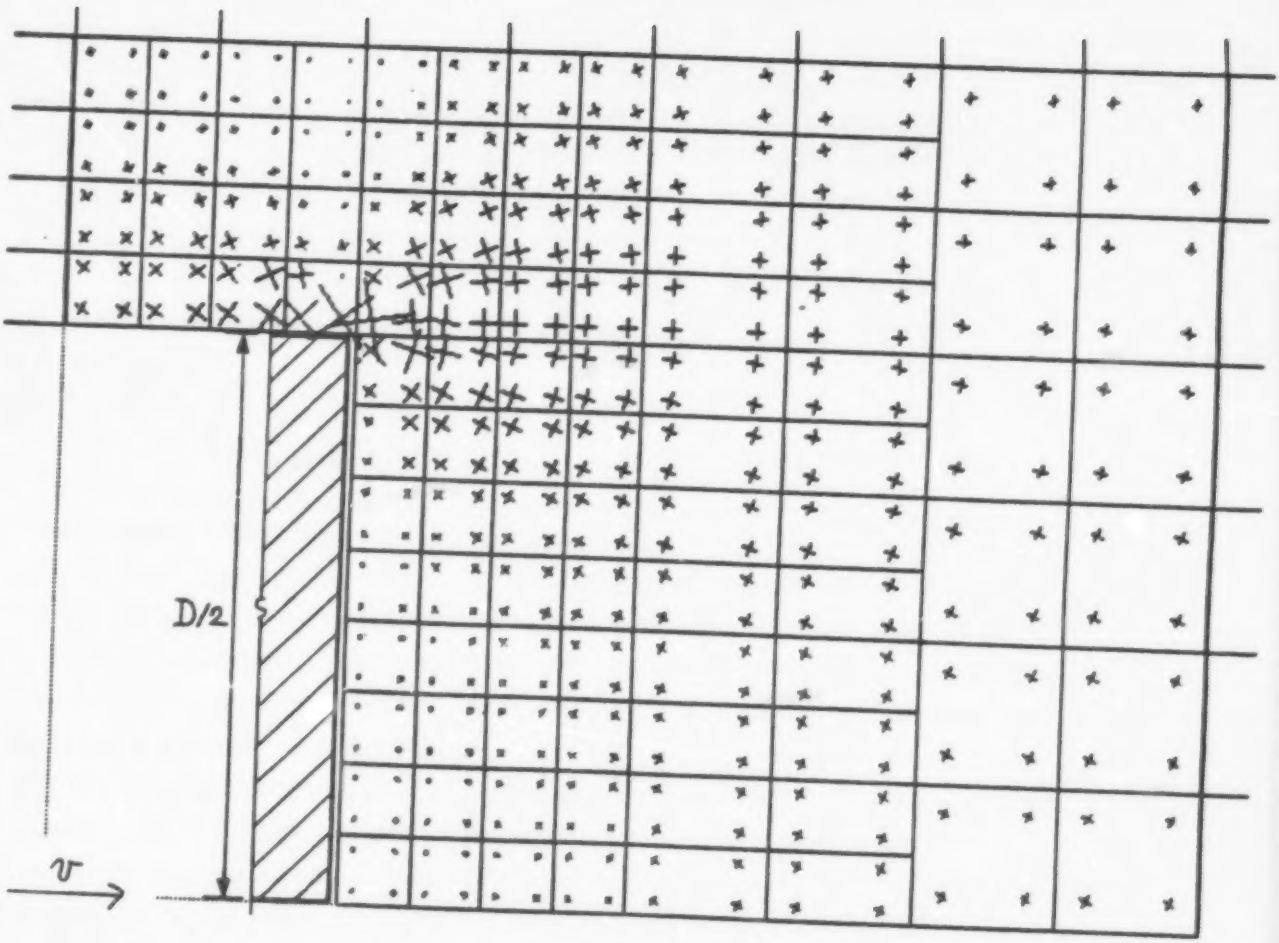

Figure 6.3. Maximum Shear Stress Distribution Under the Indenter
(Tomin et al, 1985)

The abrupt spreading of damage indicates the necessity to model the post-failure behaviour of the crushed ice zone. In the light of Fig. 6.4, the following simplified model for ice-indenter interaction is justified, that is, the ice is subdivided in just two zones:

1. undamaged ice (D = 0), with initial elastic properties; and
2. completely damaged ice (D = 100%).

Damage is consequently assumed to occur instantaneously instead of progressively. It remains connected to an excessive reduction of shearing stiffness due to brittle microcracking. The behaviour of crushed ice is analyzed in more detail in the following section.

6.2 Viscous Flow of Crushed Ice During Indentation

Kheisin et al. (1975) conducted a series of tests in which they dropped balls onto ice sheets. By the measurement of accelerations and restitution coefficients, they related the specific break-up energy to the nominal contact pressure acting on the indenter. The crushed layer of ice under the indenter was subsequently modelled in order to study the squeezing of ice between two moving surfaces; one the indenter, the other the ice break-up surface. The main goal of their experiments and their analysis was to measure the break-up energy density of ice, that is the energy required to fracture a unit volume of ice into small fragments, and to relate it to the hypothesized analytical model. Their experiments and mathematical model suggest that there is a linear relation between the average pressure p and the break-up energy density e_v, namely:

$$e_v = 0.3\,p \tag{6.2}$$

In their tests, the contact pressure reached values of 10 to 20 MPa, which exceed the uniaxial crushing strength of ice by several orders of magnitude. This can be associated with the high degree of confinement of the crushed layer. Observations made during typical indentation tests indicated that the contact pressure during plane strain conditions was typically 3 times higher than plane stress conditions.

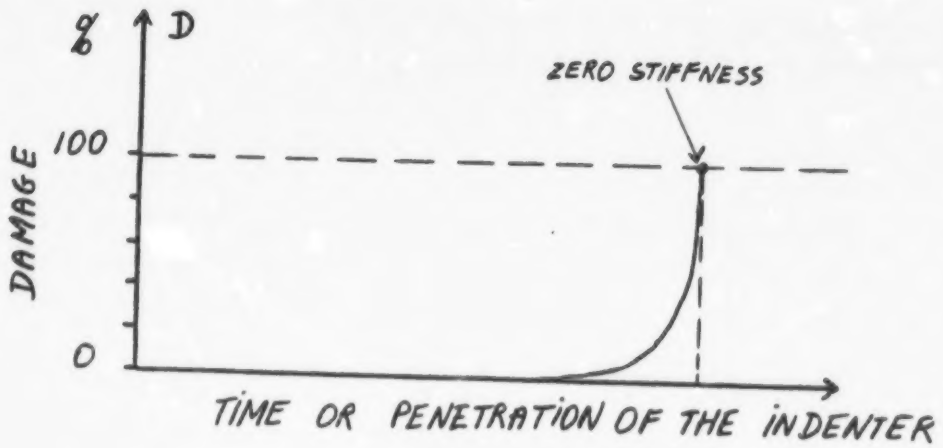

Figure 6.4. Damage Evolution at a Certain Point Under the Indenter

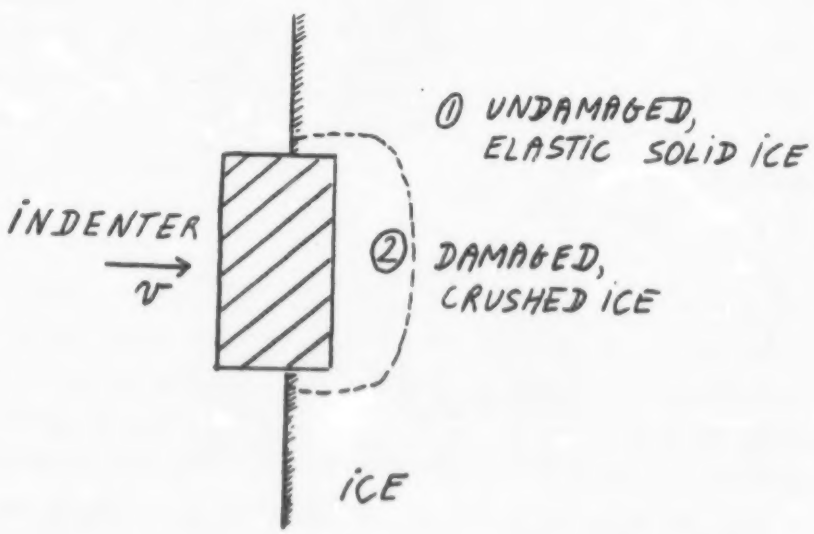

Figure 6.5. Simplified Model for Ice Indentation

Three major problems need to be addressed when developing a numerical model for the behaviour of crushed ice, during sheet indentation tests with a flat indenter. They are related to the following topics:

a. The shape of the crushed ice layer. A simple model based on an elastic stress distribution (Boussinesq-Flamant) (see, for example, Timoshenko and Goodier, 1970), together with a distribution of shear microcracks at grain boundaries would indicate that the break-up surface coincides with lines of constant shear stress, or circles passing through the corners of the indenter and aligned along the axis of symmetry (Figure 6.6(a)).

However, inspection of the photograph of a block of indented ice shows the microcracked region in front of the indenter of width D, Figure 6.6b (G. Timco, 1986). It is a zone of high microcrack density extending a distance of approximately D/4 on each side of the indenter, and extending a distance of D/2 ahead of the indenter, as shown on Figure 6-6c.

b. The viscosity of crushed ice. Kheisin et al. (1975) suggest values ranging from 10^{-2} to 10^{-1} MPa/s. In view of Eq. (5.16), it is clear that there is a linear relationship between the value of G employed in the elastic analogy and the viscosity μ of the crushed material. Therefore, the alteration of a value of the viscosity corresponds to a linear scaling of the associated stresses, pressures or velocities according to (5.16). This allows a convenient investigation of a wide range of values.

c. The choice of boundary conditions. It is important to picture the motion of the indenter through the ice sheet. The layer of crushed ice is adjacent to the indenter, and "travels" together with it. If an observer was sitting on top of the penetrating body, he would observe a stationary layer between the indenter and solid ice (Figure 6.7). As far as he can tell, the layer is fixed and there is a flow of crushed ice particles through this "channel": an inflow at the boundary of the solid and the crushed ice and an outflow on the sides, top and bottom of the transport channel. The exact apportionment of the outflow (comparable to the

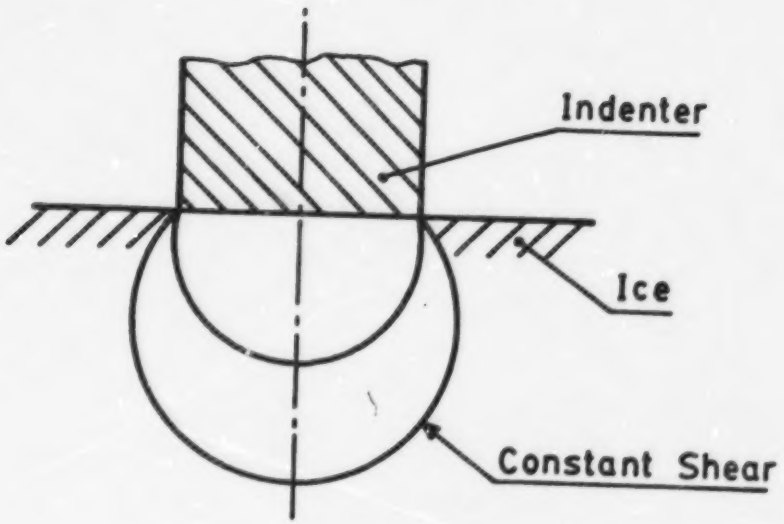

Figure 6.6 (a). Contours of Constant Shear Stress From Boussinesq-Flamant Analytical Solution

Figure 6.6 (b). Shape of Crushed Layer Under the Indenter (G. Timco, 1986)

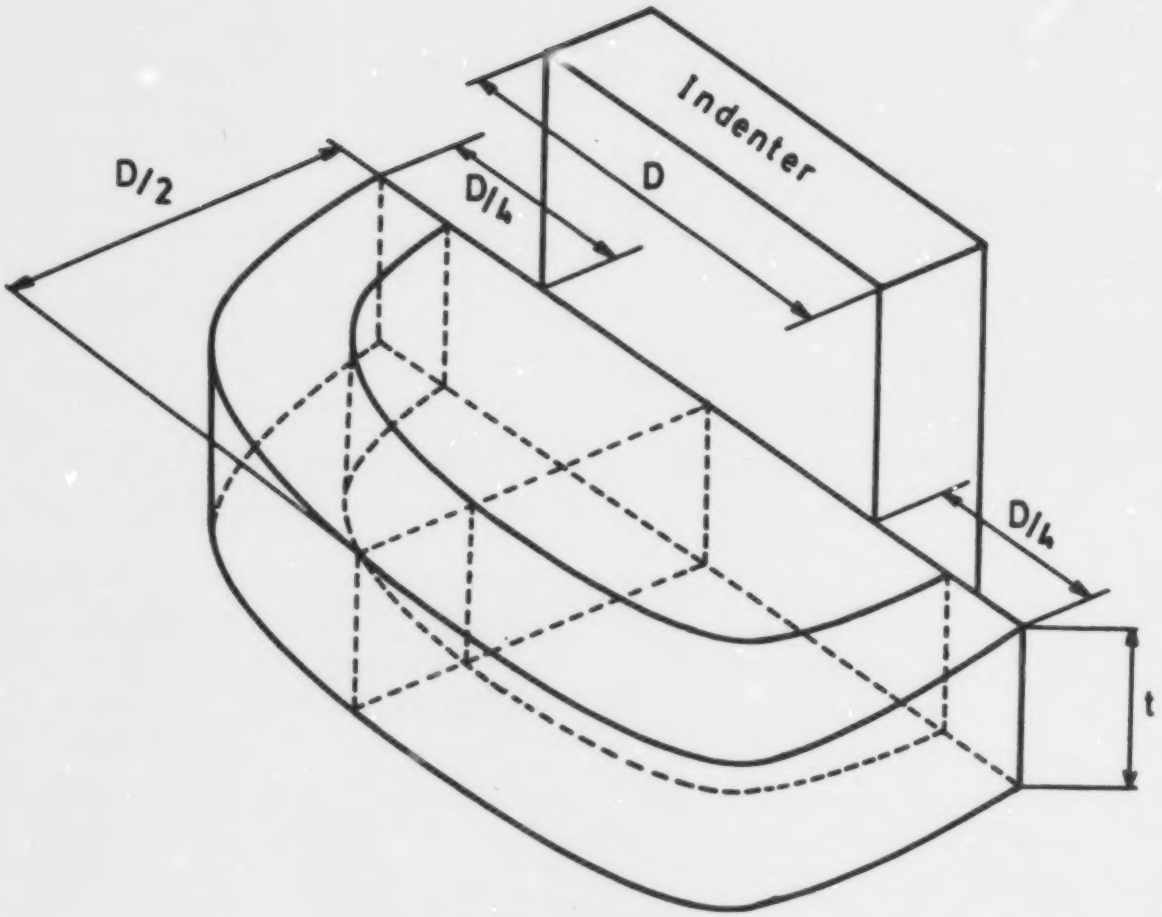

Figure 6.6 (c). Possible Shapes of the Layer of Crushed Ice

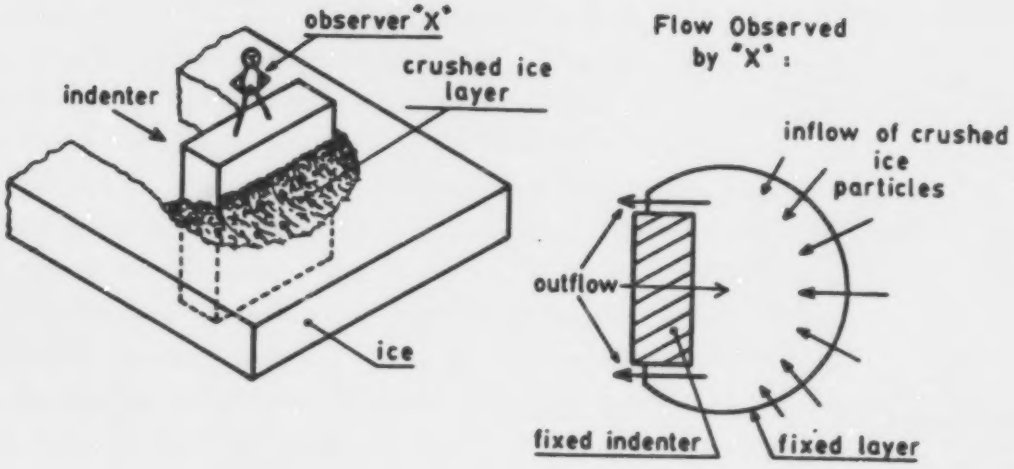

Figure 6.7. Flow of Crushed Ice in the Layer Adjacent to the Indenter

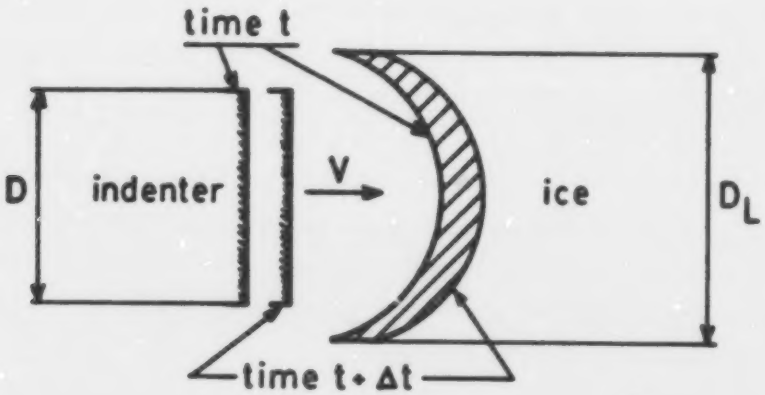

Figure 6.8. Amount of Ice Crushed During Δt in an Indentation Test

discharge of a fluid) depends on the exact geometry of both indenter and ice. Clearly, for a layer having a fixed shape and size, the total inflow of crushed ice must be related to the kinematics of the indenter with respect to the ice sheet. Assuming that the indenter moves at a constant speed v, an average amount of ice ($v \cdot \Delta t \cdot D_L \cdot h$) is crushed during the time interval Δt, where h is the ice thickness and D_L is the width of the layer (Figure 6.8). In reality, the process is not entirely uniform: pressure in the layer builds up and causes a certain amount of ice to fragment. As it clears, higher pressures are produced elsewhere, causing another local zone to crack. The present model, however, pictures an idealized homogeneous flow pattern. This simplification is permitted for the simulation of small scale tests; however, the alternation between break-up and clearance dominates the (unstationary) flow regime in the case of large scale impacts. In addition, the study of the crushed ice flow for an interaction involving natural ice, must account for the presence of flaws and weaknesses which are considerably more important than systems of microcracks in compression. As a result, a highly irregular flow of crushed ice is obtained.

In view of the elastic-viscous analogy (Section 5.2), an equivalent elastic problem is analyzed under the conditions shown in Figure 6.9; the layer is subdivided into hybrid incompressible plane stress finite elements. The unit displacement given at the right-hand boundary corresponds to a constant velocity of the indenter with respect to ice; scaling occurs in accordance with Eq. (5.16).

Various layer geometries were selected for plane stress conditions (Fig. 6.10). In plane stress, the elastic strain ε_{zz} perpendicular to the ice surface is not zero. This corresponds to a certain outflow of crushed ice on the top and the bottom of the ice surface. Recall that because of the incompressibility condition (5.9), the net inflow is necessarily equal to the net outflow.

If the same FE assemblages are used for a plane strain (with zero out-of-plane strain) or for an axysymmetric analysis (with zero radial strain), then the crushed ice is forced to flow out along the side(s) of the indenter within the plane of contact.

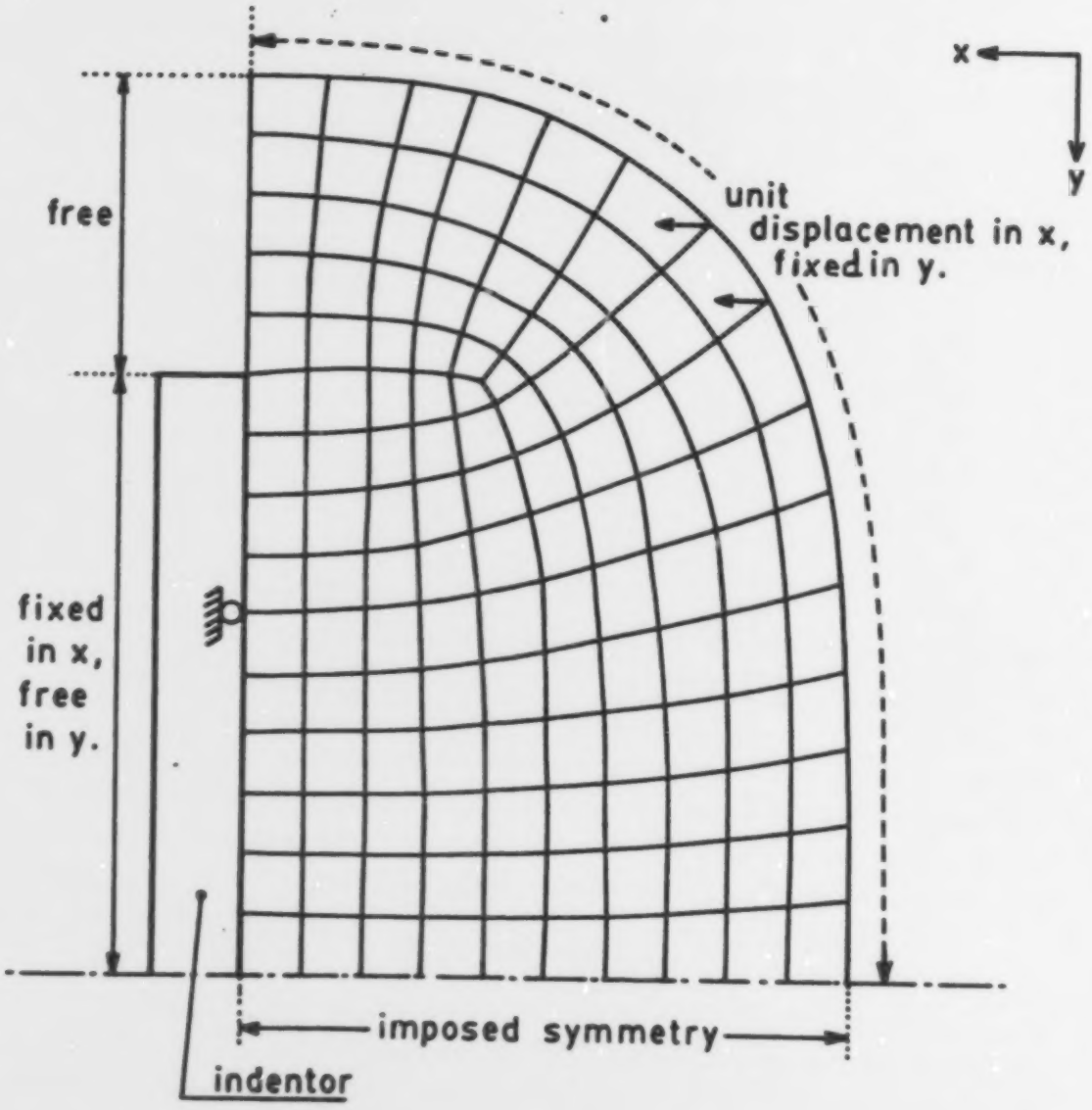

Figure 6.9. Finite Element Analysis of a Typical Layer of Crushed Ice Using the Elastic-Viscous Analogy

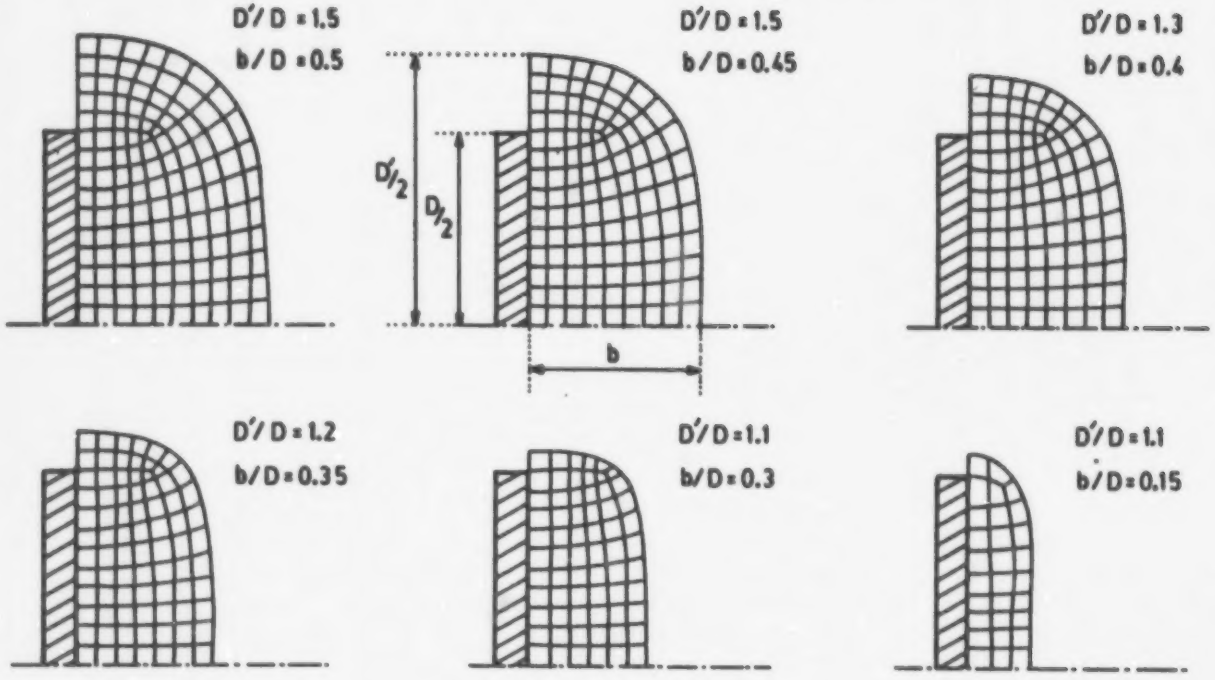

Figure 6.10. Various Layer Geometries to Model the Crushed Ice Flow in Plane-Stress

A first inspection of the results of the FE analysis show that the thickness of crushed ice layer is an important variable. Generally speaking, the thinner this layer, the higher the forces on the indenter for a given velocity.

In Figure 6.11, the distribution of stresses normal to the moving indenter is given for various layer thicknesses. Close to the axis of symmetry, the distribution is essentially uniform at the value of stress $\bar{\sigma}$ given by:

$$\bar{\sigma} = A \frac{\mu v}{b},$$

where
- μ: viscosity of crushed ice;
- v: velocity of the indenter;
- b: thickness of layer;
- D: width of the indenter; and
- A: a constant varying betwen 4 for thick layers (b > 0.3D) to approximately 3 for thin layers.

Note that the quantity $(\sigma/\mu v)$ with dimension m^{-1} in Figure 6.11 is used on the ground of the proportionality principle embodied in Eq. (5.16). Because of the variation of A with the layer geometry, the relationship between $\bar{\sigma}$ and (1/b) is not strictly linear; when the ratio (b/D) increases, the global viscous resistance and, consequently, the parameter A increase.

Stress reaches a peak at the corners of the indenter. It attains a value that is approximately the double of the stress $\bar{\sigma}$ at the centre of the indenter. Recall that the indenter is assumed to be very much stiffer than the ice. Increased structural flexibility would smoothen the stress distribution at the corners of the indenter.

The total force on the indenter is plotted as a function of (bD) in Figure 6.12. For a given velocity, the force decreases with increasing layer thickness. In Table 6.1, some plane-stress indentation test results from Timco (1986) are presented. In all six cases crushing is the basic failure mechanism. There is also some radial cracking, but this is not considered to have an important influence on the axial indentation force.

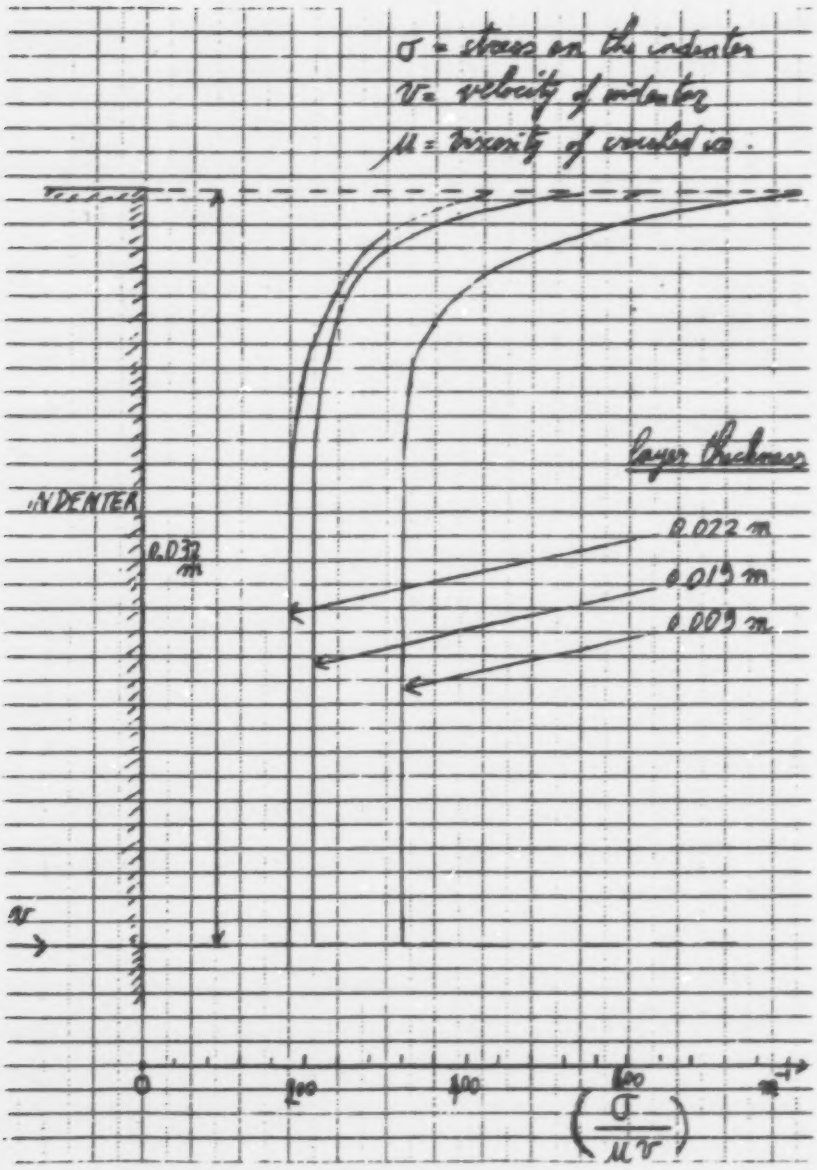

Figure 6.11. Stresses, exerted by Crushed Ice on the Indenter

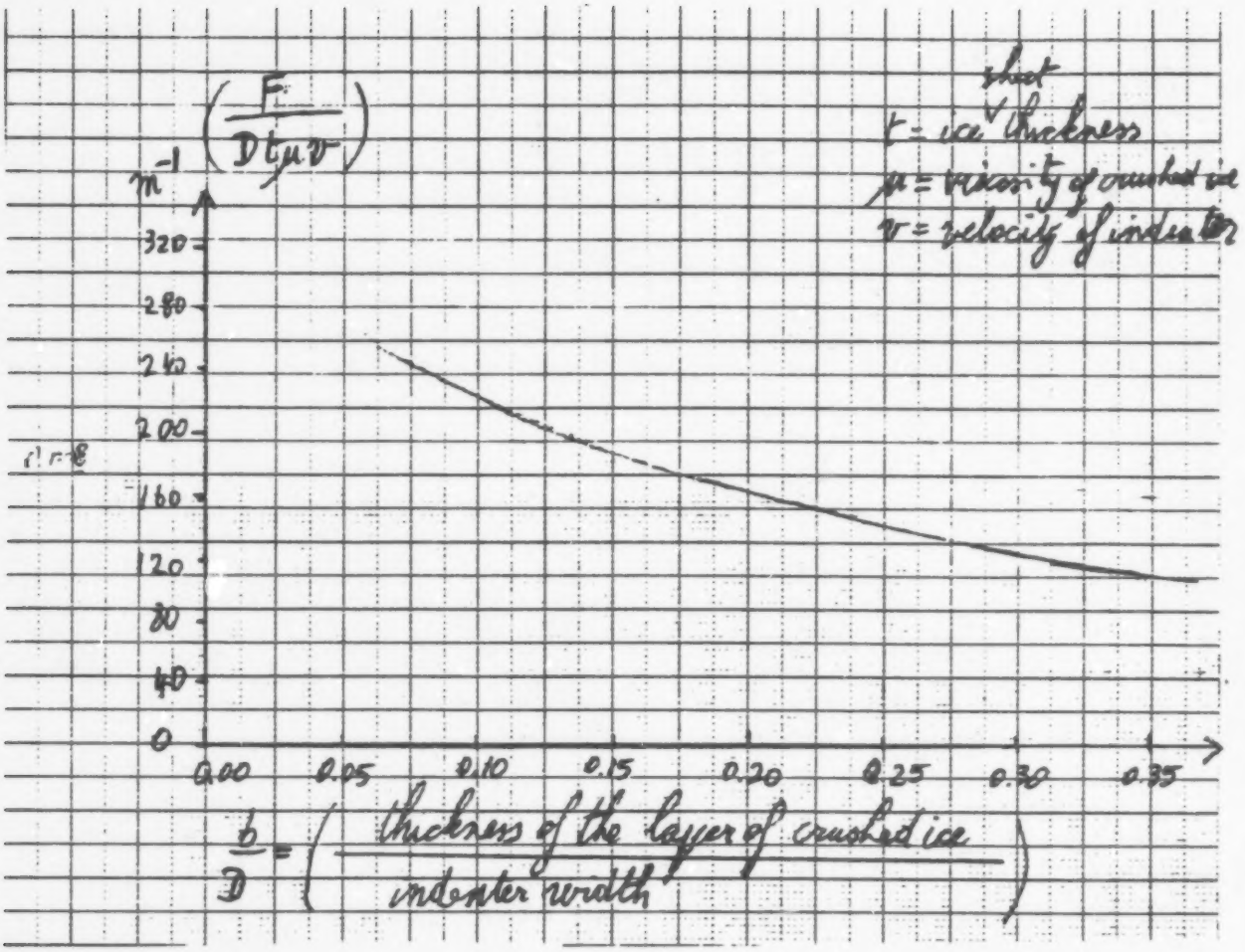

Figure 6.12. Interact Force as a Function of Thickness of the Layer of Crushed Ice

The load shown in Table 6.1 is the mean load; this selection is consistent with the assumption of stationary flow through the contact layer. As discussed earlier, the actual force oscillates around this value because of non-uniform failure of ice, resulting in an irregular flow of crushed ice.

Table 6.1. Forces From Indentation Tests (Timco, 1986)

Velocity v (m/s)	Indenter width D (mm)	Thickness of ice sheet t (mm)	Mean load F (n)	Calculated $\frac{F}{\mu Dtv}$	Calculated b/D (est.)
0.015	63.5	8.2	710	909	$\rightarrow$ 0
0.050	63.5	8.5	610	226	0.09
0.100	63.5	8.5	760	141	0.26
0.100	63.5	6.7	830	195	0.14
0.300	63.5	6.4	830	68	0.50
0.500	63.5	8.5	840	31	$>$ 0.5

The fifth column in Table 6.1 contains the calculated ratio ($F/^{\mu}Dtv$), where $^{\mu}$ is the (constant) viscosity of crushed ice, assumed to be 0.1 MPas (Kheisin et al., 1981). Figure 6.12 is used to estimate the layer thickness b. It appears that the layer is thin for low indentation speeds and becomes substantially thicker at higher speeds. This is in agreement with Timco's (1986) analysis of indentation data. Indeed, the two principal effects emerging from the present analysis are namely:

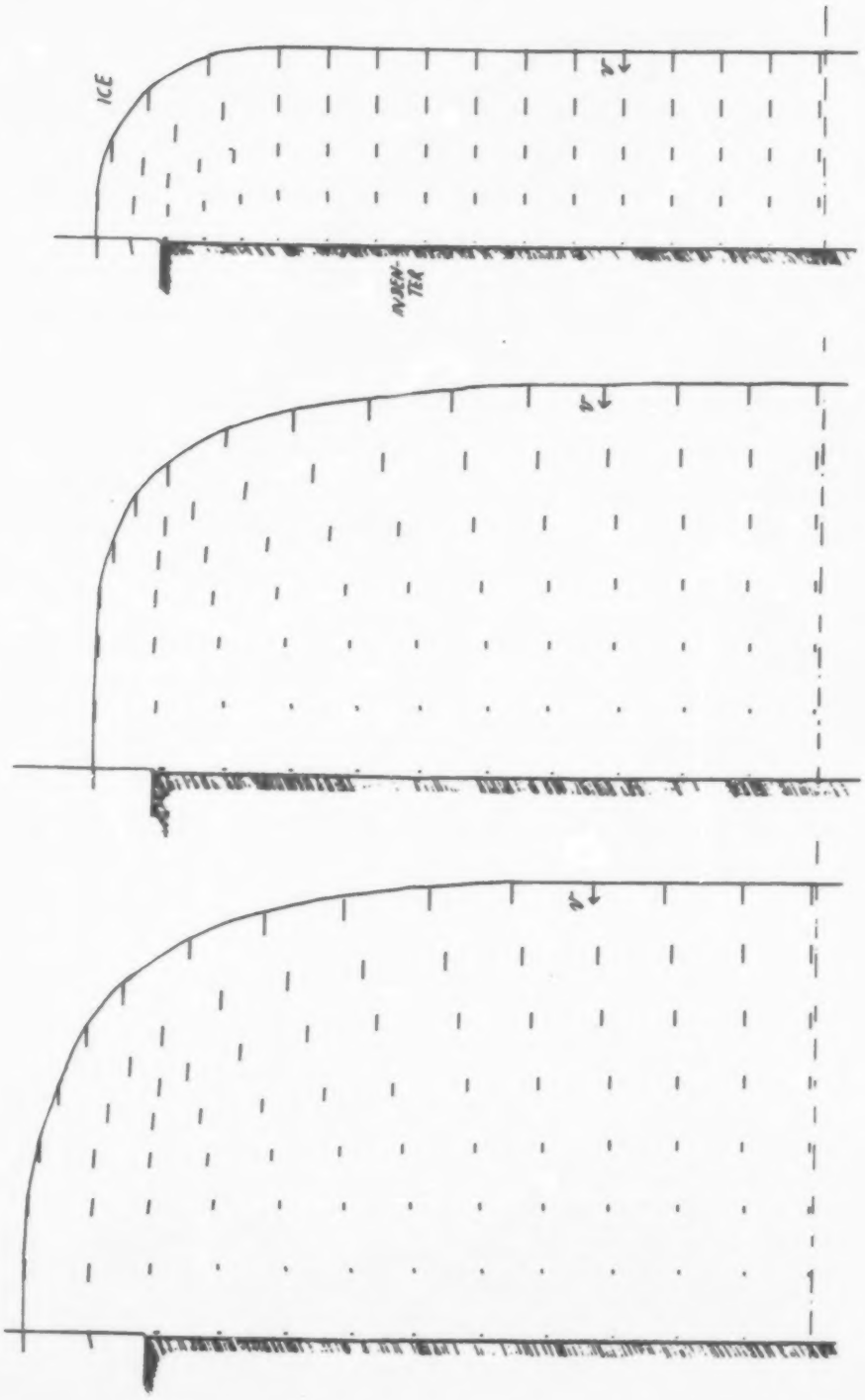

Figure 6.13. Flow of Crushed Ice in the Midplane of the Ice Sheet

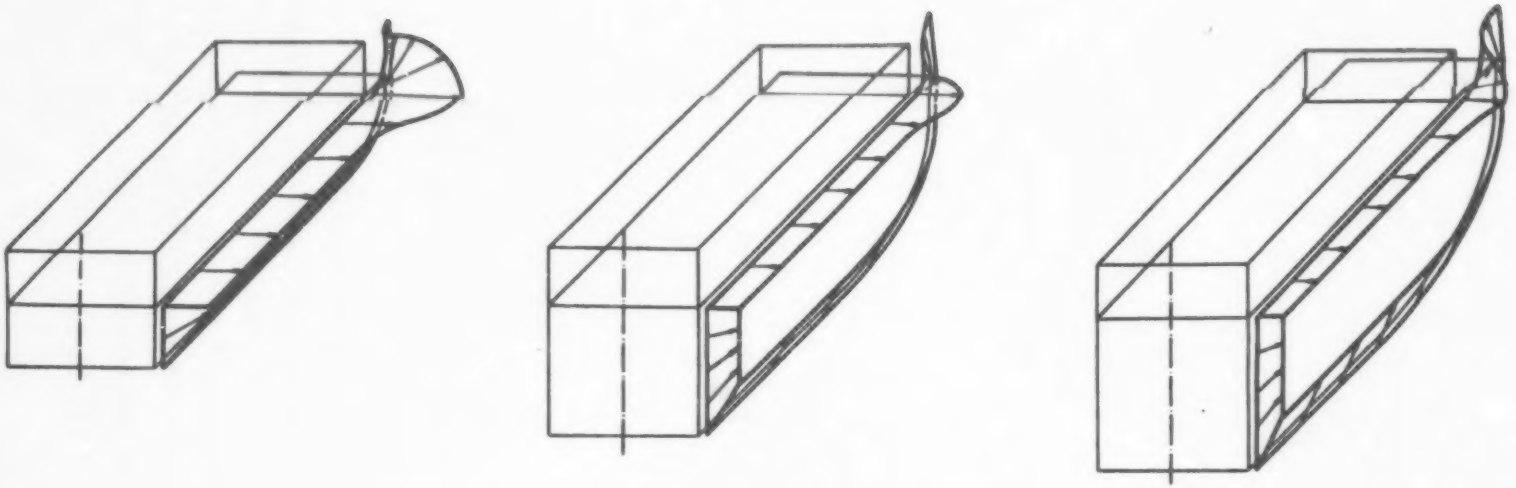

Figure 6.14. Distribution of Velocity Vectors on Top of the Ice-Layer Boundary

- increasing layer thickness for higher indentation speed, and

- decreasing force and pressure for increasing layer thickness,

seem to interact in a balanced way and result in an indentation force that is approximately independent of velocity in the brittle range.

Results from the present analysis can also be extrapolated for different aspect ratios, as long as the plain stress condition is preserved. Basically, the geometry of the crushed ice layer can be scaled up arbitrarily to fit a certain layer thickness that corresponds to a given velocity. This is a correct procedure, since the flow analysis is based on the analogy with linear elastic displacement analysis.

Finally, consider the flow pattern in the mid-plane of the ice sheet. In Figure 6.13, the inflow of magnitude v is parallel to the direction of motion of the indenter. There is an almost constant vertical outflow which is characterized by the out-of-plane strain obtained in the elastic FE analysis. Thus the velocity decreases from the value v at the ice-layer boundary to zero at the face of the indenter. This situation is schematized further in Figure 6.14, where the (total) velocity vector is plotted for in- and outgoing crushed ice.

7. CONCLUSIONS AND RECOMMENDATIONS

This study addresses two important phenomena of ice-structure interaction: progressive damage of ice in compression and the clearing of pulverized material around the indenter. Appropriate constitutive models have been developed in order to simulate and analyze the behaviour of ice on a computer using finite element methods.

In recent years, numerical techniques have enabled a wide variety of non-linear structural problems to be solved, including the modelling of complex geometries and material behaviour. The finite element method, for example, has been used extensively. Discrepancies in the results between observed and "predicted" values have often been attributed to an inadequate representation of material characteristics. This is particularly true for fracture processes. In fact, a mathematical model can only optimally represent the material for which it has been designed. Therefore, the prediction of a physical phenomenon is closely linked to the identification of the main constitutive parameters, and to the measurement of the material constants. Two numerical models for the pulverization of ice under compressive stress have been developed in the present analysis.

A number of simplifying assumptions concerning the nature and the evolution of microcracks have been made, mainly restricted by the scarcity of relevant data for ice crushing. The main inspiration was provided by existing damage theories for metals, concrete and rocks.

For compressive states, an isotropic shear degradation model with residual shear strains upon unloading was implemented in the FE program ABAQUS. The degradation of the material is governed by evolution laws which do not require the use of failure or yield surfaces. The model was tested for uniaxial loading tests, for a wide variety of loading rate conditions, and for brittle and ductile modes, both of which show strain softening effects. Furthermore, it was shown that the degradation of creep properties, can effectively simulate tertiary creep effects.

Finally, a shear damage model as successfully applied to the spread of micro-cracks during an ice sheet indentation test. The numerical solution showed a progressive spread of damage, followed by an unstable behaviour, when the load carrying capacity of the damaged ice is exceeded. Restrictions associated with the explicit time-step algorithm did not allow an accurate prediction of the shape of the crushed layer. It is felt that an implicit algorithm, together with special time-stepping procedures, could alleviate the problem, and this is proposed as a possible extension to the present work.

The evolution of the damage process in indentation shows that the formation of the crushed ice layer is almost instantaneous. An energy-based criterion could provide further insight into the accurate shape of the crushed ice layer, and this also represents an area where further development would be appropriate.

The steady flow of crushed ice in indentation tests was investigated using the analogy between incompressible elasticity and viscous flow. A finite element mesh, based on the observation of the shape of the crushed ice was modelled and tested for various thicknesses of the layer. Distribution of velocities in the flow and pressures under the indenter were obtained, together with a discussion on the appropriate boundary conditions.

A relationship between velocity, viscosity, thickness of layer and pressure on the indenter was derived and compared with indentation data and typical values for the viscosity. It is recommended that further experimental work be conducted to quantify damage. Mechanical stress/strain measurements could be obtained, in order to derive appropriate damage evolution laws and verify the validity of the basic assumptions in the model. Additional experiments on the flow of crushed ice are also necessary. Measurements of viscosity and the determination of the geometry of the crushed layer would prove very valuable to determine local ice pressure distributions. On the analysis level, a more elaborate model could include non-linear viscosity and account for the deformation of the crushed layer (spherical indenter). This would also require

a full Eulerian representation. In the long term, the solution of the following coupled problem is considered to be important: the progression of damage using Lagragian formulation, and the simultaneous motion of the break-up surface and the extrusion of crushed ice using an Eulerian representation.

REFERENCES

Ashby, M.F. and Hallam, S.D. (Cooksley) (1986): "The Failure of Brittle Solids Containing Small Cracks Under Compressive Stress States". Acta. Metall., Vol. 34, No. 3, pp. 497-510.

Bazant, Z.P., and Gambarova, P.G.: "Crack Shear in Concrete: Crack Band Microplane Model".

Bazant, Z.P. (1977): "Endochronic and Classical Theories of Plasticity in Finite Element Analysis". International Conference on Finite Elements in Nonlinear Solid and Structural Mechanics, Geilo, Norway, Aug. 29 - Sept. 1, Vol. 1.

Bazant, Z.P. (1976): "Instability, Ductility, and Size Effect in Strain-Softening Concrete". Journal of the Engineering Mechanics Division, April.

Bazant, Z.P., and Bhat, P.D. (1976): "Endochronic Theory of Inelasticity and Failure of Concrete". Journal of the Engineering Division, August.

Bazant, Z.P., and Krizek, R.J. (1975): "Endochronic Constitutive Law for Inelastic Shear and Densification of Sand". Proceedings of the Fifth Canadian Congress of Applied Mechanics, Fredericton, New Brunswick.

Burt, N.J., and Dougill, J.W. (1977): "Progressive Failure in a Mode Heterogeneous Medium". Journal of the Engineering Mechanics Division, June.

Carpinteri, A., and Sih, G.C. (1983): "Damage Accumulation and Crack Growth in Bilinear Materials with Softening: Application of Strain Energy Density Theory". Lehigh University, Institute of Fracture and Solid Mechanics, Report No. IFSM-83-115.

Chaboche, J.L. (1979): "The Continuous Damage Mechanics: A Tool to Describe Phenomena Before Crack Initiation". 2nd Int. Seminar on Incl. Analysis and Life Prediction in High Temp. Env., pp. C9-C14.

Chen, E.P., Kipp, M.E., and Grady, D.E. (1984): "A Strain-Rate Sensitive Rock Fragmentation Model". To appear in Mechanics of Oil Shale, edited by K.P. Chong and J.W. Smith, Applied Science Ltd.

Davison, L., and Stevens, A.I. (1973): "Thermomechanical constitution of Spalling Elastic Bodies". Journal of Applied Physics, Vol. 44, pp. 667-674.

Dienes, J.K.: "Fracture, Failure, and Fragmentation". Theoretical Division, Group T-3, Los Alamos National Laboratory, Los Alamos, New Mexico.

Dougill, J.W.: "An Approximate Assessment of the Effects of Heterogeneity on the Strength and Mode of Failure of Concrete Systems". University of London King's College, Civil Engineering Department.

Dougill, J.W. (1983): "Path Dependence and a General Theory for the Progressively Fracturing Solid". Proc. R. Soc. Lond., A390, 341-351, Great Britain.

Dougill, J.W. (1983): "Constitutive Relations for Concrete and Rock: Applications and Extensions of Elasticity and Plasticity Theory". William Prager Symposium on Mechanics of Geomaterials, Rocks, Concretes, Soils, September 11-15.

Dougill, J.W., Lau, J.C., and Burt, N.J. (1976): "Towards a Theoretical Model for Progressive Failure and Softening in Rock, Concrete and Similar Materials". To be presented at the American Society of Civl Engineering Mechanics Division Specialty Conference of Mechanics in Engineering Univeristy of Waterloo, Ontario, May 26-28.

Dougill, J.W. (1976): "On Stable Progressively Fracturing Solids". Reprint from Journal of Applied Mathematics and Physics, Vol. 27, Fasc. 4, ZAMP, pp. 423-437.

Dougill, J.W. (1975): "Some Remarks on Path Independence in the Small in Plasticity". Quarterly of Aplied Mathematics, October.

Dougill, J.W., and Rida, M.A.M. (1980): "Further Consideration of Progressively Fracturing Solids". The Journal of Engineering Mechanics Division, October.

Evans, A.G. et al. (1984): "Indentation Spalling of Edge-Loaded Ice Sheets". IAHR Ice Symposium 1984, Hamburg.

Garcia, N.B., et al. (1985): "Ice Penetration Tests". Cold Regions Research and Engineering Technology, 11, pp. 223-36.

Gerard, R. (1976): "A Simple Field Measure of Ice Strength". Third International Symposium on Ice Problems, IAHR, Hanover, NH, U.S.A.

Glen, J.W. (1975): The Mechanics of Ice. CRREL Monograph II-C2b.

Gold, L.W. (1972): "The Failure Process in Columnar-Grained Ice". NRCC Paper No. 369.

Hayhurst, D.R., Dimmer, P.R., and Chernuka, M.W. (1975): "Estimates of the Creep Rupture Lifetime of Structures Using the Finite-Element Method". Journal of Mechanics and Physics of Solids, Vol. 23, pp. 335-355.

Hibbitt, Karlsson and Sorensen Inc. (1985-1): ABAQUS User's Manual. Version 4.5.

Hibbitt, Karlsson and Sorensen Inc. (1985-2): ABAQUS Theory Manual.

Horii, H., and Nemat-Nasser, S. (1982): "Overall Moduli of Solids With Microcracks: Load-Induced Anisotropy". J. Mech. Phys. Solids., Vol.31, No. 2, pp. 155-171.

Jordaan, I.J., Tomin, M.J., Cormeau, A. (1985): "Development of Analytical Models Related to Experimental Work on Ice Structure Interaction". Veritas Report No. CGY 033/85.

Jordaan, I.J. (1986): "Numerical and Finite Element Techniques in Calculaton of Ice-Structure Interaction". 8th Symposium on Ice, Iowa City, August.

Kachanov, L.M. (1958): "Time to Failure Under Creep Conditions". Isz. AN SSSR OTN, No. 8.

Karr, D.G. (1985): "Constitutive Equations for Ice as a Damaging Material". Proc. Civil Eng. in the Arctic Offshore, ASCE, San Francisco, March 25-57.

Kheisin, D.E., and Likhomanov, V.A. (1973): "An Experimental Determination of the Specific Energy of Mechanical Crushing in Ice by Impact". Problemy Arktiki i Antarktiki, Vol. 41, pp. 55-61.

Krajcinovic, D., and Fonseka, G.U. (1981): "The Continuous Damage Theory of Brittle Materials". Journal of Applied Mechanics, December, Vol. 48.

Kurdyumov, V.A., and Kheisin, D.E. (1976): "Hydrodynamic Model of the Impact of a Solid on Ice". Prikladnaya Mekhanika, Vol. 12, No. 10, pp. 103-109.

Lainey, L., and Tinarvi, R. (1984): "The Mechanical Properties of Sea Ice - A Compilation of Available Data". Can. J. Civ. Eng. 11, 884-923.

Leckie, F.A. (1978): "The Constitutive Equations of Continuum Creep Damage Mechanics". Philosophical Transactions of the Royal Society, London, Series A, 288, 27-47.

Leckie, F.A. and Hayrust, D.R. (1974): "Creep Rupture of Structures". Proceedings of the Royal Society, London, Series A., Vol. 340, 1974, pp. 323-347.

Lemaitre, J., and Chaboche, J.L. (1985): "Mécanique des Matérieux Solides". First Edition, Dunod.

Lemaitre, J., and Chaboche, J.L. (1978): "Aspect Phenomenologique de la Rupture par Endommagement". Journal de Mecanique Appliquee, Vol. 2, pp. 317-365.

Likhomanov, V.A., and Kheisin, D.E. (1971): "Experimental Investigation of Solid Body Impact on Ice". Problemy Arctiki i Antarktiki, Vol. 38, pp. 105-111.

Nemat-Nasser, S., and Horii, H. (1984): "Micro-Mechanics of Fracture and Failure of Geo-Materials in Compression". Advances in Fracture Research, Proceedings of the 6th International Conference on Fracture (ICF6), New Delhi, India. Dec. 4-10.

Nemat-Nasser, S., and Horii, H. (1984): "Rock Failure in Compression". Int. J. Engng. Sci., Vol.22, No. 8-10, pp. 999-1011.

Nemat-Nasser, S., and Horii, H. (1982): "Growth of Microcracks in Rocks, and Load-Induced Anisotropy". Symposium on Fracture Mechanics Approach to Hydraulic Fracturing and Geothermal Energy, Sendai, Japan, November 8.

Resende, L., and Martin, J.B.: "Constitutive Modelling and Finite Element Analysis in Rock Mechanics - Part I: The Internal Damage Model and Parameter Identification". AMRU Rep. No. 57 (to be published).

Resende, L., and Martin, J.B.: "Constitutive Modelling and Finite Element Analysis in Rock Mechanics - Part II: Finite Element Solution of Boundar Value Problems". AMRU Rep. No. 58 (to be published).

Resende, L. and Martin, J.B. (1983): "Damage Constitutive Model for Geotechnical Applications". University of Cape Town, Rondebosch, Cape Town, South Africa, Nonlinear Structural Mechanics Research Unit, Technical Report No. 44.

Resende, L., and Martin, J.B. (1983): "A Progressive Damage Continuum Model for Granular Materials". Computer Methods in Applied Mechanics and Engineering 42 (1984) 1-18 North-Holland.

Ross, B. (1969): "Perforation of the Arctic Sea-Ice Cover by Projectile Impact". Journal of Hydronautics, Vol. 3, No. 3, July.

Sinha, N. (1984): "Delayed-Elastic Model for Initiation and Assimiliation of Creep Cavitation at High Temperatures". Sixth International Conference on Fracture, New Delhi, December 4-10.

Spooner, D.C., and Dougill, J.W. (1975): "A Quantitative Assessment of Damage Sustained in Concrete During Compressive Loading". Reprinted from Magazine of Concrete Research, Vol. 27, No. 92, September, pp. 151-160.

Stankowski, T., and Gerstle, K.H. (1983): "Simple Formulation of Concrete Behaviour Under Load Histories". Paper submitted for Publication in Jnl. A.C.I., September.

Timco, G.W. (1986): "Indentation and Penetration in Freshwater Ice". 5th Symposium on Offshore Mechanics and Arctic Engineering, OMAE, Japan, April 13-17.

Timoshenko, S.P., and Goodier, J.N. (1970): "Theory of Elasticity". Third Edition, McGraw Hill.

Vakulenko, A.A., and Kachanov, M.L. (1971): "Continuum Theory of Cracked Media". Mekh Tverdogo Tela, Vol. 6, pp. 159-166.

Willam, K.J., and Sture, S. (1985): "A Composite Fracture Model for Localized Failure in Cementitious Materials". Paper presented at second Symposium on the Interaction of Non-Nuclear Munitions with Structures, Panama City Beach, Florida, April.

Willam, K.J., Bicanic, N., and Sture, S. (1984): "Constitutive and Computational Aspects of Strain-Softening and Localization in Solids". Presented at A.S.M.E. - WAM'84 Symposium on Constitutive Equations: Micro, Macro and Computational Aspects", New Orleans, December 10-14.

Yen, Y-C, et al. (1970): "Impact of Spheres on Ice". Proc. A.S.C.E., Eng. Mech. Division, Vol. 36, No. EM5, October.

Yuceoglu, U., Sierakowski, R.L., and Glasgow, D.A. (eds.) (1983), "Advances in Aerospace Structures, Materials and Dynamics - A Symposium on Composites". Presented at the Winter Annual Meeting of the American Society of Mechanical Engineers, November 13-18.

Zhurkov, S.N. and Sanfirova, T.P. (1958): "The Relationship Between Strength and Creep in Metals and Alloys". Zhurnal Teoreticheskoi Fyziki, Vol. 28, No. 8.

Zienkiewicz, O.C. (1977): "The Finite Element Method". Third Edition, McGraw Hill.

APPENDIX A

RELATIONSHIP BETWEEN STRESS AND STRAIN INCREMENTS FOR PARTICULAR CONSTRAINT CONDITIONS AND STATES OF STRESS

In this appendix, specific forms of stress/strain rate relationships are developed for various types of applied stress and strain constraints. In order to simplify the matrix notation in what follows, a single superscript has been used to denote a vector whereas a double superscript signifies an array.

In any stress state, the vectors of stress and strain can be readily partitioned into dependent and independent components (denoted d and i respectively), thus:

$$\Delta\bar{\varepsilon} = \begin{Bmatrix} \Delta\bar{\varepsilon}_i \\ \Delta\bar{\varepsilon}_d \end{Bmatrix}; \qquad \Delta\bar{\sigma} = \begin{Bmatrix} \Delta\bar{\sigma}_i \\ \Delta\bar{\sigma}_d \end{Bmatrix}; \qquad \bar{s} = \begin{Bmatrix} \bar{s}_i \\ \bar{s}_d \end{Bmatrix}$$

It will be recalled that the stress/strain rate equation (4.23) was written as:

$$\Delta\bar{\sigma} = \bar{\bar{J}}\,\Delta\bar{\varepsilon} - f\bar{s}\,\Delta t \tag{A1}$$

where

$$f = \left(\frac{\dot{D}}{1-D} + \frac{2\tilde{G}}{s}\,\dot{e}^{rd}\right)$$

and D, $\tilde{G}$, s, and $\dot{e}$ are understood to mean current damage, current shear modulus, equivalent deviatoric stress and conjugate total strain rate, respectively.

Separating Eq. (A1) into its dependent and independent components yields

$$\begin{matrix} \bar{\sigma}_i \\ \Delta\bar{\sigma}_d \end{matrix} = \begin{matrix} \bar{\bar{J}}_{ii} & \bar{\bar{J}}_{id} \\ \bar{\bar{J}}_{di} & \bar{\bar{J}}_{dd} \end{matrix} \begin{matrix} \Delta\bar{\varepsilon}_i \\ \Delta\bar{\varepsilon}_d \end{matrix} - f\Delta t \begin{matrix} \bar{s}_i \\ \bar{s}_d \end{matrix} \tag{A2}$$

Now assume, for example, that uniaxial load conditions exist in the x direction in which case one can write:

$$\bar{\Delta\sigma}_d \equiv \begin{matrix} \Delta\sigma_{yy} \\ \Delta\sigma_{zz} \\ \Delta\tau_{xy} \\ \Delta\tau_{xz} \\ \Delta\tau_{yz} \end{matrix} ; \quad \text{and} \quad \bar{\Delta\sigma}_i \equiv \{\Delta\sigma_{xx}\}$$

Similarly, if plane stress conditions existed in the XY plane, one could write

$$\bar{\Delta\sigma}_d \equiv \begin{matrix} \sigma_{zz} \\ \Delta\tau_{xz} \\ \Delta\tau_{yz} \end{matrix} ; \quad \text{and} \quad \bar{\Delta\sigma}_i \equiv \begin{matrix} \Delta\sigma_{xx} \\ \Delta\sigma_{yy} \\ \tau_{xy} \end{matrix}$$

It can be seen from the above that the constraint condition is of order 5 for uniaxial conditions and of order 3 in the case of plane stress. In general, the constraint condition can be written as:

$$\bar{\Delta\sigma}_d = 0 \qquad \text{(A3)}$$

Substituting the constraint equation (A3) into equation (A2), and rearranging enables the dependent strains $\bar{\Delta\epsilon}_d$ to be written as:

$$\bar{\Delta\epsilon}_d \equiv \bar{J}_{dd}^{-1} \left(f\, {}^{\Delta t}\bar{S}_d - \bar{J}_{di}\ \bar{\Delta\epsilon}_i \right).$$

This expression may then be further used on Eq. (A2) to establish that:

$$\Delta\bar{\sigma}_i = (\bar{J}_{ii} - \bar{J}_{id}\,\bar{J}_{dd}^{-1}\,\bar{J}_{di})\,\Delta\bar{\epsilon}_i + f\,\Delta t(\bar{J}_{id}\bar{S}_d - \bar{S}_i), \tag{A4}$$

which shows that increments of independent stresses are a function of the full stress deviator (S_d, S_i).

For plane strain or axisymmetric conditions, analogous conditions for dependent stress can be prescribed on the dependent strain components as follows:

$$\Delta\bar{\epsilon}_d = \bar{0} \tag{A5}$$

In this case, Eq. (2) becomes

$$\Delta\bar{\sigma}_i = \bar{J}_{ii}\,\Delta\bar{\epsilon}_i - f\,\Delta t\;\bar{S}_i$$

$$\Delta\bar{\sigma}_d = \bar{J}_{di}\,\Delta\bar{\epsilon}_i - f\,\Delta t\;\bar{S}_d \tag{A6}$$

Equations (A4) and (A6) both show that the stress increments are related to strain increments through specific elastic stiffness matrices derived from the appropriate particular states of stress (uniaxial, plane stress and strain, axisymmetric). Furthermore, in order to evaluate the equivalent stress s, six components of the stress deviator need to be stored.

```
      SUBROUTINE UMAT(STRESS,STATEV,DDSDDE,SSE,SPD,SCD,STRAN,DSTRAN,
     1 TIME,DTIME,TEMP,DTEMP,PREDEF,DPRED,MATERL,NDI,NSHR,NTENS,NSTATV,
     2 PROPS,NPROPS,COORDS)
C
CPU PURPOSE:
CPU     DUMMY ROUTINE TO ALLOW FOR VARIABLE DIMENSIONS IN UMAT40
C
      DIMENSION STRESS(NTENS)
      DIMENSION DDSDDE(NTENS,NTENS)
      DIMENSION STRAN(NTENS),DSTRAN(NTENS)
      DIMENSION PREDEF(1),DPRED(1),PROPS(NPROPS),COORDS(3)
      DIMENSION STATEV(NSTATV)
      DIMENSION RJACM1(25),RJACCO(25)
C
      NTENCO=6-NTENS
      IF(NSTATV.NE.14)THEN
         PRINT*,'$ ***** ERROR : NUMBER OF STATEV IS NOT 14 '
         STOP
      ENDIF
      IF(NTENCO.EQ.0)NTENCO=1
      CALL UMAT40(STRESS,STATEV,DDSDDE,SSE,SPD,SCD,STRAN,DSTRAN,
     1 TIME,DTIME,TEMP,DTEMP,PREDEF,DPRED,MATERL,NDI,NSHR,NTENS,NSTATV,
     2 PROPS,NPROPS,COORDS,RJACCO,RJACM1,NTENCO)
      RETURN
      E N D
C
C*****************************************************
C*****************************************************
C
      SUBROUTINE UMAT40(STRESS,STATEV,DDSDDE,SSE,SPD,SCD,STRAN,DSTRAN,
     1 TIME,DTIME,TEMP,DTEMP,PREDEF,DPRED,MATERL,NDI,NSHR,NTENS,NSTATV,
     2 PROPS,NPROPS,COORDS,RJACCO,RJACM1,NTENCO)
C
CPU PURPOSE:
CPU     USER MATERIAL ROUTINE  U M A T 4 0
CPU     SHEAR DAMAGE MODEL (ELASTIC) AND SHEARING RESIDUAL STRAINS
CPU     (UNLOADING) BOTH DEFINED BY EQUIVALENT EVOLUTION LAWS
CPU     EVOLUTION LAWS ARE INTEGRATED WITH FORWARD TIME INTEGRATION
CPU     SCHEME
CPU     PURE ELASTIC BULK BEHAVIOUR (NOT AFFECTED BY DAMAGE)
C
CAI ARGUMENT INPUT:
CAI     NTENCO          SIZE OF RJACM1 AND RJACCO MATRICES
CAI     STRAN(.)        TOTAL STRAINS
CAI                     NOTE: (.) MEANS VARIABLE SIZE (1D, 2D, AX OR 3D)
CAI     DSTRAN(.)       INCREMENTS OF TOTAL INDEPENDENT STRAINS
CAI     TIME            TIME AT START OF INCREMENT
CAI     DTIME           TIME INCREMENT
CAI     NDI             NUMBER OF DIRECT STRESS COMPONENTS
CAI     NSHR            NUMBER OF SHEAR STRESS COMPONENTS
CAI     NSTATV          NUMBER OF SOLUTION DEPENDENT VARIABLES
CAI     PROPS(.)        ARRAY OF MATERIAL CONSTANTS
CAI           1         YUNG0
CAI           2         RNU0
CAI           3         NOT USED
CAI           4         EMAX0
CAI         5 --> 15    DEFINE RATE OF DAMAGE
CAI           5         CONSTANT
CAI         6 --> 10    LINEAR VARIATION (DAM, EQ, DEQ, SQ, DSQ)
CAI        11 --> 15    QUADRATIC VARIATION
CAI          16         NOT USED
CAI        17 --> 27    DEFINE RATE OF PERMANENT DEFORMATION
CAI          17         CONSTANT
CAI        18 --> 22    LINEAR VARIATION (DAM, EQ, DEQ, SQ, DSQ)
```

```
CAI       23 --> 27  QUADRATIC VARIATION
CAI     NPROPS       NUMBER OF MATERIAL CONSTANTS (27)
CAI     COORDS(3)    ARRAY OF CURRENT COORDINATES AT THIS POINT
C
CIV INTERNAL VARIABLES:
CIV                  NOTE: 0 INDICATES VIRGIN PROPERTIES
CIV                        1 INDICATES CURRENT DEGRADED VALUES
CIV                          AT BEGINNING OF INCREMENT
CIV                        2 INDICATES CURRENT DEGRADED VALUES
CIV                          AT END OF INCREMENT
CIV                        D MEANS RATE, INCREMENT OR PERTURBUTION
CIV                        S MEANS STRESS
CIV                        E MEANS TOTAL STRAIN
CIV                      DEV MEANS DEVIATOR
CIV     DE(6)        TOTAL STRAIN INCREMENT
CIV     DEPSV        TOTAL INCREMENT IN VOLUME STRAIN
CIV     SDEV1(6)     STRESS DEVIATOR
CIV     SDEV2(6)
CIV
CIV     LOCZ(3)      LOCALISATION OF OUT OF PLANE COMPONENTS (STRESS)
CIV     LOCP(3)      LOCALISATION OF IN PLANE (X,Y) COMPONENTS
CIV
CIV     LOCA(4)      LOCALISATION OF AXISYM/PLANE STRAIN COMPONENTS
CIV     LOCT(2)      LOCALISATION OF NON AXISYM/PLANE COMPONENTS
CIV
CIV     LOCX(1)      LOCALISATION OF UNIAX. COMPONENT
CIV     LOCS(5)      LOCALISATION OF NON UNIAX. COMPONENTS
CIV
CIV     ISTATE       FLAG DEFINING STATE OF STRESS
CIV        1         AXIAL STRESS (NTENS=1)
CIV        3         PLANE STRESS (NTENS=3)
CIV        4         PLANE STRAIN/AXIAL SYMMETRY (NTENS=4)
CIV        6         3D (NTENS=6)
CIV     YUNG0, YUNG1 YOUNG MODULUS
CIV     RNU0, RNU1   POISSON RATIO
CIV     SHE0, SHE1   SHEAR MODULUS
CIV     BULK0, BULK1 BULK MODULUS
CIV     DAM1, DAM2   PERMANENT DAMAGE
CIV     EMAX0        EQUIVALENT STRAIN AT START OF DAMAGE
CIV     EQ1, EQ2     EQUIVALENT STRAIN
CIV     DEQ1, DEQ2   RATE OF EQUIVALENT STRAIN (SDEV:DE/SQ)
CIV     SQ1, SQ2     EQUIVALENT MISES STRESS (3/2 SDEV:SDEV) ** 1/2
CIV     SM1, SM2     MEAN STRESS 1/3 TR(S)
CIV     DSQ1, DSQ2   RATE OF EQUIVALENT MISES STRESS
CIV     DEQ          INCREMENT OF EQUIVALENT STRAIN
CIV     RJAC66(6,6)  MATERIAL JACOBIAN FOR FULL 3D STATE OF STRESS
CIV                  (UNI, PLANE, AXI, NOT 3D), WRITTEN IN VECTOR
C
CAO ARGUMENT OUTPUT:
CAO                  NOTE:
CAO                  VARIABLES TO UPDATE AT END OF INCREMENT ARE PASSED
CAO                  IN FOR INFO AT BEGIN OF INCREMENT
CAO     DDSDDE(.,.)  JACOBIAN MATRIX
CAO     STRESS(.)    STRESS TO UPDATE
CAO     STATEV(.)    STATE VARIABLES TO UPDATE
CAO         (1)      DAMAGE
CAO         (2)      EQUIVALENT TOTAL STRAIN
CAO         (3)      EQUIVALENT TOTAL STRAIN RATE
CAO         (4)      EQUIVALENT MISES STRESS
CAO         (5)      EQUIVALENT MISES STRESS RATE
CAO         (6)      MEAN STRESS
CAO         (7)      MAXIMUM EQUIVALENT STRAIN
CAO     (8) --> (13) STRESS DEVIATOR
CAO     SSE          STRAIN ENERGY DENSITY (RECOVERABLE)
CAO     SPD          DENSITY OF ELASTIC RECOVERY ENERGY (DUE TO
CAO                  DAMAGE OF ELASTIC PROPERTIES)
```

```
CAO      SCD           DISSIPATION DENSITY (DUE TO RESIDUAL PERMANENT
CAO                    STRAINS)
C
      COMMON /CEL    / GASH1(3),IEL,IGP,GASH2(57)
C
      SAVE YUNG0,RNU0,SHE0,BULK0,EMAX0
C
      DIMENSION ENER2(2,7)
      DIMENSION STRESS(NTENS),SDEV1(6),SDEV2(6),S1(6),S2(6)
      DIMENSION DDSDDE(NTENS,NTENS),RJAC66(6,6)
      DIMENSION RJACCO(NTENCO,NTENCO),RJACM1(NTENCO,NTENCO)
      DIMENSION STRAN(NTENS),DSTRAN(NTENS),DE(6)
      DIMENSION PREDEF(1),DPRED(1),PROPS(NPROPS),COORDS(3)
      DIMENSION STATEV(NSTATV)
      DIMENSION LOCP(3),LOCZ(3), LOCX(1),LOCS(5), LOCA(4),LOCT(2)
      DIMENSION LOC3(6)
C
      EQUIVALENCE (ENER2(1,2),WEM2),(ENER2(2,2),DWEM2)
      EQUIVALENCE (ENER2(1,1),WEQ2),(ENER2(2,1),DWEQ2)
      EQUIVALENCE (ENER2(1,3),WE2),(ENER2(2,3),DWE2)
      EQUIVALENCE (ENER2(1,4),WD2),(ENER2(2,4),DWD2)
      EQUIVALENCE (ENER2(1,5),WR2),(ENER2(2,5),DWR2)
      EQUIVALENCE (ENER2(1,6),W2),(ENER2(2,6),DW2)
      EQUIVALENCE (ENER2(1,7),WT2),(ENER2(2,7),DWT2)
C
      DATA LOCP /1,2,4/,LOCZ /3,5,6/
      DATA LOCX /1/, LOCS/2,3,4,5,6/
      DATA LOCA /1,2,3,4/, LOCT/5,6/
      DATA LOC3 /1,2,3,4,5,6/
C=================================================
C ENTRY SECTION
C STATE VARIABLES AT BEGINNING OF INCREMENT
C=================================================
      T1=TIME
      T2=TIME+DTIME
      DAM1=STATEV(1)
      EQ1 =STATEV(2)
      DEQ1=STATEV(3)
      SQ1 =STATEV(4)
      DSQ1=STATEV(5)
      SM1 =STATEV(6)
      DO 10 I=1,6
      SDEV1(I)=STATEV(7+I)
      S1(I)   =SDEV1(I)
      IF(I.LE.3)S1(I)=S1(I)+SM1
10    CONTINUE
C=================================================
C FIND MATERIAL CONSTANTS FOR VIRGIN AND DEGRADED
C (AT BEGINNING OF INCREMENT) STATES
C=================================================
C
C VIRGIN ELASTIC PROPERTIES
C
      IF(TIME.EQ.0.)THEN
         SSE=0.
         SPD=0.
         SCD=0.
         YUNG0=PROPS(1)
         RNU0 =PROPS(2)
         BULK0=YUNG0/(3.*(1.-2.*RNU0))
         SHE0 =YUNG0/(2.*(1.+RNU0))
         EMAX0=PROPS(4)
         STATEV(7)=EMAX0
      ENDIF
      IF(IEL.EQ.1.AND.IGP.EQ.1.AND.DSTRAN(1).NE.0.)THEN
         IPSW =INT(PROPS(3))
```

```
      ELSE
         IPSW=0
      ENDIF
C
C PRINT STATE VARIABLES AT BEGINNING OF INCREMENT
C
      IF(IPSW.GE.6.OR.IPSW.EQ.-6)CALL PRMAT(T1,STATEV,1,7,
     +                              'STATEV BEGIN OF INC')
      IF(IPSW.GE.7.OR.IPSW.EQ.-7)CALL PRMAT(T1,S1,1,6,
     +                              'STRESS BEGIN OF INC')
      IF(IPSW.GE.7.OR.IPSW.EQ.-7)CALL PRMAT(T1,SDEV1,1,6,
     +                              'SDEV BEGIN OF INC')
C
C ELASTIC PROPERTIES FOR DAMAGED MATERIAL AT BEGINNING OF INCREMENT
C
      SHE1 =(1.-DAM1)*SHE0
      BULK1=BULK0
      RNU1 =-(2.*SHE1-3.*BULK0)/(2.*SHE1+6.*BULK0)
      YUNG1= 2.*SHE1*(1.+RNU1)
C
C STATE OF STRESS
C
      ISTATE=NTENS
C=================================================
C FORM JACOBIAN MATRIX (6 X 6) AT BEGIN. OF INCR.
C=================================================
      C1=2.*SHE1*(1.-RNU1)/(1.-2.*RNU1)
      C2=C1*RNU1/(1.-RNU1)
      C3=SHE1
      DO 50 I=1,6
      DO 40 J=1,6
      IF(I.EQ.J)THEN
         IF(I.LE.3)THEN
            RJAC66(I,J)=C1
         ELSE
            RJAC66(I,J)=C3
         ENDIF
      ELSE
         IF(I.LE.3.AND.J.LE.3)THEN
            RJAC66(I,J)=C2
         ELSE
            RJAC66(I,J)=0.
         ENDIF
      ENDIF
40    CONTINUE
50    CONTINUE
C
C FORMAT JACOBIAN (6 X 6) INTO JACOBIAN (NTENS X NTENS) FOR INDEPENDENT
C VARIABLES. THIS TRANSFORMATION DEPENDS ON STATE OF STRESS (ISTATE)
C THE RELATION LINKING DEPENDENT VARIABLES TO INDEPENDENT VARIABLES
C IS STORED IN RJACCO (NTENCO X NTENCO)
C
       CALL MATJAC(RJAC66,DDSDDE,RJACCO,RJACM1,NTENS,NTENCO,ISTATE)
C
C PRINT MATERIAL JACOBIAN AND ASSOCIATED MATRICES
C
      IF(IPSW.GE.10.OR.IPSW.EQ.-10)THEN
         CALL PRMAT(T1,RJAC66,6,6,'MATERIAL JACOBIAN (3D)')
         CALL PRMAT(T1,DDSDDE,NTENS,NTENS,
     +              'MATERIAL JACOBIAN (NTENS X NTENS)')
         IF(NTENCO.GT.1)THEN
            CALL PRMAT(T1,RJACCO,NTENCO,NTENS,
     +                 'DEP. VAR./ INDEP. VAR. RELATION')
            IF(ISTATE.LE.2)THEN
            CALL PRMAT(T1,RJACM1,NTENCO,NTENCO,
     +                 'INVERTED DEP. VAR. MATRIX')
```

```
            ENDIF
         ENDIF
      ENDIF
C*************************************************
C 3D STRAIN INCREMENT (ENG NOTATION)
C*************************************************
C
C DAMAGE RATE AND PERMANENT STRAIN RATE
C
      DDA1=DAMRAT(STATEV,NSTATV,PROPS,NPROPS,SSE,SPD,SCD)
      DEE1=REERAT(STATEV,NSTATV,PROPS,NPROPS,SSE,SPD,SCD,DDA1)
      DDAM=DDA1*DTIME
      IF(DAM1.LT.1.)THEN
         FAC1=DDA1/(DAM1-1.)
      ELSE
         FAC1=0.
      ENDIF
      IF(SQ1.NE.0.)THEN
         FAC2=2.*SHE1*DEE1/SQ1
      ELSE
         FAC2=0.
      ENDIF
      FAC=(FAC1-FAC2)*DTIME
      IF(IPSW.GE.50.OR.IPSW.EQ.-50)THEN
         PRINT*,'$ DDA1=',DDA1
         PRINT*,'$ DEE1=',DEE1
         PRINT*,'$ FAC1=',FAC1
         PRINT*,'$ FAC2=',FAC2
         PRINT*,'$ FAC =',FAC
      ENDIF
C
C NOTE:
C       II, I : INDEP. VARIABLES
C       JJ, J : DEP. VARIABLES
C           L : SUMMATION
C
C UNIDIMENSIONAL STRESS
C
      IF(ISTATE.EQ.1)THEN
         II=LOCX(1)
         DE(II)=DSTRAN(1)
         DO 110 J=1,5
         JJ=LOCS(J)
         GASH=RJACCO(J,1)*DSTRAN(1)
         DO 100 L=1,5
         LL=LOCS(L)
         GASH=GASH-FAC*RJACM1(J,L)*SDEV1(LL)
100      CONTINUE
         DE(JJ)=GASH
110      CONTINUE
C
C PLANE STRESS
C
      ELSEIF(ISTATE.EQ.3)THEN
         DO 310 J=1,3
         II=LOCP(J)
         JJ=LOCZ(J)
         DE(II)=DSTRAN(J)
         GASH=0.
         DO 300 L=1,3
         LJ=LOCZ(L)
         GASH=GASH-FAC*RJACM1(J,L)*SDEV1(LJ)+RJACCO(J,L)*DSTRAN(L),
300      CONTINUE
         DE(JJ)=GASH
310      CONTINUE
C
```

```
C PLANE STRAIN / AXISYMMETRIC
C
      ELSEIF(ISTATE.EQ.4)THEN
         DO 400 I=1,4
         II=LOCA(I)
         DE(II)=DSTRAN(I)
400      CONTINUE
         DO 410 J=1,2
         JJ=LOCT(J)
         DE(JJ)=0.
410      CONTINUE
C
C FULL STATE OF STRESS (3D)
C
      ELSEIF(ISTATE.EQ.6)THEN
         DO 600 I=1,6
         II=LOC3(I)
         DE(II)=DSTRAN(I)
600      CONTINUE
      ENDIF
C
C INCREMENT OF STRAIN IN VOLUME
C
      DEPSV=DE(1)+DE(2)+DE(3)
      IF(IPSW.GE.3.OR.IPSW.EQ.-3)CALL PRMAT(T2,DE,1,6,
     +                                  'STRAIN INCREMENT (3D)')
      IF(IPSW.GE.4.OR.IPSW.EQ.-4)CALL PRMAT(T2,DSTRAN,1,NTENS,
     +                                  'STRAIN INCREMENT (INDEP)')
C================================================
C UPDATE STRESS
C================================================
C
C INCREMENT OF MEAN STRESS
C
      DSM=BULK1*DEPSV
C
C 3D STRESS
C
      DO 720 I=1,6
      IF(I.LE.3)THEN
         DS    =FAC*SDEV1(I)+2.*SHE1*(DE(I)-DEPSV/3.)+DSM
      ELSE
         DS    =FAC*SDEV1(I)+SHE1*DE(I)
      ENDIF
      S2(I)=S1(I)+DS
720   CONTINUE
C
C MEAN STRESS END OF INCREMENT
C
      SM2=(S2(1)+S2(2)+S2(3))/3.
C
C STRESS DEVIATOR AT END OF INCREMENT
C
      DO 721 I=1,6
      IF(I.LE.3)THEN
         SDEV2(I)=S2(I)-SM2
      ELSE
         SDEV2(I)=S2(I)
      ENDIF
721   CONTINUE
C
C EQUIVALENT MISES STRESS
C
      GASH=0.
      DO 730 I=1,6
      S=SDEV2(I)
```

```
      IF(I.LE.3)THEN
         GASH=GASH+S*S
      ELSE
         GASH=GASH+2.*S*S
      ENDIF
730   CONTINUE
      SQ2=SQRT(1.5*GASH)
      DSQ =(SQ2-SQ1)
      DSQ2=DSQ/DTIME
C
C DIRECT INDEPENDENT STRESSES
C
      DO 740 ITENS=1,NDI
      STRESS(ITENS)=S2(ITENS)
740   CONTINUE
C
C SHEAR INDEPENDENT STRESSES
C
      IF(NSHR.NE.0)THEN
         DO 750 ITENS=1,NSHR
         STRESS(ITENS+NDI)=S2(3+ITENS)
750      CONTINUE
      ENDIF
C*************************************************
C UPDATE STATE VARIABLES AT END OF INCREMENT
C*************************************************
      NITER=1
      IF(TIME.EQ.0.)NITER=2
      DO 700 ITER=1,NITER
C
C DAMAGE
C
      DAM2=DAM1+DDAM
      IF(DAM2.GT.1.)DAM2=.9999
      SHE2=SHE0*(1.-DAM2)
C
C INCREMENT OF EQUIVALENT STRAIN
C
      DEQ=DEE1*DTIME*2./3.+(SQ2/(3.*SHE2))-(SQ1/(3.*SHE1))
      EQ2=EQ1+DEQ
      DEQ2=DEQ/DTIME
C
C STORE VALUES IN STATE VARIABLE VECTOR
C
      STATEV(1)=DAM2
      STATEV(2)=EQ2
      STATEV(3)=DEQ2
      STATEV(4)=SQ2
      STATEV(5)=DSQ2
      STATEV(6)=SM2
      STATEV(7)=AMAX1(STATEV(7),EQ2)
      DO 800 I=1,6
      STATEV(I+7)=SDEV2(I)
800   CONTINUE
C
C EVALUATE DAMAGE RATE AT END OF INCREMENT FOR FIRST INCREMENT
C RATES OF STRESS/STRAIN CAN ONLY BE ESTIMATED AT THE END OF THE
C FIRST INCREMENT (CONSTANT STRAIN RATE TEST)
C
      IF(TIME.EQ.0.)THEN
      DDA1=DAMRAT(STATEV,NSTATV,PROPS,NPROPS,SSE,SPD,SCD)
         DDAM=DDA1*DTIME
      ENDIF
700   CONTINUE
C*************************************************
C ENERGY AND DISSIPATION INCREMENTS
```

```
C*****************************************************
C
C PRINT VARIABLES FOR ENERGY CALCULATION
C
      IF(IPSW.GE.50.OR.IPSW.EQ.-50)THEN
         PRINT*,'$ SHE1,SHE2 =',SHE1,SHE2
         PRINT*,'$ SQ1,SQ2,DSQ =',SQ1,SQ2,DSQ
         PRINT*,'$ BULK0,BULK1 =',BULK0,BULK1
         PRINT*,'$ SM1,SM2 =',SM1,SM2
         PRINT*,'$ DAM1,DAM2,DDAM =',DAM1,DAM2,DDAM
         PRINT*,'$ DEQ =',DEQ
      ENDIF
C
C ELASTIC STRAIN ENERGY DENSITY
C
      WEM1  =SM1*SM1/(2.*BULK1)
      WEM2  =SM2*SM2/(2.*BULK1)
      DWEM  =WEM2-WEM1
      DWEM2 =DWEM/DTIME
C
      WEQ1  =SQ1*SQ1/(6.*SHE1)
      WEQ2  =SQ2*SQ2/(6.*SHE2)
      DWEQ  =WEQ2-WEQ1
      DWEQ2 =DWEQ/DTIME
C
      DWE   =DWEM+DWEQ
      DWE2  =DWE/DTIME
      WE2   =WEM2+WEQ2
      SSE   =WE2
C
C ELASTIC RESTITUTION THROUGH DAMAGE
C
      IF(DDAM.GT.0.)THEN
         DWD=SQ1*SQ2*((1./SHE2)-(1./SHE1))/6.
      ELSE
         DWD  =0.
      ENDIF
      DWD2  =DWD/DTIME
      WD2   =SPD+DWD
      SPD   =WD2
C
C DISSIPATION THROUGH PERMANENT DEFORMATION
C
      DWR2 =DTIME*(SQ1+0.5*DSQ)*DEE1*2./3.
      WR2  =SCD+DWR2
      SCD  =WR2
C
C TOTAL ENERGY DENSITY
C
      W2    =WE2+WD2+WR2
      DW2   =DWE2+DWD2+DWR2
C
      DWT   =(SQ1+.5*DSQ)*DEQ+DWEM
      WT2   =STATEV(14)+DWT
      STATEV(14)=WT2
      DWT2 =DWT/DTIME
C*****************************************************
C PRINT STATE VARIABLES AT END OF INCREMENT
C*****************************************************
      IF(IPSW.GE.7.OR.IPSW.EQ.-7)CALL PRMAT(T2,S2,1,6,
     +                                'STRESS END OF INC')
      IF(IPSW.GE.1.OR.IPSW.EQ.-1)CALL PRMAT(T2,STATEV,1,7,
     +                                'STATEV END OF INCREMENT')
      IF(IPSW.GE.2.OR.IPSW.EQ.-2)CALL PRMAT(T2,SDEV2,1,6,
     +                                'STRESS DEVIATOR END OF INCREMENT')
      IF(IPSW.GE.5.OR.IPSW.EQ.-5)CALL PRMAT(T2.ENER2.2.7.
```

```
     +                                  'ENERGY EQ,EM,E,D,R,TOT,TOT')
      RETURN
      E N D
      SUBROUTINE PRMAT(TIME,RMAT,N,M,CMESS)
C
CPU PURPOSE:
CPU     PRINT MATRIX RMAT(N,M) AND HEADING CMESS
C
      DIMENSION RMAT(N,M),VECT(10)
C
      CHARACTER*(*) CMESS
C
      PRINT*,'$ '
      PRINT*,'$',CMESS,' TIME=',TIME
      DO 20 ILINE=1,N
      DO 25 JCOL=1,M
      V=RMAT(ILINE,JCOL)
      IF(ABS(V).LT.1.E-10)V=0.
      VECT(JCOL)=V
25    CONTINUE
      WRITE(*,'(1P,1X,A3,7E10.3)')'$$ ',(VECT(JCOL),JCOL=1,M)
20    CONTINUE
      RETURN
      E N D
C
C*****************************************************
C*****************************************************
C
      SUBROUTINE MATJAC(RJAC66,DDSDDE,RJACCO,RJACM1,NTENS,NTENCO,
     + ISTATE)
C
CPU PURPOSE :
CPU     1) FORMAT THE 3D MATERIAL JACOBIAN RJAC66 INTO DDSDDE
CPU        DEPENDING ON STRESS STATE ISTATE
CPU     2) ESTABLISH RELATION BETWEEN DEPENDENT AND INDEPENDENT
CPU        VARIABLES (RJACCO)
C
CAI ARGUMENT INPUT :
CAI     RJAC66 FULL 3D MATERIAL JACOBIAN
CAI     ISTATE STATE OF STRESS
CAI        1 = UNIAXIAL STRESS IN PLANE
CAI        2 = UNIAXIAL STRESS IN SPACE
CAI        3 = PLANE STRESS
CAI        4 = PLANE STRAIN
CAI        5 = AXI-SYMMETRIC
CAI        6 = 3D
CAI     NTENS  NUMBER OF ACTIVE STRESSES
CAI     NTENCO NUMBER OF COMPLEMENTARY STRESSES
C
CIV INTERNAL VARIABLES :
CIV     LOC.(.)     LOCALISATION VECTORS
C
CAO ARGUMENT OUTPUT :
CAO     RJACCO(.,.) COMPLEMENTARY PART OF MATERIAL JACOBIAN
CAO     DDSDDE(.,.) MATERIAL JACOBIAN REDUCED TO NTENS X NTENS
CAO     RJACM1(.,.) INVERTED COMPLEMENTARY JACOBIAN
C
      DIMENSION LOC3(6)
      DIMENSION RJAC66(6,6),RJACCO(NTENCO,NTENS),DDSDDE(NTENS,NTENS)
      DIMENSION RJACM1(NTENCO,NTENCO)
      DIMENSION LOCP(3),LOCZ(3),RJACZZ(3,3)
      DIMENSION LOCX(1),LOCS(5),RJACSS(5,5)
      DIMENSION LOCA(4),LOCT(2)
C
      DATA LOC3 /1,2,3,4,5,6/
      DATA LOCP /1,2,4/  LOCZ /3,5,6/
```

```
      DATA LOCX /1/, LOCS /2,3,4,5,6/
      DATA LOCA /1,2,3,4/, LOCT /5,6/
C*****************************************************
C ENTRY SECTION
C BRANCH ACCORDINGLY TO STRESS STATE
C*****************************************************
       GOTO (1000,9000,3000,4000,9000,6000)ISTATE
C*****************************************************
C UNIAXIAL STRESS
C*****************************************************
1000  CONTINUE
C
C STORE SS COMPONENT OF RJAC66 IN RJACSS, AND INVERT RJACSS (RJACM1)
C
      DO 1020 I=1,5
      II=LOCS(I)
      DO 1010 J=1,5
      JJ=LOCS(J)
      RJACSS(I,J)=RJAC66(II,JJ)
1010  CONTINUE
1020  CONTINUE
C
      CALL AINVND(RJACSS,RJACM1,NTENCO)
C
C DEPENDENT COMPONENTS (RJACM1 * RJACSX)
C
      JJ=LOCX(1)
      DO 1040 I=1,5
      GASH=0.
      DO 1050 L=1,5
      LL=LOCS(L)
      GASH=GASH+RJACM1(I,L)*RJAC66(LL,JJ)
1050  CONTINUE
      RJACCO(I,1)=-GASH
1040  CONTINUE
C
C INDEPENDENT COMPONENTS RJACXS * ( RJACM1 * RJACSX )
C
      GASH=0.
      II=LOCX(1)
      DO 1060 L=1,5
      LL=LOCS(L)
      GASH=GASH+RJAC66(II,LL)*RJACCO(L,1)
1060  CONTINUE
      DDSDDE(1,1)=RJAC66(II,JJ)+GASH
      GOTO 8000
C*****************************************************
C PLANE STRESS
C*****************************************************
3000  CONTINUE
C
C STORE ZZ COMPONENTS OF RJAC66 IN RJACZZ, AND INVERT IT (RJACM1)
C
      DO 3020 I=1,3
      II=LOCZ(I)
      DO 3010 J=1,3
      JJ=LOCZ(J)
      RJACZZ(I,J)=RJAC66(II,JJ)
3010  CONTINUE
3020  CONTINUE
C
      CALL AINVND(RJACZZ,RJACM1,NTENCO)
C
C DEPENDENT COMPONENTS RJACM1 * RJACZP
C
      DO 3070 I=1,3
```

```
      DO 3060 J=1,3
      JJ=LOCP(J)
      GASH=0.
      DO 3050 L=1,3
      LL=LOCZ(L)
      GASH=GASH+RJACM1(I,L)*RJAC66(LL,JJ)
3050  CONTINUE
      RJACCO(I,J)=-GASH
3060  CONTINUE
3070  CONTINUE
C
C INDEPENDENT COMPONENTS
C
      DO 3100 I=1,3
      II=LOCP(I)
      DO 3090 J=1,3
      JJ=LOCP(J)
      GASH=0.
      DO 3080 L=1,3
      LL=LOCZ(L)
      GASH=GASH+RJAC66(II,LL)*RJACCO(L,J)
3080  CONTINUE
      DDSDDE(I,J)=RJAC66(II,JJ)+GASH
3090  CONTINUE
3100  CONTINUE
      GOTO 8000
C=============================================
C AXISYMMETRIC / PLANE STRAIN
C=============================================
4000  CONTINUE
C
C INDEPENDENT COMPONENTS
C
      DO 4020 I=1,4
      II=LOCA(I)
      DO 4010 J=1,4
      JJ=LOCA(J)
      DDSDDE(I,J)=RJAC66(II,JJ)
4010  CONTINUE
4020  CONTINUE
C
C DEPENDENT COMPONENTS
C
      DO 4040 I=1,2
      II=LOCT(I)
      DO 4030 J=1,4
      JJ=LOCA(J)
      RJACCO(I,J)=RJAC66(II,JJ)
4030  CONTINUE
4040  CONTINUE
      GOTO 8000
C=============================================
C 3-D
C=============================================
6000  CONTINUE
      DO 6200 I=1,6
      II=LOC3(I)
      DO 6100 J=1,6
      JJ=LOC3(J)
      DDSDDE(I,J)=RJAC66(II,JJ)
6100  CONTINUE
6200  CONTINUE
      GOTO 8000
C=============================================
C EXIT SECTION
C=============================================
```

```
 8000  CONTINUE
       RETURN
C*****************************************************
C ERROR SECTION
C*****************************************************
 9000  CONTINUE
       PRINT*,'***** ERROR IN MATJAC'
       PRINT*,'      UNKNOWN STATE OF STRESS - STOP'
       STOP
       E N D
C
C*****************************************************
C*****************************************************
C
      FUNCTION DAMRAT(STATEV,NSTATV,PROPS,NPROPS,SSE,SPD,SCD)
C
CPU PURPOSE :
CPU     FUNCTION DEFINING THE RATE OF DAMAGE
CPU     CAN BE DEPENDENT ON CURRENT DAMAGE SO FAR, EQUIVALENT
CPU     UNIAXIAL QUANTITIES SUCH AS STRAIN, STRAIN RATE, STRESS,
CPU     STRESS RATE
C
CAI ARGUMENT INPUT:
CAI     SSE    STRAIN ENERGY DENSITY
CAI     SPD    DENSITY OF STRAIN ENERGY RESTITUTION (DAMAGE)
CAI     SCD    DISSIPATION DENSITY (PERMANENT STRAINS)
CAI     STATEV STATE VARIABLES
CAI      (1)   DAMAGE
CAI      (2)   EQUIVALENT TOTAL STRAIN
CAI      (3)   RATE OF EQUIVALENT TOTAL STRAIN
CAI      (4)   EQUIVALENT UNIAXIAL STRESS
CAI      (5)   RATE OF EQUIVALENT UNIAXIAL STRESS
CAI     NPROPS NUMBER OF CONSTANTS FOR CURRENT MATERIAL
CAI     PROPS(.) ARRAY OF MATERIAL CONSTA NTS
C
CIV INTERNAL VARIABLES:
CIV     INXST0 START ADDRESS (0+) FOR CONSTANT
CIV     INXST1 START ADDRESS (0+) FOR FIRST POWER OF S.V.
CIV     INXST2 START ADDRESS (0+) FOR SECOND POWER OF S.V.
C
C
CAO ARGUMENT OUTPUT:
CAO     STATEV STATE VARIABLES
CAO       (7)  MAXIMUM STRAIN (EQUIVALENT)
CAO     DAMRAT RATE OF DAMAGE
C
      DIMENSION PROPS(NPROPS),STATEV(NSTATV)
C
      DATA INXST0 /4/, INXST1 /5/, INXST2 /10/
C
C ENTRY SECTION
C
      IF(STATEV(2).GE.STATEV(7))THEN
         DAMRAT=PROPS(INXST0+1)
         DO 10 INX=1,5
         GASH=STATEV(INX)
         DAMRAT=DAMRAT+(PROPS(INXST1+INX)+
     +                  PROPS(INXST2+INX)*GASH)
     +                  *GASH
10       CONTINUE
      ELSE
         DAMRAT=0.
      ENDIF
      RETURN
      E N D
C
```

```
C*****************************************************
C*****************************************************
C
      FUNCTION REERAT(STATEV,NSTATV,PROPS,NPROPS,SSE,SPD,SCD,DDAI)
C
CPU PURPOSE :
CPU     FUNCTION DEFINING THE RATE OF PERMANENT STRAINS
CPU     CAN BE DEPENDENT ON CURRENT DAMAGE SO FAR, EQUIVALENT
CPU     UNIAXIAL QUANTITIES SUCH AS STRAIN, STRAIN RATE, STRESS,
CPU     STRESS RATE
C
CAI ARGUMENT INPUT:
CAI     SSE     STRAIN ENERGY DENSITY
CAI     SPD     DENSITY OF STRAIN ENERGY RESTITUTION (DAMAGE)
CAI     SCD     DISSIPATION DENSITY (PERMANENT STRAINS)
CAI     DDAI    DAMAGE RATE
CAI     STATEV STATE VARIABLES
CAI       (1)   DAMAGE
CAI       (2)   EQUIVALENT TOTAL STRAIN
CAI       (3)   RATE OF EQUIVALENT TOTAL STRAIN
CAI       (4)   EQUIVALENT UNIAXIAL STRESS
CAI       (5)   RATE OF EQUIVALENT UNIAXIAL STRESS
CAI     NPROPS NUMBER OF CONSTANTS FOR CURRENT MATERIAL
CAI     PROPS(.) ARRAY OF MATERIAL CONSTANTS
C
CAO ARGUMENT OUTPUT:
CAO     REERAT RATE OF PERMANENT EQUIVALENT STRAINS
C
      DIMENSION PROPS(NPROPS),STATEV(NSTATV)
C
      DATA INXST0 /16/, INXST1 /17/, INXST2 /22/
C
C ENTRY SECTION
C
      REERAT=PROPS(INXST0+1)
      DO 10 INX=1,5
      GASH=STATEV(INX)
      REERAT=REERAT+(PROPS(INXST1+INX)+
     +               PROPS(INXST2+INX)*GASH)
     +               *GASH
10    CONTINUE
      REERAT=REERAT+PROPS(16)*DDAI
      RETURN
      E N D
END OF FILE
```

APPENDIX B

COMPARISON BETWEEN AN ANALYTICAL AND AN FE SOLUTION TO A UNIAXIAL DAMAGE PROBLEM

In order to determine the accuracy of the numerical integration of the F.E. damage model, an exact analytical solution for the particular case of a uniaxial sample subjected to a strain, ε_x that increases linearly in time t,

$$\varepsilon_x(t) = Bt \tag{B1}$$

is derived, and then compared to the FE solution; B is a given constant. The following evolution law is considered (Eq. (4.39)):

$$\dot{D} = A\dot{e} \tag{B2}$$

$$\dot{e}^{rd} = 0 \tag{B3}$$

where A is a given constant.

In a strain-driven test, a solution is required for the history of axial stress $\sigma_x(t)$. Because of the simple loading conditions, the damage law (B2) can be integrated in closed form.

For uniaxial conditions, the conjugate deviatoric strain rate $\dot{e}$, defined in (4.17), is equal to:

$$\dot{e} = \frac{2}{3}\ \text{sign}\ (\sigma_x)\ (1 + \tilde{\nu})\ \varepsilon_x, \tag{B4}$$

and

$$1 - D = \frac{3K}{2G}\ \frac{1-2\tilde{\nu}}{1+\tilde{\nu}} \tag{B.5}$$

In these equations, K and G are the original bulk and shear modulus, respectively, X and ν is the current value of Poisson's ratio, which increases from its original value to the value 0.5 when damage attains 100%, according to the following history:

$$1 + \tilde{\nu}(t) = \frac{3}{4AB\ \mathrm{sign}(\sigma_x)t}\left(1 + \frac{3K}{G}\right) - \left(\left(1 + \frac{3K}{G}\right)^2 - \frac{12ABK}{G}\ \mathrm{sign}(\sigma_x)t\right)^{1/2} \tag{B6}$$

The fundamental stress-strain relation (4.14) yields stress as a function of time:

$$\sigma_x(t) = \frac{4GB}{3}(1 - D(t))(1 + \tilde{\nu}(t))t + KB(3 - 2(1+\tilde{\nu}(t)))t \tag{B7}$$

where $1 + \tilde{\nu}(t)$ is given by (B6) and total damage is given by the following equation:

$$1 - D(t) = \frac{3K}{G}\left(\frac{3}{2(1 + \tilde{\nu}(t))} - 1\right) \tag{B8}$$

The analytical solution given by dotted lines is compared to the finite element solution given by solid lines in Figures B.1 to B.4 for stress history, damage history, Poisson's ratio history, and deviatoric and volumetric strain history, respectively. The figures show that there is good agreement between the analytical and numerical solutions.

Due to the numerical time integration method (i.e. a simple Euler scheme), stress and strain are slightly over-estimated and damage is very slightly underestimated. The numerical solution shows an instability at time t = 3.5 s, when damage reaches values larger than 90%; at that point, the time increment reaches its critical value and numerical integration becomes inaccurate. Note that incompressibility is reached at a state of full damage: Poisson's ratio attains 0.5 and the volumetric strain becomes zero.

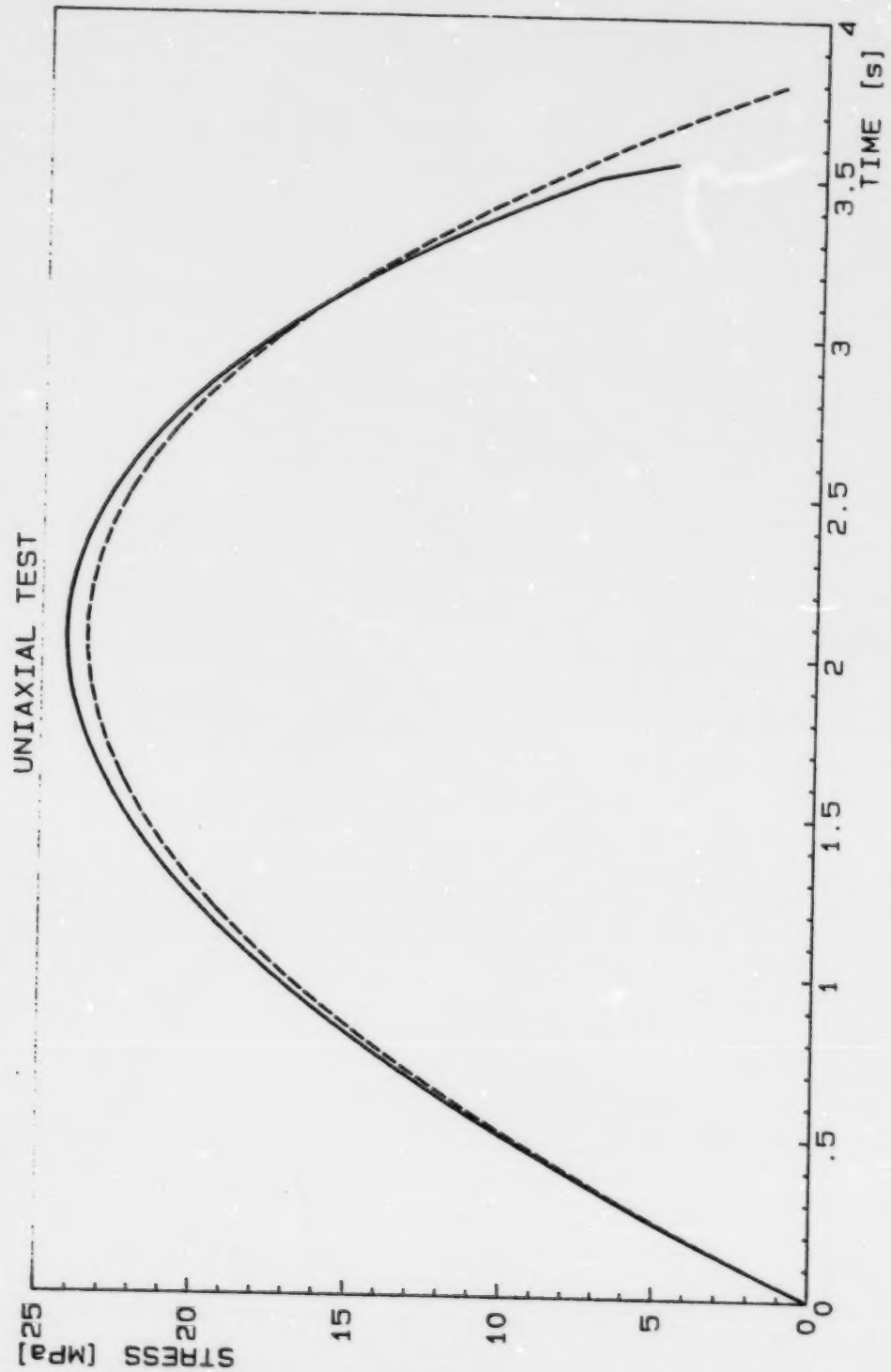

Figure B.1. Uniaxial Stress History

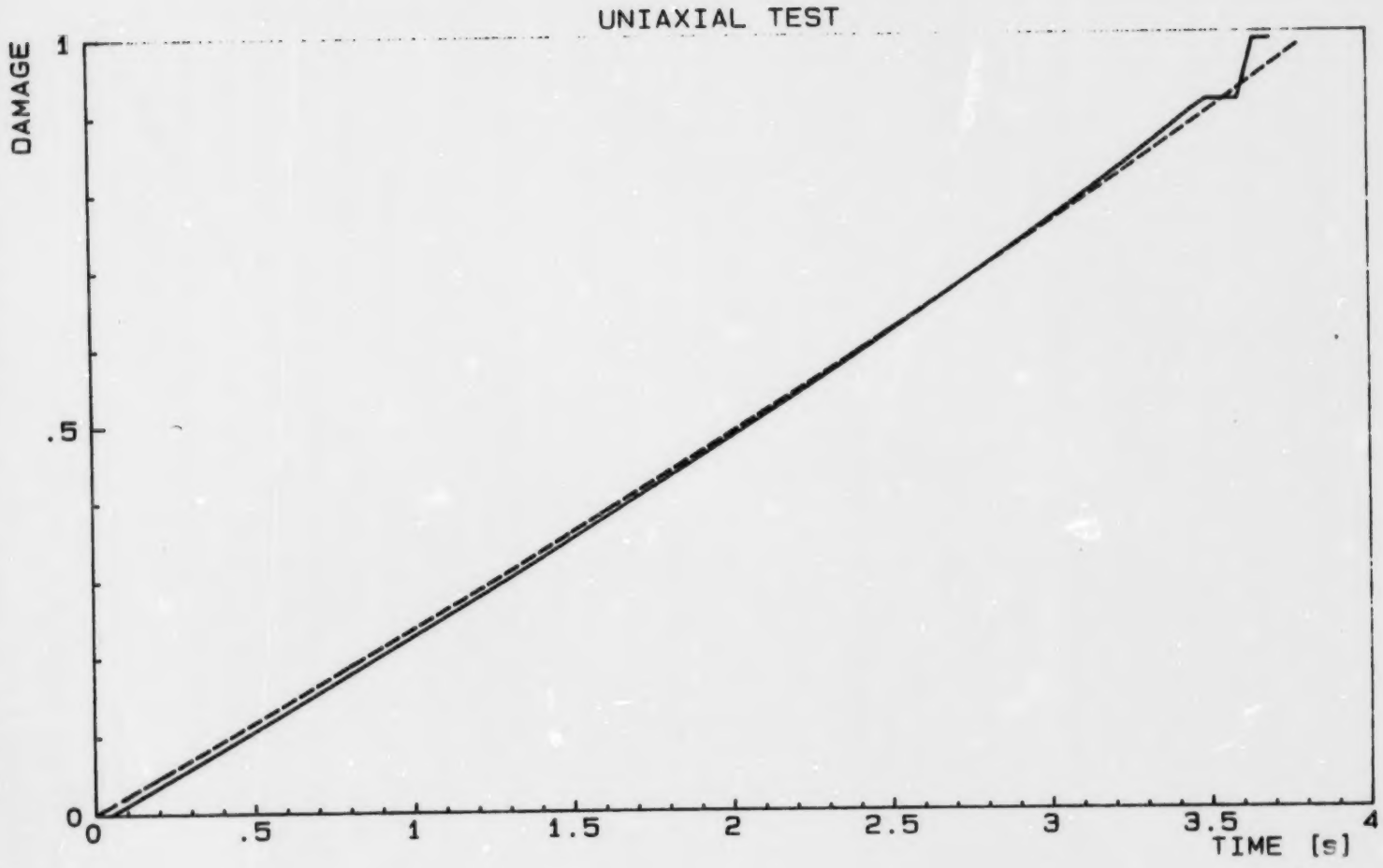

Figure B.2. Damage Accumulation

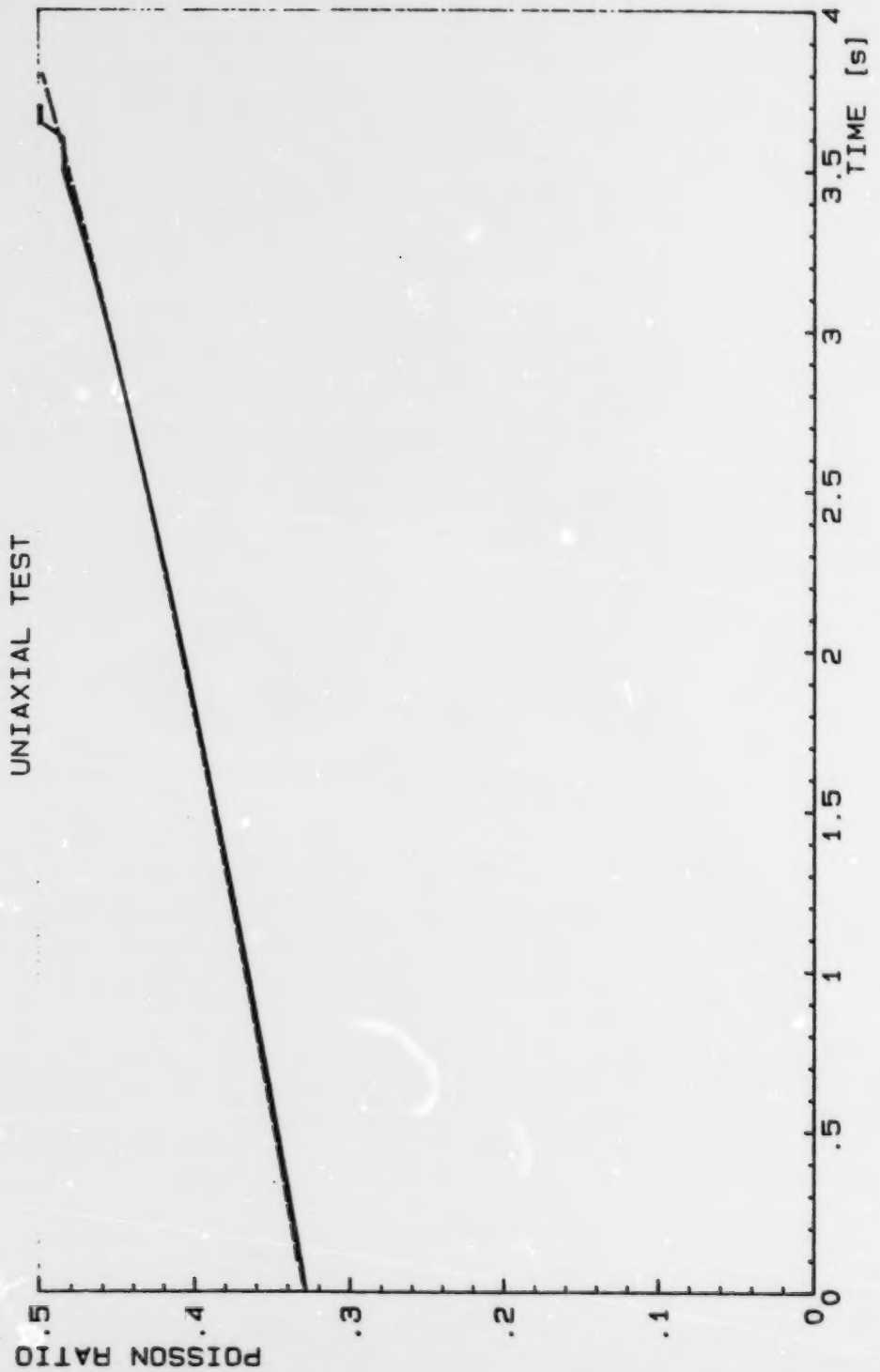

Figure B.3. History of Poisson's Ratio

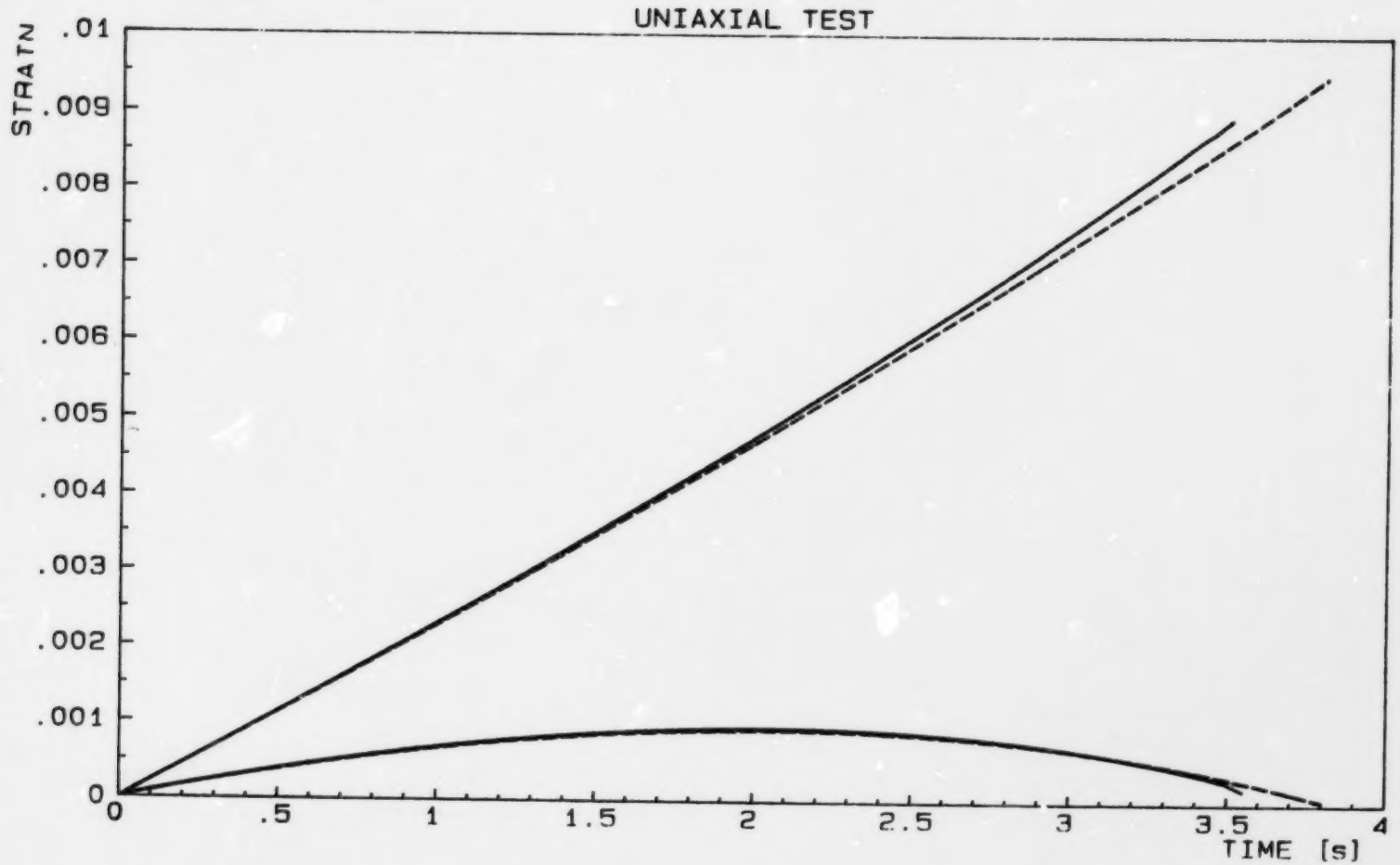

Figure B.4. Equivalent Deviatoric and Volumetric Strain